

UNIVERSITY FOR DEVELOPMENT STUDIES

**TRANSMUTED TYPE I GENERAL EXPONENTIAL
FAMILY OF DISTRIBUTIONS**

ALBERT AYI ASHIAGBOR

2021



UNIVERSITY FOR DEVELOPMENT STUDIES

TRANSMUTED TYPE I GENERAL EXPONENTIAL FAMILY
OF DISTRIBUTIONS

BY

ALBERT AYI ASHIAGBOR (MPhil in Statistics)

(UDS/DAS/0001/18)

THESIS SUBMITTED TO THE DEPARTMENT OF
STATISTICS, FACULTY OF MATHEMATICAL SCIENCES,
UNIVERSITY FOR DEVELOPMENT STUDIES, IN PARTIAL
FULFILLMENT OF THE REQUIREMENTS FOR THE AWARD
OF DOCTOR OF PHILOSOPHY DEGREE IN APPLIED
STATISTICS

MAY, 2021



DECLARATION

Student

I hereby declare that this thesis is the result of my own original work and that no part of it has been presented for another degree in this University or elsewhere;

Candidate's Signature:..... Date:.....

Albert Ayi Ashiagbor

Supervisors'

We hereby declare that the preparation and presentation of this thesis was supervised in accordance with the guidelines on supervision of thesis laid down by the University for Development Studies.

Principal Supervisor's Signature..... Date:.....

Abukari Alhassan, PhD

Co-Supervisor's Signature..... Date:.....

Suleman Nasiru, PhD



ABSTRACT

The Transmuted Type I General Exponential family of distributions as a new generator is proposed and studied. The new generator has a closed form and therefore very tractable, its hazard rate function has the flexibility to model different kinds of the bathtub shapes. Also, a comprehensive description of the statistical properties of the new generator including explicit expressions for the ordinary and incomplete moments, moments generating function, order statistics and stochastic ordering property are derived. Five special models were derived from the proposed generator. The unknown parameters of the models were estimated and the Monte Carlo Simulation technique was used to assess the performance of the maximum likelihood estimators in terms of the average biases and the root mean squared errors, and it was found that the estimators are stable. The dynamism of the proposed generator was demonstrated by using real datasets and it was shown that the special models of the proposed generator provide a better fit than other competing models. It is recommended that the new family of distributions can be used in broad application in real life situation.



ACKNOWLEDGEMENT

Finishing this thesis is really a humble experience for me. It is really exciting, interesting and also challenging. I am greatly indebted to my supervisors, Dr. Alhassan Abukari and Dr. Suleman Nasiru for their constant encouragement and supports.

I would like to express my utmost gratitude to Dr. Nasiru, for the opportunity to tap into his vast knowledge and technical expertise in statistical distributions and probability theories. I cannot find words to express my gratitude to him and also to Dr. Abukari for introducing Dr. Nasiru to me. I am really grateful.

I would also like to thank the members of my thesis committee for their valuable advises: Professor Albert Lugerterah; Professor Atinuke O. Adebajji; Dr. Solomon Sarpong; Dr. Salifu Katara and Dr. Jakperik Dioggban.

I also wish to express my gratitude to the Department of Statistics, Faculty of Mathematical Sciences, and the University for Development Studies for offering me an admission to further my studies.

I express my special thankfulness to all who have supported me during this study. I would like to thank my family and friends who helped and provided much information through discussions. It is impossible to list the people who have played a role in the completion of this thesis. Their supports have been invaluable, and without this thesis would not exist.



DEDICATION

To the memories of my parents and to everyone who makes genuine contributions for a better world.



TABLE OF CONTENTS

DECLARATION	i
ABSTRACT.....	ii
ACKNOWLEDGEMENT	iii
DEDICATION.....	iv
TABLE OF CONTENTS.....	v
LIST OF TABLES	x
LIST OF FIGURES	xii
LIST OF ABBREVIATION	xiv
CHAPTER ONE	1
INTRODUCTION	1
1.1 Background of the Study.....	1
1.2 Problem Statement	2
1.3 Objectives of the Study	3
1.3.1 General Objective	3
1.3.2 Specific Objectives	3
1.4 Significance of the Study	4
1.5 Outline of the Study	5
CHAPTER TWO	6
LITERATURE REVIEW	6
2.1 Introduction	6
2.2 Methods for Developing New Distributions	6
2.3 Technique of Adding Parameters	6



2.4	Transmuted Family of Distributions and Extensions	7
2.5	Some Important Continuous Probability Distributions	10
2.5.1	Weibull Distribution	10
2.5.2	Rayleigh Distribution	13
2.5.3	Fréchet Distribution	14
2.5.4	Exponentiated Exponential Distribution.....	15
2.5.5	Lomax Distribution.....	16
CHAPTER THREE		18
METHODOLOGY		18
3.1	Introduction	18
3.2	The TIGE Class of Distributions.....	18
3.3	The Quadratic Rank Transmutation Map.....	19
3.4	Method of Estimation.....	21
3.4.1	Properties of Maximum Likelihood Estimators.....	22
3.4.1.1	Consistency	22
3.4.1.2	Asymptotic Normality	23
3.4.1.3	Asymptotic Efficiency	24
3.4.1.4	Invariance Property	24
3.5	Information Matrix and Confidence Intervals.....	25
3.6	Optimization Technique.....	25
3.7	Monte Carlo Simulation Study.....	26
3.8	Model Selection Criteria	27
3.8.1	Goodness of Fit Tests.....	28



3.8.2	The Kolmogorov-Smirnov Test.....	28
3.8.3	Cramér-von Mises Test.....	29
3.8.4	Anderson-Darlings.....	29
3.9	Information Criteria.....	30
3.9.1	The Akaike Information Criterion	30
3.9.2	The Corrected Akaike Information Criterion	31
3.9.3	Bayesian Information Criterion	31
3.10	Total Time on Test Transform.	32
3.11	Data used and Sources.....	33
CHAPTER FOUR.....		36
THEORETICAL RESULTS.....		36
4.1	Introduction	36
4.2	The T-TIGE Family of Distributions	36
4.2.1	Mixture Representation.....	38
4.3	Statistical Properties of T-TIGE Family	40
4.3.1	The Quantile Function	40
4.3.2	Moments	41
4.3.3	Moment Generating Function	42
4.3.4	Incomplete Moment	43
4.3.5	Inequality Measures	44
4.3.5.1	Lorenz Curve	45
4.3.5.2	Bonferroni Curve	45



4.3.6	Mean Residual Life.....	46
4.3.7	Stochastic Ordering Property	47
4.3.8	Distribution of Order Statistics	49
4.4	Estimators of the T-TIGE Family	52
4.5	Special T-TIGE Distributions	54
4.5.1	The T-TIGE Rayleigh Distribution.....	54
4.5.2	The T-TIGE Weibull Distribution	58
4.5.3	The T-TIGE Fréchet Distribution	62
4.5.4	The T-TIGE Exponentiated Exponential Distribution.....	66
4.5.5	The T-TIGE Lomax Distribution.....	70
4.6	The Monte Carlo Simulation Studies	74
CHAPTER FIVE		85
EMPIRICAL RESULTS AND APPLICATIONS.....		85
5.1	Introduction	85
5.2	The Application of the T-TIGER Distribution.....	85
5.3	The Application of the T-TIGEW distribution	104
5.4	The Application of the T-TIGEFr Distribution.....	111
5.5	The Application of the T-TIGEEE Distribution	121
CHAPTER SIX.....		125
SUMMARY, CONCLUSIONS AND RECOMMENDATIONS.....		125
6.1	Introduction	125
6.2	Summary	125
6.3	Conclusions	126



6.4 Recommendations	127
REFERENCES	129
APPENDICES	151
Appendix A1: The tax revenue data and the application of the T-TIGER model.....	151
Appendix A2: The Kiamo dataset and the application of the T-TIGER model.....	152
Appendix A3: The dataset and the application of the T-TIGER distribution	153
Appendix B: The Aircraft windshield failure rate dataset and the application of the T-TIGEW	154
Appendix C1: The rainfall dataset and the application of the T-TIGEFr distribution	155
Appendix C2: The breaking strength dataset and the application of the T-TIGEFr model	156
Appendix D: The fibre strength dataset and application of the T-TIGEEE distribution	157



LIST OF TABLES

Table 4.1: The RMSE of the MLE of T-TIGEW distribution 75

Table 4.2: The AB of the MLE of T-TIGEW distribution 76

Table 4.3: The RMSE of the MLE of T-TIGER distribution 77

Table 4.4: The AB of the MLE of T-TIGER distribution..... 78

Table 4.5: The RMSE of the MLE of T-TIGEFr distribution 79

Table 4.6: The AB of the MLE of T-TIGEFr distribution..... 80

Table 4.7: The RMSE of the MLE of T-TIGEEE distribution 81

Table 4.8: The average biases (AB) of the MLE of T-TIGEEE distribution .. 82

Table 4.9: The RMSE of the MLE of T-TIGEL distribution 83

Table 4.10: The AB of the MLE of T-TIGEL distribution..... 84

Table 5.1: Descriptive statistic of the tax revenue data 86

Table 5.2: The MLE estimates using the tax revenue data 88

Table 5.2: The MLE estimates using the tax revenue data (Cont'd) 89

Table 5.3: Confidence Interval for the model parameters 89

Table 5.4: The negative log-likelihood, information criteria and goodness of fit statistics for tax revenue data 90

Table 5.5: Descriptive statistic of Kiamo Blowhole Data 92

Table 5.6: The maximum likelihood estimates of parameters of the 95
Kiamo Blowhole data 95

Table 5.7: Confidence Interval for the model parameters 96

Table 5.8: The negative log-likelihood, information criteria and goodness of fit statistics for the Kiamo Blowhole data..... 97

Table 5.9: The descriptive summary of the Applied Life Data 98

Table 5.10: The MLE estimates of the applied life data..... 101



Table 5.11: The negative log-likelihood, information criteria and goodness of fit statistics for the applied life dataset	102
Table 5.12: Confidence Interval for the model parameters	102
Table 5.13: Descriptive statistic of the Aircraft Windshield data.....	104
Table 5.14: The MLE estimates of the aircraft windshield data.....	107
Table 5.14: The MLE estimates of the aircraft windshield data (cont'd).....	108
Table 5.15: The negative log-likelihood, information criteria and goodness of fit statistics for the Aircraft windshield failure data	109
Table 5.16: Confidence Interval for the model parameters	109
Table 5.17: Descriptive statistic of the rainfall data	111
Table 5.18. The MLE estimates of parameters of the rainfall data.....	113
Table 5.19: The negative log-likelihood, information criteria and goodness of fit statistics for the Rainfall dataset.....	114
Table 5.20: Confidence Interval for the model parameters	114
Table 5.21: Descriptive statistic of the breaking stress data.....	116
Table 5.22. The MLE estimates of the breaking stress dataset.....	118
Table 5.23: The negative log-likelihood, information criteria and goodness of fit statistics for the Breaking Stress dataset	119
Table 5.24: Confidence Interval for the model parameters	120
Table 5.25: Descriptive statistic of the fibre strength data	121
Table 5.26: The MLE estimates of models using the fibre strength data	123
Table 5.27: The negative log-likelihood, information criteria and goodness of fit statistics for the Fibre Strength data	124



LIST OF FIGURES

Figure 4.1: The CDF plots of the T-TIGER distribution 55

Figure 4.2: The PDF plots of T-TIGER distribution 56

Figure 4.3. Survival function plots of T-TIGER model..... 56

Figure 4.4: Hazard rate plots of T-TIGER distribution 57

Figure 4.5: The CDF plots of T-TIGEW model 58

Figure 4.6: The PDF plots of T-TIGEW distribution 59

Figure 4.7: The Survival functions of T-TIGEW model 60

Figure 4.8: Hazard rate plots of T-TIGEW distribution 61

Figure 4.9: The CDF plots of T-TIGEFr distribution 62

Figure 4.10: The PDF plots of T-TIGEFr distribution 63

Figure 4.11: The survival plots of T-TIGEFr distribution..... 64

Figure 4.12: Hazard rate function plots of T-TIGEFr model..... 65

Figure 4.13: The CDF plots of T-TIGEEE distribution 67

Figure 4.14: The PDF plots of T-TIGEEEE distribution 67

Figure 4.15: The survival plots of T-TIGEEEE distribution..... 68

Figure 4.16: Hazard rate function plots of T-TIGEEEE model 69

Figure 4.17: The CDF plots of T-TIGEL model..... 71

Figure 4.18: The PDF of T-TIGEL model..... 72

Figure 4.19: The survival plots of T-TIGEL distribution 72

Figure 4.20: Hazard rate function plots of T-TIGEL model..... 73

Figure 5.1: A graphical summary of the tax revenue dataset 86

Figure 5.2: The TTT-transform plot for tax revenue data 87

Figure 5.3: Plots of empirical density and densities of the fitted models. 91

Figure 5.4: A graphical summary of the Kiamo Blowhole dataset..... 93



Figure 5.5: The TTT-transform plot for Kiamo Blowhole data.....	94
Figure 5.6: Empirical and densities plots of the fitted models.	98
Figure 5.7: A graphical summary of the applied life dataset	99
Figure 5.8: The TTT-transform plot for applied life data	100
Figure 5.9: Plots of empirical and densities of the fitted models.....	103
Figure 5.10: A graphical summary of the windshield failure dataset	105
Figure 5.11: The TTT-transform plot for windshield failure data	106
Figure 5.12: Plots of empirical and densities of the fitted models.....	110
Figure 5.13: A graphical summary of the rainfall data	111
Figure 5.14: The TTT-transform plot for rainfall dataset	112
Figure 5.15: Plots of empirical and densities of the fitted model	115
Figure 5.16: A graphical summary of the breaking stress data.....	116
Figure 5.17: The TTT-transform plot for breaking stress data	117
Figure 5.18: Empirical and densities plots of the fitted	120
Figure 5.19: A graphical summary of the fibre strength data	121
Figure 5.20: The TTT-transform plot for fibre strength data.....	122
Figure 5.21: Empirical and densities plots of the fitted models	124



LIST OF ABBREVIATION

A*	Anderson Darling Test
AB	Average Bias
AIC	Akaike Information Criteria
AICc	Corrected Akaike Information Criteria
BFGS	Broyden-Fletcher-Goldfarb-Shanno
BIC	Bayesian Information Criteria
BXFr	Burr-X Fréchet Distribution
CI	Confidence Interval
CDF	Cumulative Distribution Function
E	Exponential Distribution
EE	Exponentiated Exponential Distribution
EFr	Exponentiated Fréchet Distribution
EGTR	Exponentiated Generalized Transmuted Rayleigh Distribution
EGFr	Exponentiated Generalized Fréchet Distribution
ETGR	Exponentiated Transmuted Generalized Rayleigh
EWE	Exponentiated Weibull Exponential Distribution
Fr	Fréchet Distribution



GE	Generalized Exponential Distribution
GR	Generalized Rayleigh Distribution
GTFr	Generalized Transmuted Fréchet Distribution
GTR	Generalized Transmuted Rayleigh Distribution
HQ	Hannan–Quinn information criterion
KDE	Kernel Density Estimation
K-S	Kolmogorov-Smirnov
L	Lomax Distribution
Max	Maximum
MGF	Moment Generating Function
Min	Minimum
MLE	Maximum Likelihood Estimation
PDF	Probability Density Function
PL	Power Lomax Distribution
Q(u)	Quantile Function
QRTM	Quadratic Rank Transmutation Map
R	Rayleigh Distribution
RMSE	Root Mean Square Error



Sd	Standard Deviation
S(x)	Survival Function
SBIC	Schwarz Bayesian Information Criterion
TEMW	Transmuted Exponentiated Modified Weibull Distribution
TIGE	Type I Generalized Exponential
TR	Transmuted Rayleigh Distribution
T-TIGE	Transmuted Type I General Exponential
TIGEW	Transmuted Type I General Exponential Weibull Distribution
T-TIGEEE	Transmuted Type I General Exponential Exponentiated Exponential Distribution
T-TIGEFr	Transmuted Type I General Exponential Fréchet Distribution
T-TIGEL	Transmuted Type I General Exponential Lomax Distribution
T-TIGER	Transmuted Type I General Exponential Rayleigh Distribution
T-TIGEW	Transmuted Type I General Exponential Weibull Distribution
TTT	Total Time on Test
W	Weibull Distribution
W*	Cramer von Misses Test



WFr Weibull-Fréchet Distribution

X Random Variable

Z(x) Hazard Rate Function



CHAPTER ONE

INTRODUCTION

1.1 Background of the Study

Statistical distributions are very essential in modeling and analysing lifetime data in many areas of applied sciences such as actuarial science (Boland, 2007; Frees et al., 2014), risk management (Embrechts et al., 2011; Willmot and Lin, 2011; Guo, 2017), insurance (Achieng and No, 2010; Paula et al., 2012; Adcock et al., 2015), biomedical research (Lang, 2004; Ishak et al., 2013) among others.

In many practical situations, the existing models are not able to provide adequate fit and flexibility to real data because most datasets are believed to arise from dynamic processes. Available literature (Merovic, 2013a; Yousof et al., 2015; Mahdavi and Kundu, 2017) indicate that by introducing an additional parameter, more flexibility is brought into a distribution and hence can be very useful for data analysis purposes. In fact, most of the compounded models are noted to perform better in terms of flexibility when compared with their baseline distribution. This is because the additional parameter helps to change the weight of the tail of the new models thereby inducing it with skewness (Lee et al., 2013; Rezaei et al., 2017).

For instance, the traditional normal distribution lacks robustness in terms of analysing asymmetric data, hence cannot be relied upon as a good choice. The introduction of an additional parameter in the normal distribution by Azzalini (1985) led to the establishment of the skewed normal distribution which brings more flexibility to the normal distribution.



There are many techniques in literature that can be adopted to extend existing standard distributions. For instance, a model can be enhanced by means of generalization which involves using the available model or generalized family of distributions. When a model or family of distributions is generalized, an extra parameter would have been added.

A closer look at the existing statistical literature indicate a huge interest among statisticians and practitioners in developing new family of distributions. Some of these well-known families of distributions include: Quadratic Rank Transmutation Map (QRTM) by Shaw and Buckley (2007), Lomax-G by Cordeiro et al. (2014), Kumaraswamy Marshall-Olkin-G by Alizadeh et al. (2015), Beta Transmuted-H family by Afify et al. (2017), Topp-Leone Odd log-logistic family by Brito et al. (2017), Type I General Exponential class of distributions by Hamedani et al. (2018), T-Pareto-G by Hamed et al. (2018), Z-family of distributions by Ahmad et al. (2020).

1.2 Problem Statement

The introduction of the Type I General Exponential (TIGE) class of distributions by Hamedani et al. (2018) is timely; because it contributes to the theory of probability distributions and relatively better fits for modeling unimodal data.

However, the work of Hamedani et al. (2018) is not flexible enough to provide a better parametric fit for modeling phenomenon with varied failure rates such as bathtub and bimodal failure rates which can be present in many practical fields such as medical, risk management as well as reliability studies.



In order to overcome this drawback of the TIGE class of distributions, a minimum of two shape parameters are required (Gomes-Silva et al., 2017; Nasiru, 2018a). This study therefore seeks to develop an extended form of the TIGE class of distributions by adding an extra parameter to the existing family of distributions.

1.3 Objectives of the Study

1.3.1 General Objective

The general objective of this study is to develop and study the statistical properties of Transmuted Type I General Exponential (T-TIGE) family of distributions.

1.3.2 Specific Objectives

The specific objectives are to;

1. Develop the T-TIGE family of distributions.
2. Derive the statistical properties of the T-TIGE family of distributions.
3. Develop maximum likelihood estimators for parameters of the T-TIGE family.
4. Develop some special distributions using the T-TIGE generator.
5. Study the behaviour of the estimators using the Monte Carlo Simulation.
6. Demonstrate the applications of the special models using real datasets.



1.4. Significance of the Study

Developing and studying of probability distributions, generally in the sense of properties of suitable family of distributions, has ever been a persistent theme of theoretical and applied statistics for many decades. The knowledge of appropriate statistical distribution of real data sets greatly improves the sensitivity, power and efficiency of the statistical test associated with the data sets (Nasiru, 2018b).

Therefore, developing new generator for modifying existing distributions to improve their goodness-of-fit cannot be overemphasized. Thus, this study makes significant contribution in terms of theoretical and empirical literature as a result of introduction of a new generator called T-TIGE, to improve upon the existing distributions.

Another significant contribution of the current study which cannot be over-emphasized is the development of T-TIGE family, which is a very versatile generalization of the TIGE generator with tractable distributions and very important in statistical analysis of dataset characterized by both monotonic and non-monotonic failure rates.

It is equally important to know that the new T-TIGE generator is also capable in controlling skewness, kurtosis and tail variation of distributions that are common in actuarial science, risk management, insurance, biological, medical, and survival analysis applications among others.

This new family of distributions has several advantages and it will give practitioners additional option for analyzing skewed life time data sets. It is also envisaged that practitioners, academicians and other researchers will



benefit from the necessary background and the relevant references about this distribution because it may serve as a knowledge base for academicians and researchers working on related topics.

1.5 Outline of the Study

The organization of this study is in six chapters. Chapter one deals with the introduction of the study, with focus on the background of the study, the problem statement, the objective of the study and significance of the study. Chapter two is a review of the relevant studies that underpin the current study. Chapter three is on the methods that help in addressing the research objectives. Chapter four is about the theoretical results which highlight the development of the new generator and some statistical properties. The chapter also highlights the development of the estimators and the Monte Carlo simulations. Chapter five is about the empirical results which focuses on the applications of the special distributions derived to real datasets. Chapter six presents the summary of findings, recommendations and concluding remarks of the study.



CHAPTER TWO

LITERATURE REVIEW

2.1 Introduction

This chapter reviews relevant literature relating to current study with focus on broad-spectrum of studies that were developed and current developments in the field of statistical distributions and probability theories. Some important continuous distributions which are also relevant to this study are also being highlighted.

2.2 Methods for Developing New Distributions

There are general methodologies that underpinned the development and construction of new statistical distributions. These include methods of differential equations (Pearson, 1895, 1916; Burr, 1942), methods of quantile function (Hastings et al., 1947; Tukey, 1960), methods of transformation (Johnson, 1949; Birnbaum and Saunders, 1969; Athayde et al., 2012), skewed distributions generating methods (Azzalini, 1985), method of adding parameters to existing distributions (Mudhokar and Srivastava, 1993; Gupta and Kundu, 2001; Nadarajah and Kotz, 2006).

2.3 Technique of Adding Parameters

Mudholker and Srivastava (1993) initiated the addition of parameters to an existing distribution. This concept posits that adding parameter to an existing distribution makes it more flexible and simple. The addition of the parameter can either be in the form of scale parameter, shape parameter, or location parameter.



A scale parameter has the effect of widening or shrinking the graph of a distribution. A shape parameter is the one that affects the shape of the distribution, and the location parameter is when a change in the value results in either a shift to the left or to the right of the curve. The concept of adding parameter was boosted by the work of various researchers.

For instance, Gupta et al. (1998) gave many accounts on adding of parameters on the exponential distribution. Marshall-Olkin (2007) also developed another method of adding an extra parameter to a lifetime model, for which they studied in details the aspects or cases of exponential and Weibull models.

Shaw and Buckley (2007) also introduced a generator called QRTM family of distributions. This has brought about a huge boost in adding a parameter to existing distribution, because the QRTM has led to the development of more family of distributions and extension of some existing distributions.

2.4 Transmuted Family of Distributions and Extensions

The transmuted family has being receiving increased attentions for the past two (2) decades. The concept of the transmuted family of distributions was engineered to provide parametric models that would provide flexibility and also provide tractability of distributions.

The QRTM uses a functional composition of a cumulative function of one distribution with the quantile function of another, which allows the quadratic rank transmutation map to generate a flexible family of distributions. Thus the use of QRTM generator provides a platform to induce skewness and kurtosis of a given distribution or family of distributions. That is, the quadratic rank transmutation map is a vehicle available to generate a flexible family of



distributions. The generated family, also called the transmuted extended distribution, includes the parent distribution as a special case and gives more flexibility to model various types of data. There are many kinds of extensions to the transmuted family of distributions.

For instance, Bourguignon et al. (2016) had modified the QRTM family to include the general results, as well as bivariate and multivariate extensions. The Generalized Transmuted-G by Nofal et al. (2017), the Beta transmuted-H families by Afify et al. (2017), and the Cubic Rank Transmuted distributions by Granzotto et al. (2017).

As a way of contributing to the development of the QRTM literature, Azalideh et al. (2017) introduced and studied general mathematical properties of a new generator of continuous distributions called the Generalized Transmuted family.

The various statistical properties such as the ordinary and incomplete moments, moment generating function, Bonferroni, Lorenz, Shannon and Rényi entropies and order statistics are computed. Azalideh et al. (2017) employed the maximum likelihood method among other to estimate the model parameters and illustrate the potential application of the model via real data.

Rahman et al. (2018) have proposed and studied generalized transmuted models with emphasis on the Cubic Transmuted (CT) family.

The CT family was derived as a result of the combination of the T-X family by Alzaatreh et al. (2013) and the QRTM family. A special model, called the Cubic Transmuted Exponential distribution, was derived from the CT family



of distributions and various statistical properties of the distribution were studied. The Cubic Transmuted Exponential model was fitted to two different datasets to investigate its applicability.

The Transmuted Kumaraswamy-G Family for modeling reliability dataset was proposed and studied by Khan et al. (2017) as an extension to the QRTM family. The new extended family was derived by the combination of the quadratic rank transmutation map method, which possesses a bathtub shape for its hazard rate. Some special models in the new family were derived.

Khan et al. (2020) studied the various statistical properties of the new family, including the probability weighted moment, ordinary moments, and moment generating functions, quantile function, and formulated the PDF of r^{th} order statistics. The method of maximum likelihood was used by Khan et al. (2020) for the estimation of the parameters.

Louzada and Granzotto (2016) introduced and studied the transmuted log-logistic model which represents a general class of survival regression models.. This model was formed by combining the quadratic rank transmutation map and the usual log-logistic distribution.

Also, the QRTM was used by various authors to extend existing distributions. For instance, Aryal and Tsokos (2009) applied the QRTM to extend the Gumbel distribution to a new distribution called the Transmuted Gumbel distribution. Aryal and Tsokos (2011) embedded a two parameter Weibull model into the family of the QRTM to develop a new Weibull model known as the Transmuted Weibull model. Aryal and Tsokos (2011) studied and provided comprehensive statistical attributes of the Transmuted Weibull



distribution. The usefulness of the Transmuted Weibull model was compared with other models.

Elbatal (2013) derived the Transmuted Generalized Inverted Exponential model via the combination of the QRTM family and the generalized Inverted Exponential model was developed by Abouammoh and Alshingiti (2009). The properties of the Transmuted Generalized Inverted Exponential model such as the moments, the order statistics among others were discussed. Abouammoh and Alshingiti (2009) also used the maximum likelihood estimation technique to estimate the parameters of the model. Other generalization or extensions of the Transmuted family or generator can be found in the works of Merovci et al. (2016), Merovci et al.(2017), Afify et al. (2017), Alizadeh et al. (2018) and Mansour et al. (2019) among others.

2.5 Some Important Continuous Probability Distributions

In this section some important continuous parametric probability models that are relevant to this study are introduced.

2.5.1 Weibull Distribution

Weibull model is named after its pioneer, Waloddi Weibull, a Swedish scientist, who developed and used it in 1939 to study the distribution of breaking strength of materials.

This model continue to attract extensive use in real life analysis such as survival analysis, weather forecasting, general insurance claim, reliability



analysis, extreme value theory, among others. Thus, Weibull distribution has wider applications in modeling practical issues in engineering and medicine.

In addition, The Weibull model is equally important for modeling reliability (Bourguignon et al., 2016). Because of its versatility, it has attracted significant attentions and modifications. The Weibull model is a popular lifetime model in reliability engineering.

However, this model does not have a bathtub or upside-down bathtub shaped hazard rate function (hrf), and thus cannot be used to model the lifetime of certain systems. To overcome this shortcoming, several generalizations of the classical Weibull model have been discussed by different authors in recent years. Many studies have introduced improved Weibull models to handle more complex data and to obtain better fits.

The extensions of the Weibull as well as other traditional models is to provide a theoretical interpretation that would help to explain the mechanism of data generation and also introducing a model whose empirical fit better suits a given dataset.

Tahir et al. (2018) proposed and studied the Transmuted New Weibull-Pareto model from the New Weibull-Pareto model by Nasiru and Luguterah (2015). The quadratic equation by Shaw and Buckley (2007) and the work of Nasiru and Luguterah (2015) have been compounded to develop the generalization.

For instance, as extension to the family of the Weibull distribution, Alzaatreh and Ghosh (2015) introduced and studied some properties of the Weibull-X family. The Weibull-logistic distribution, which belongs to the Weibull-X



family, was found to be unimodal and the shape can be symmetric, right skewed or left skewed.

Tahir et al. (2016) also introduced and studied a new generator based on the Weibull distribution known as the Weibull-G family, and some statistical properties were studied. The flexibility of special-models of the Weibull-G family were exhibited in their PDFs in terms of the special models to be symmetrical, left-skewed, right-skewed, bathtub and reversed-J shaped, and has increasing, decreasing, bathtub, and S-shaped hazard rates. Tahir et al. (2016) obtained various statistical expressions which include the Renyi entropy, ordinary and incomplete moments, quantile and generating functions, order statistics and reliability. Tahir et al. (2016) also used the method of maximum likelihood to estimate the model parameters.

As said earlier, there are several extensions of the Weibull model that have been developed by use of the QRTM technique. For instance, Carrasco et al. (2008) generalized the Weibull distribution into a four parameter model, which enabled it to model a bathtub-shaped hazard rate. Ashour and Eltehiwy (2013a) also proposed the Transmuted Exponentiated Modified Weibull model, making use of the QRTM techniques.

The Transmuted Modified Weibull was also developed by Khan and King (2013) making use of the QRTM family of distributions. Application with real dataset was provided and it was confirmed that Khan and King (2013) was relatively better in terms of flexible compared with its competing models. Other generalization of the Weibull distribution can be found in the works of Nasiru and Luguterah (2015).



2.5.2 Rayleigh Distribution

This is one of the important lifetime distributions, introduced by Lord Rayleigh in the early 1880s. Rayleigh model is very useful in physics and its related fields in modeling phenomenon such as wave heights, sound and light radiations. Its application has been seen in other areas of studies in literature. The greater interest in the use of Rayleigh model has led to many extensions.

For instance, Blumenson and Miller (1963) generalized and studied the properties of the Rayleigh model in order to improve on the problem of computing the Rayleigh model in a useful form for arbitrary covariance matrices that appears intractable. The Transmuted Rayleigh model was developed by Merovci (2013c) by compounding the Rayleigh distribution and the QRTM family of distributions. The mathematical properties of the Transmuted Rayleigh model along with its reliability behaviour were studied. The transmuted Rayleigh model was applied to real dataset and it was confirmed that the work by Merovci (2013c) had a better fit compared with its competitors.

Khan and King (2015) proposed the Transmuted Modified Inverse Rayleigh model. This was achieved by using the QRTM, and the Modified Inverse Rayleigh model. The various statistical properties of the Transmuted Modified Inverse Rayleigh model were discussed. The usefulness of the model was illustrated using real lifetime data.

Usman and Yakubu (2018) proposed and studied a five parameter Generalized Transmuted-Generalized Rayleigh (GTGR) model which serves as a new distribution. Some of the mathematical expressions for this model included the



survival function and hazard function. Application of GTGR model with a dataset indicates that the model performs better than the other competing models with smallest value of Akaike information criteria.

2.5.3 Fréchet Distribution

The Fréchet model as one of versatile model was developed by a French Mathematician, Maurice Fréchet in 1927. This model has attracted a lot of attention recently because it emerged as a sub-model of the generalized extreme model and can be used to model maximum values in a dataset.

Many studies proposed several generalization of the Fréchet distribution. For example, Nadarajah and Gupta (2004) studied the Beta Fréchet model, Nadarajah and Kotz (2013) proposed and studied the Exponentiated Fréchet model, Krishna et al. (2013) introduced the Marshall-Olkin Fréchet model.

Ul Haq et al. (2017) derived a new five parameter Fréchet model for extreme value model and studied its various statistical properties. The new five-parameter which was an extension of Fréchet model was arrived at by compounding the Weibull-Fréchet model (Afify et al., 2016) and the Transmuted-G family.

Again, Mead (2014) developed and studies the Kumaraswamy Fréchet model, Afify et al. (2015), developed and studies the properties of the transmuted Marshall-Olkin Fréchet model.

Moolath, and Jayakumar (2018) proposed and studied the Exponentiated-Transmuted Fréchet distribution. Tablada and Cordeiro (2016) proposed a three-parameter extended Fréchet model and titled it as the Modified Fréchet



model. UIHaq and Elagarhy (2018) developed and studied the Odd Fréchet generator, and this family was further extended by the works of Nasiru (2018b) and named it as the Extended Odd Fréchet-G family.

Riffi et al. (2019) recently developed Generalized Transmuted Fréchet (GTFr) model, a generalized version of the quadratic rank transmuted Fréchet model that generalizes the standard Fréchet model by incorporating extra shape parameters into its distribution functions.

The main mathematical and statistical properties studied under the GTFr distribution include the hazard rate function, moments, moment-generating function, quantile function, order statistics, moments of order statistics, probability weighted moment, L-moments and maximum likelihood estimator.

2.5.4 Exponentiated Exponential Distribution

There are wide usages of the exponential distributions in literature, especially with regards to time to failure data, and a situation where the hazard rate function is fairly constant. There are great efforts in literature to improve upon the versatility of the Exponential model and this led to the development of various extension of this model.

For instance, Gupta and Kundu (2001) have developed a generator called the Exponentiated Exponential family of distributions, which had encouraged lot of researchers in generalizing related Exponentiated Exponential model.

The Exponentiated Exponential family of distribution has two parameters namely the scale parameter and the shape parameter. It is a right skewed unimodal distribution. The probability density function as well as the hazard



function of the Exponentiated Exponential model is quite similar to the density function and hazard function of the Gamma or Weibull model hence can be used to analyze lifetime data in place of Gamma or Weibull model.

Also, Merovci (2013a) developed and studies the Transmuted Exponentiated Exponential model by compounding the works of Shaw and Buckley (2007) and the Exponentiated Exponential family.

2.5.5 Lomax Distribution

Lomax model is named after its pioneer, K.S. Lomax, and this was used by Lomax (1954) to analysis the business lifetime data. The Lomax model is also referred to as a Pareto type II. It is basically a Pareto model that was shifted so as to allow its support at zero.

Lomax model is essentially a heavy tailed model and versatile in its applications. For instance, its application is pronounced in actuarial science, business, economics, queuing theory, and internet traffic modeling among others.

There are various generalizations of the Lomax family in literature. For instance, Oguntunde et al. (2017) recently generalized the Lomax model. This new generalization was derived by compounding the Gompertz's generalized family of distributions and the Lomax model. Excerpt from the literature indicates that the Gompertz Lomax model performed better than some of existing distributions such as the Beta Lomax distribution (Rajab et al., 2013), and Weibull-Lomax model (Tahir et al., 2015).



Recently, Cordeiro et al. (2014) proposed and studied a new class of distributions known as the Lomax generator with two extra positive parameters. This generalization has opened the frontier of the Lomax family. Some special models such as the Lomax-normal, Lomax–Weibull, Lomax-log-logistic and Lomax–Pareto models are were also derived.

The wider usage of the Lomax model and other related models discussed so far clearly indicate that there is the need for the extensions of these traditional models.



CHAPTER THREE

METHODOLOGY

3.1 Introduction

This chapter presents the various methods used in achieving the stated objectives. The chapter discusses the TIGE class of distributions, Quadratic Rank Transmutation Map (QRTM), compounding of the TIGE and the QRTM, the statistical properties, the concept of the maximum likelihood estimation, model selection criteria, optimization technique, the total time on test transform plot, data and sources of data used in this study.

3.2 The TIGE Class of Distributions

The first objective of this thesis is to develop the T-TIGE family of distributions. In order to achieve this objective, the Type I General Exponential (TIGE) generator by Hamedani et al. (2018) was one of the tools used. TIGE is a family of univariate continuous distributions and has two parameters, namely the scale and shape parameters. The CDF of the TIGE class of distributions are represented as:

$$F(x; \boldsymbol{\varphi}) = e^{\lambda(1-H(x; \boldsymbol{\varphi}))^{-\alpha}}, \quad \alpha > 0, \quad \lambda > 0, \quad x \in R. \quad (3.1)$$

where λ is a scale parameter, α is a shape parameter and $\boldsymbol{\varphi} = (\varphi_k) = (\varphi_1, \varphi_2, \dots)$ is a parameter vector. Differentiating (3.1) gives the PDF of TIGE as:

$$f(x; \boldsymbol{\varphi}) = \lambda \alpha h(x; \boldsymbol{\varphi}) H(x; \boldsymbol{\varphi})^{-(\alpha+1)} e^{\lambda(1-H(x; \boldsymbol{\varphi}))^{-\alpha}}. \quad (3.2)$$



Henceforth $H(x; \boldsymbol{\varphi}) = H(x)$ and $h(x; \boldsymbol{\varphi}) = h(x)$ are the arbitrary baseline CDF and PDF distributions respectively.

The survival and the instantaneous failure rate (hazard) function of the TIGE family are defined respectively by

$$S(x) = 1 - F(x) = 1 - e^{-\lambda(1-H(x))^{-\alpha}}, \quad (3.3)$$

and

$$\tau(x) = \frac{f(x)}{S(x)} = \frac{\lambda \alpha h(x) H(x)^{-(\alpha+1)} e^{\lambda(1-H(x))^{-\alpha}}}{1 - e^{\lambda(1-H(x))^{-\alpha}}}. \quad (3.4)$$

The mathematical attributes of the TIGE class of distributions include expansions for the ordinary and incomplete moments, generating function, mean deviations, order statistics, probability weighted moments.

3.3 The Quadratic Rank Transmutation Map

Another important tool used to achieve the first objective of this study was the Quadratic Rank Transmutation Map (QRTM) by Shaw and Buckley (2007) which help to generate more distributional flexibility. Transmutation map provides a powerful technique for turning the ranks of one distribution in to the ranks of another (Hussein et al., 2018).

The general rank transmutation as defined by Shaw and Buckley (2007) is given as $R_{G_{12}}(u) = F_2(F^{-1}(u))$ and $R_{G_{21}}(u) = F_1(F^{-2}(u))$ for which F_1 and F_2 are cumulative distribution functions (CDF) of two distributions with a common sample space. The quantile function or the inverse of the cumulative



distribution is expressed as $F^{-1}(y) = \inf_{x \in R} \{F(x) \geq y\}$ for $y \in [0,1]$. The functions $R_{G_{12}}(u)$ and $R_{G_{21}}(u)$ both map the unit interval $I = [0,1]$ into itself, and under suitable assumptions are mutual inverses and they satisfy $R_{G_{ij}}(0) = 0$ and $R_{G_{ij}}(1) = 1$. The QRTM is defined as $R_{G_{12}}(u) = u + \gamma u(1-u)$, from which it follows that the CDF's satisfy the relationship in equation (3.5)

$$T(x) = (1 + \gamma)F(x) - \gamma F(x)^2. \quad (3.5)$$

The corresponding PDF of equation (3.5) was arrived at by differentiation, which gives equation (3.6) as follows:

$$t(x) = f(x) [1 + \gamma - 2\gamma F(x)], \quad |\gamma| \leq 1, \quad (3.6)$$

$F(x)$ and $f(x)$ are the CDF and PDF of the base distribution respectively. If the transmutation parameter is zero, that is, $\gamma = 0$, then the transmuted model reduces to the parent model.

For more detail about the QRTM, see the works of Shaw and Buckley (2007), and Elgarhy et al. (2016).

The QRTM thus provides a platform to induce skewness and kurtosis into a given model or family of distributions.

The process of developing the new Transmuted Type I General Exponential (T-TIGE) family of distribution was therefore achieved by compounding the works of Hamedani et al. (2018) and that of Shaw and Buckley (2007).



3.4 Method of Estimation

There are various methods of estimation; however, this study adopts the maximum likelihood estimation technique in order to achieve the third objective of this thesis. The maximum likelihood estimation technique is one of the widely used methods in estimating parameters of a model, because of its desirable properties under certain general conditions (Nasiru, 2018a).

The algorithm selects the set of values of the model parameters that maximizes the likelihood function; it also gives a unified approach to estimation. That is, it helps provide the maximum information about the properties of the estimated parameters.

The likelihood function, which is an essential and integral part of the MLE is defined as the joint density, $f(X|\theta) = \prod_{i=1}^n f(X_i; \theta)$, as a function of the parameters θ . Let us consider X as a random variable, with PDF $f(x_i; \theta)$, where $i = 1, 2, \dots, n$. and θ is unknown parameter with $x_1, x_2, x_3, \dots, x_n$ as the observed values. The likelihood function of the sample as presented in (3.7) was arrived at by multiplying the probabilities of independent events;

$$l(\theta|X) = \prod_{i=1}^n f(X_i; \theta) \quad (3.7)$$

Thus, log-likelihood function $L(\theta)$, is also arrived at by taking natural logarithm of equation (3.7). That is,

$$L(\theta|X) = \ln \left[\prod_{i=1}^n f(X_i; \theta) \right] \quad (3.8)$$



The likelihood function attains its maximum at a specific value of the parameters. Since logarithm is a monotone function, the maximization of equation (3.7) is the same as the maximization of the equation (3.7), and vice versa.

The maximum likelihood estimates for the parameters are obtained by solving the system of log-likelihood equations in (3.9). That is, a point estimate is chosen such that the value $\hat{\theta}$ maximizes $L(\theta)$. That is

$$\frac{\partial}{\partial \theta_i} L(\theta | x_1, x_2, x_3, \dots, x_n) = 0, i = 1, 2, 3, \dots, k. \quad (3.9)$$

3.4.1 Properties of Maximum Likelihood Estimators

This subsection explains some important (desirable) properties of the maximum likelihood estimators which make it more attractive. Also, we used these properties of the MLE in examining the behaviour of the MLE based on the Monte Carlo simulation conducted in chapter four.

3.4.1.1 Consistency

An estimator is said to be consistent when the value of $\hat{\theta}$ converges in probability to the true value as the sample size get infinitely large. Consider X_1, X_2, \dots, X_n which are independent identically distributed (iid) random sample from a population X with density function $f(x, \theta)$. If $\hat{\theta}$ is an estimator based on n observations, then it is said to be consistent if the probability of making an error of any size ε , tends to zero as n tends to infinity. This is written mathematically as



$$\lim_{n \rightarrow \infty} P(|\hat{\theta}_n - \theta| \geq \varepsilon) = 0, \quad (3.10)$$

for any $\varepsilon > 0$.

In the nutshell, an estimator $\hat{\theta}_n$ based on the sample size n is consistent for θ if and only if the following theorem holds (Ofosu et al., 2016)

$$\lim_{n \rightarrow \infty} E(\hat{\theta}_n) = \theta \text{ and } \lim_{n \rightarrow \infty} V(\hat{\theta}_n) = 0. \quad (3.11)$$

This indicates that the estimator converges to the true parameter values as the sample size increases.

3.4.1.2 Asymptotic Normality

The distribution of the estimator converges to a multivariate normal variate as the sample size increases. Hence

$$\sqrt{n}(\hat{\theta}_n - \theta) \xrightarrow{Dist} N(\mathbf{0}, I^{-1}(\theta)) \quad (3.12)$$

where $\mathbf{0}$ is a K -dimensional mean zero vector, \xrightarrow{Dist} represents convergence in distribution and, $I(\theta)$ is the $K \times K$ dimensional Fisher information matrix, which is represented as the negative expectation of the second partial derivative matrix of the log-likelihood function evaluated at the true parameter (see, Nasiru, 2018). That is,

$$I(\theta) = -E \left[\frac{\partial^2 f(x|\theta)}{\partial \theta \partial \theta'} \right] = - \int_{-\infty}^{\infty} \left[\frac{\partial^2 f(x|\theta)}{\partial \theta \partial \theta'} \right] f(x) dx. \quad (3.13)$$



The inverse of the Fisher information matrix yields the variance-covariance matrix of parameter θ .

3.4.1.3 Asymptotic Efficiency

Whenever there is more than one consistent estimator in a class of unbiased estimators, there is the need to compare those estimators and select the one with the least variance. The estimator with the least variance in this class of unbiased estimators is known as the most efficient. The maximum likelihood estimators are asymptotically most efficient. Mathematically, if there are alternative unbiased estimator $\hat{\theta}$, such that

$$\sqrt{n}(\hat{\theta}_n - \theta) \xrightarrow{Dist} N(\mathbf{0}, I^{-1}(\Omega)), \quad (3.14)$$

then $I^{-1}(\Omega) \geq I^{-1}(\theta)$ always.

3.4.1.4 Invariance Property

Another desirable property of the method of maximum likelihood is its invariance to one-to-one transformations of the parameters of the log-likelihood.

Suppose that $f(\theta)$ is a differentiable function, then the maximum likelihood estimator of $f(\theta)$ is equal to the function evaluated at the maximum likelihood estimator of $f(\theta)$. This means that if $\hat{\theta}$ is the maximum likelihood estimator of θ , then $f(\hat{\theta})$ is the maximum likelihood estimator of $f(\theta)$, and further

$$\sqrt{n}(f(\hat{\theta}) - f(\theta)) \xrightarrow{Dist} \left(0, \left[\frac{\partial f(\theta)}{\partial \theta} \right] I^{-1}(\theta) \left[\frac{\partial f(\theta)}{\partial \theta} \right]' \right). \quad (3.15)$$



3.5 Information Matrix and Confidence Intervals

In order to determine the likely range within which our estimates lie, and to be confident about that, we computed the confidence interval by making the use of the estimated values and the information matrix.

A 95% confidence interval is indicative that we are 95% certain that the true value of the population falls within a given range of values (lower and upper values).

Consider the following $\omega_1, \omega_2, \dots, \omega_n$ as the parameters of the distribution and $\Sigma_{11}, \Sigma_{22}, \dots, \Sigma_{kk}$ as their respective variances. Making use of the multivariate normal approximation, the approximate $100(1 - \alpha)\%$ confidence intervals for the parameters are estimated as:

$$\omega_1 \in \hat{\omega}_1 \pm z_{\alpha/2} \sqrt{\Sigma_{11}}, \omega_2 \in \hat{\omega}_2 \pm z_{\alpha/2} \sqrt{\Sigma_{22}}, \dots, \omega_k \in \hat{\omega}_k \pm z_{\alpha/2} \sqrt{\Sigma_{kk}}, \quad (3.16)$$

where $z_{\alpha/2}$ is the upper half percentile of the standard normal.

3.6 Optimization Technique

The maximum likelihood estimates of the special distributions (T-TIGER, T-TIGEW, T-TIGEFr, T-TIGEEE and T-TIGEL) parameters are obtained using the independent works of Broyden (1970), Fletcher (1970), Goldfarb (1970) and Shanno (1970) collectively known as the BFGS algorithm. The BFGS algorithm has iterative approach for finding solution to unconstrained optimization problems.

This technique was applied to maximize the MLE by using the subroutine `mle2` and the `bbmle` package in R (R version 3.6.2) which uses a wide range of



initial values. The *bbmle* is an R in-built package, named after its developer Bolker (2017).

The iterative processes of the algorithm may lead to more than one maximum value, thus in such cases, the largest maxima is chosen as the maximum likelihood estimate. In cases where no maximum value is identified for the chosen initial values, a new set of initial values are used and the optimization is repeated until a maximum is obtained.

3.7 Monte Carlo Simulation Study

The Monte Carlo simulation is a technique that makes use of repeated random sampling in order to study properties of a statistic's sampling distribution and its behaviour. In other words, a Monte Carlo approach is a general tool for conducting and analyzing the behaviour of MLE since the process can be too complex for analytic manipulation. This technique helps to address our fifth objective of the study. That is, the Monte Carlo study was conducted to examine the performance (stability of point estimates) of MLE of the special models by conducting various simulations for different sample sizes and different parameter values. The quantile function of each of the special models was used to generate the random data.

That is, the Monte Carlo was conducted to study the behaviour of the properties of the estimators of the various special distributions. The Monte Carlo Simulation steps are as follows:

Step1: Specify the sample size and values of the parameters;

Step2: Generate the random samples of size $n= 25, 50, 75$ and 100 from the



special distributions of T-TIGE generator using their respective quantile functions;

Step3: Find the maximum likelihood estimates for the parameters

Step4. Repeat steps 2-3 for N=1000 times.

The average bias (AB) of the MLE $\hat{\phi}_i$ ($\hat{\phi}_i = \alpha, \beta, \theta, \lambda, \gamma$) parameter is defined as

$$AB = \frac{1}{N} \sum_{i=1}^n (\hat{\phi}_i - \phi), \quad (3.17)$$

Also, the root mean square errors (RMSE) of the MLE $\hat{\phi}_i$ of the estimated parameters are defined in equation (3.18) as follows:

$$RMSE = \sqrt{\frac{1}{N} \sum_{i=1}^n (\hat{\phi}_i - \phi)^2}. \quad (3.18)$$

An RMSE is bounded by zero and a lower value of RMSE indicates a better fit.

3.8 Model Selection Criteria

The goal of the real-life application with regard to modeling is to select the most appropriate model from the competing models. To accomplish this, various statistical tests such as the goodness of fit and information loss criteria tests were conducted.



3.8.1 Goodness of Fit Tests

In order to test whether a given random variable comes from a specified distribution, we employed the goodness-of-fit tests. These tests include the Cramér-von Mises test (W^*), the Kolmogorov-Smirnov (K-S) and Anderson-Darling (A^*) tests.

The goodness of fit statistic K-S , W^* and A^* were tabulated and used as an analytical tool for establishing the best fitting model for the particular dataset in question. As a rule of thumb, the smaller values of A^* , K-S and W^* give a better distributional fit.

3.8.2 The Kolmogorov-Smirnov Test

The K-S test (Kolmogorov, 1933; Smirnov, 1939) was used to decide if a random sample $x_1, x_2, x_3, \dots, x_n$ comes from a population with a given distribution. That is, K-S test is based on the empirical distribution function. The test statistic measures the distance between the empirical distribution function, $F_n(x)$ of the given sample and the estimated cumulative distribution function of the candidate (theoretical) distribution, $F^*(x)$.

The null and the alternative hypotheses in relation to the K-S test stated as follows:

H_0 : the data do not follow a specified distribution

H_1 : the data follow a specified distribution.

The test statistic of the K-S is defined as;



$$K-S \text{ test} = \text{Max}_{1 \leq i \leq n} \left[F^*(x) - \frac{i-1}{n}, \frac{1}{n} - F^*(x) \right]. \quad (3.19).$$

3.8.3 Cramér-von Mises Test

This test was also employed to judge the goodness of fit of a cumulative distribution function compared to a given distribution function. When comparing the models, the one with the least value of the test statistic, W^* is usually the best. Let $x_1, x_2, x_3, \dots, x_n$ be the observed values in a random sample of size n of X in increasing (that is, ascending) order. The test statistic is given by

$$W^* = n\omega^2 = \sum_{i=1}^n \left[\frac{2i-1}{2n} - F(x_i) \right]^2 + \frac{1}{2n} \quad (3.20)$$

where
$$\omega^2 = \int_{-\infty}^{\infty} [F_n(x) - F^*(x)]^2 \partial F^*(x). \quad (3.21)$$

$F^*(x)$ and $F_n(x)$ are the theoretical and the empirically observed distributions respectively.

The Cramér-von Mises test is most of the time, considered as an alternative to the Kolmogorov-Smirnov (K-S) test.

3.8.4 Anderson-Darlings

The Anderson Darlings (A^*) test is a modification of the Cramér-von Mises test. This test gives more weight to the tails than the K-S test. The A^* test statistic is computed as:

$$A^* = -n - \sum_{i=1}^n \left[\frac{2i-1}{n} \left(\log(1 - F\tilde{x}_{n-i+1}) + \log(F(\tilde{x}_i)) \right) \right], \quad (3.22)$$



where $\tilde{x}_1 < \tilde{x}_2 < \tilde{x}_3 < \dots < \tilde{x}_n$ is the sorted data (ordered statistics) and $(F(\tilde{x}_i))$ is the cumulative distribution function of the specified model, the A* test can detect differences between models over their entire width. One drawback of this test is that the model of the test statistic depends on the specific distribution being tested, so no general expression can be given.

3.9 Information Criteria

This study uses the following frequently used information criteria: the Akaike Information Criterion, the Corrected the Akaike Information Criterion, and Bayesian Information Criterion.

The information criterion selects model with smaller values of AIC, AICc, and BIC for a given set of candidate models and specified data set.

3.9.1 The Akaike Information Criterion

This is one of the many benchmarks used in selecting the relatively better statistical models for a given data set. The Akaike information criterion (AIC), named after its developer Akaike (1973, 1974), is a measure of the quality of each model, relative to each of the other models. AIC quantifies information lost when the data generating process is represented by a statistical model by obtaining equilibrium in the trade-off between goodness-of-fit of the model and its complexity. It thus provides a means for model selection. The AIC value of the test statistic is defined as follows:

$$AIC = 2k - 2l(\hat{\theta}), \quad (3.23)$$



where k the number of estimated parameters for the model. The preferred model to be selected is the one with the minimum AIC value from a given set of candidate models for a given data set. Thus, AIC is better candidate for the goodness-of-fit (as assessed by the likelihood function), but it also includes a penalty that is an increasing function of the number of parameters (k). This penalty helps to discourage over fitting of a model, since increasing the k in the model always improves the goodness-of-fit. That is with relatively large sample size, the AIC improves the model selection. However, its limitation is exposed with relatively small sample size and biasedness.

3.9.2 The Corrected Akaike Information Criterion

The disadvantages inherent in the AIC in terms of sample size, large number of k in the model, and biasedness has led to the development of the Corrected Akaike Information Criterion (AICc) as a further improvement to overcome these challenges and improve upon it (Sugiura, 1978; Hurvich and Tsai, 1989).

The test statistic of AICc is defined as follows;

$$AICc = AIC + \frac{2k(n+1)}{n-(k+1)}. \quad (3.24)$$

3.9.3 Bayesian Information Criterion

The Bayesian Information Criterion (BIC) also known as the Schwartz Bayesian Criterion (SBC) was also developed by Schwartz (1978) by approximating the Bayes factor on the assumption that the data is independent and identically distributed. The test statistic is given as

$$BIC = k \ln(n) - 2 \ln(\hat{\theta}), \quad (3.25)$$



where, n is the sample size and $\ln l(\hat{\theta})$ is natural log of the likelihood function.

The BIC has the power to penalize models with many parameters compared to the AIC and AICc in both large and small samples.

It is therefore important to use the BIC together with AIC and AICc when selecting a best model among competing model (Nasiru, 2018).

3.10 Total Time on Test Transform.

Total time on test transform (TTT-transform), developed by Barlow and Doksum (1972) provides avenue for researchers to graphically view the shape of the hazard rate function. The TTT-transform is defines as:

$$H^{-1}(x) = \int_0^{G^{-1}(x)} R(x)dx, x \in [0,1], \quad (3.26)$$

where, $R(x) = 1 - G(x)$ is the reliability (survival) function. Refer to (Barlow and Doksum, 1972; Arset, 1987) for more detail.

The scaled TTT-transform is calculated using the relation

$$\psi(p) = \frac{H^{-1}(p)}{H^{-1}(1)}. \quad (3.27)$$

The curve $\psi(p)$ versus $0 \leq p \leq 1$ is called the TTT-transform curve. The TTT-transform can help to identify the various shapes of a hazard rate function, either it is the upside down bathtub or unimodal shape (Barlow and Doksum, 1972; Nasiru et al., 2017). For instance, a hazard rate function is



upside down bathtub or unimodal shape if the TTT-transform curve is first concave above the 45 degrees line and then convex below the 45 degrees line.

Let us consider an ordered sample $X_{1:n}, X_{2:n}, X_{3:n} \dots \dots X_{n:n}$, with the TTT statistics as:

$$TTT_i = \sum_{j=1}^i (n-j+1)(x_{j:n} - x_{j-1:n}), i = 1, 2, 3, \dots, n. \quad (3.28)$$

The empirical scaled TTT-transform is given by

$$G(r/t) = \frac{TTT_i}{TTT_n}, \quad (3.29)$$

where $0 \leq G(r/t) \leq 1$. In the nutshell, the empirical TTT-transform curve is

obtained by plotting $\frac{i}{n}$ versus $G(r/t) = \left[\left(\sum_{i=1}^r y_{(i)} \right) + (n-1)y_{(r)} \right] / \sum_{i=1}^n y_{(i)}$

against r/n , where $r = 1, 2, \dots, n$ and $y_{(i)}$ ($i = 1, 2, \dots, n$) are the order statistics of the sample.

3.11 Data used and Sources

This section highlights on the different datasets that were used and their sources. Different datasets were used to demonstrate applications of the special models. The sources of these datasets are secondary data from articles and journals. These tried and tested datasets

The flexibility of the T-TIGE model was demonstrated by using the first three datasets for the T-TIGER model. The first data set relates to monthly tax



revenue obtained from Nassar and Nada (2011). It is recently studied by Klakattawi (2019). The dataset are given in Appendix A1.

The second dataset relates to the waiting times between sixty-five consecutive eruptions of a blowhole, called the Kiamo Blowhole (Pinho et al., 2012) was also used to demonstrate the usefulness of the T-TIGEW distribution. The Kiamo Blowhole is a tourist attraction located nearly 120km to the south of Sydney, Australia. The data set are given in Appendix A2.

The third data set used is called the Applied Life, emanates from the analyses on the time to breakdown of an insulating fluid at a voltage of 34 kV. The dataset was initially from the works of Nelson (1982) and were later used by Abbas and Tang (2015). This dataset is represented in an Appendix 3.

In order to examine the flexibility of the special model known as the Transmuted Type I General Exponential Weibull (T-TIGEW) distribution, the aircraft windshield failure dataset was used in the analysis. This dataset relates to failure time. This dataset was recently used by Nasir et al (2019), and had been previously studied by Ibrahim et al. (2017), Tahir et al. (2015), Ramos et al. (2013) and Murthy et al. (2004) among others. The data set consist of 85 failed windshields and it is presented in an Appendix B.

Another dataset that was used is called the rainfall dataset which was obtained from the work of Mansoor et al. (2016). This dataset was also used in the analysis to determine the flexibility of the special model known as the the Transmuted Type I General Exponential Fréchet (T-TIGEFr) model. This dataset is displayed in an Appendix C1.



An Appendix C2 displayed uncensored dataset from the work of Nichols and Padgett (2006) which was also used to demonstrate the flexibility of T-TIGEFr model of the new generator. The dataset gives one hundred (100) data-points on breaking stress of carbon fibres (in Gba). This dataset is recently used by Mahmoud and Mandouh (2013).

The seventh dataset called the fiber strength was used to examine the performance of the of T-TIGEFr model of the proposed T-TIGE family. This dataset was taken from the work of Selim and Badr (2016). It is a fibre strength data originally considered by Badar and Priest (1982). It is represented in Appendix D.



CHAPTER FOUR

THEORETICAL RESULTS

4.1 Introduction

This chapter presents the results of the first five objectives of the studies. This include the T-TIGE generator, the statistical properties and the estimators of the T-TIGE generator. Five (5) special models of the T-TIGE family were also derived. The chapter further presents the results of the Monte Carlo Simulation.

4.2 The T-TIGE Family of Distributions

A random variable X is said to follows the T-TIGE family if it's CDF has the form:

$$T(x; \boldsymbol{\varphi}) = e^{\lambda(1-H(x;\boldsymbol{\varphi}))^{-\alpha}} \left(1 + \gamma - \gamma e^{\lambda(1-H(x;\boldsymbol{\varphi}))^{-\alpha}} \right), \quad x \in R, \quad (4.1)$$

where the shape, scale and the transmutation parameters are respectively $\alpha > 0$, $\lambda > 0$ and $|\gamma| \leq 1$. The $\boldsymbol{\varphi} = (\boldsymbol{\varphi}_k) = (\varphi_1, \varphi_2, \dots)$ is a vector parameter.

The CDF of T-TIGE family was arrived at by substituting the TIGE generator into the QRTM generator.

The corresponding PDF of the T-TIGE was obtained by differentiating the CDF of T-TIGE hence the PDF is given as:

$$t(x; \boldsymbol{\varphi}) = \lambda \alpha h(x; \boldsymbol{\varphi}) H(x; \boldsymbol{\varphi})^{-(\alpha+1)} e^{\lambda(1-H(x;\boldsymbol{\varphi}))^{-\alpha}} \left(1 + \gamma - 2\gamma e^{\lambda(1-H(x;\boldsymbol{\varphi}))^{-\alpha}} \right). \quad (4.2)$$



$H(x; \varphi)$ and $h(x; \varphi)$ are CDF and PDF of arbitrary baseline distribution respectively. Henceforth, the study write simply $T(x; \varphi) = T(x)$ and $t(x; \varphi) = t(x)$.

The T-TIGE family of distributions appears to be more flexible and could be used for modeling various types of data. The T-TIGE families of distributions can also very useful models in characterizing failure time of a given system because of its analytical structure.

As a result of equation (4.1) and (4.2), the survival function $S(x)$, (also refers to as the reliability function) defines the probability that an entity or system or an individual will survive beyond a specified time. In other words, it is the probability of an item not failing prior to some specified time. The usefulness of the survival function is paramount in many fields of studies including the actuarial science. For instance, in life contingencies, there is always the need to calculate the probability that an individual will survive to a certain age. The reliability or survival function for the T-TIGE family is defined as:

$$S(x) = 1 - e^{-\lambda(1-H(x))^{-\alpha}} \left(1 + \gamma - \gamma e^{\lambda(1-H(x))^{-\alpha}} \right).$$

The hazard rate function is yet another useful characteristic of interest, which is also known as instantaneous

failure rate is defined as $Z(x) = \frac{t(x)}{[1-T(x)]}$, which is an important quantity

characterizing life phenomenon. The instantaneous failure (hazard) rate function of the T-TIGE family is defined as



$$Z(x) = \frac{\lambda \alpha h(x) H(x)^{-(\alpha+1)} e^{\lambda(1-H(x)^{-\alpha})} \left(1 + \gamma - 2\gamma e^{\lambda(1-H(x)^{-\alpha})}\right)}{1 - e^{\lambda(1-H(x)^{-\alpha})} \left(1 + \gamma - \gamma e^{\lambda(1-H(x)^{-\alpha})}\right)}.$$

4.2.1 Mixture Representation

This section provides the mixture representation for the PDF of the T-TIGE which can be used to study the mathematical characteristics of this new generator (Nasiru, 2018b).

Lemma 4.1. The PDF of the T-TIGE family can be expressed as a mixture

representation in terms of the density as: $t(x) = \lambda \alpha \sum_{i=0}^{\infty} \sum_{j=0}^{\infty} \sum_{k=0}^j C_{ijk} h(x) H(x)^k$.

where $C_{ijk} = \binom{\alpha(i+1)+j}{j} \binom{j}{k} \left(\frac{(1+\gamma)e^{\lambda}(-1)^i \lambda^i}{i!} - \frac{2\gamma e^{2\lambda}(-1)^i (2\lambda)^i}{i!} \right)$.

Proof. The PDF of T-TIGE family, that is equation (4.2), could be written as

$$t(x) = \lambda \alpha h(x) H(x)^{-(\alpha+1)} \left((1+\gamma) e^{\lambda} e^{-\lambda H(x)^{-\alpha}} - 2\gamma e^{2\lambda} e^{-2\lambda H(x)^{-\alpha}} \right).$$

Using the expansion, $e^{-\lambda H(x)^{-\alpha}} = \sum_{i=0}^{\infty} \frac{(-1)^i \lambda^i H(x)^{-\alpha i}}{i!}$, the PDF of the T-TIGE

becomes

$$t(x) = \lambda \alpha h(x) H(x)^{-(\alpha+1)} \left[(1+\gamma) e^{\lambda} \sum_{i=0}^{\infty} \frac{(-1)^i \lambda^i H(x)^{-\alpha i}}{i!} - 2\gamma e^{2\lambda} \sum_{i=0}^{\infty} \frac{(-1)^i (2\lambda)^i H(x)^{-\alpha i}}{i!} \right]$$

and with simplification, gives

$$t(x) = \lambda \alpha h(x) H(x)^{-(\alpha+1)} \sum_{i=0}^{\infty} H(x)^{-\alpha i} \left(\frac{(1+\gamma) e^{\lambda} (-1)^i \lambda^i}{i!} - \frac{2\gamma e^{2\lambda} (-1)^i (2\lambda)^i}{i!} \right).$$



Further simplification leads to

$$t(x) = \lambda \alpha h(x) H(x)^{-(\alpha+1)} \sum_{i=0}^{\infty} H(x)^{-[(\alpha+i)+1]} \left(\frac{(1+\gamma)e^{\lambda}(-1)^i \lambda^i}{i!} - \frac{2\gamma e^{2\lambda}(-1)^i (2\lambda)^i}{i!} \right).$$

But $H(x)^{-[(\alpha+i)+1]} = [1 - (1 - H(x))]^{-[(\alpha+i)+1]}$, and using the negative binomial

expansion; $(1-b)^{-\eta} = \sum_{j=0}^{\infty} \binom{\eta+j-1}{j} b^j, |b| \leq 1,$

which gives

$$t(x) = \lambda \alpha h(x) H(x)^{-(\alpha+1)} \sum_{i=0}^{\infty} \sum_{j=0}^{\infty} \binom{\alpha(i+1)+1+j-1}{j} [1-H(x)]^j \left(\frac{(1+\gamma)e^{\lambda}(-1)^i \lambda^i}{i!} - \frac{2\gamma e^{2\lambda}(-1)^i (2\lambda)^i}{i!} \right)$$

and this leads to the expression;

$$t(x) = \lambda \alpha h(x) H(x)^{-(\alpha+1)} \sum_{i=0}^{\infty} \sum_{j=0}^{\infty} \binom{\alpha(i+1)+j}{j} \binom{j}{k} H(x)^k \left(\frac{(1+\gamma)e^{\lambda}(-1)^i \lambda^i}{i!} - \frac{2\gamma e^{2\lambda}(-1)^i (2\lambda)^i}{i!} \right)$$

hence, $t(x) = \lambda \alpha \sum_{i=0}^{\infty} \sum_{j=0}^{\infty} \sum_{k=0}^j C_{ijk} h(x) H(x)^k$. This completes the proof.



4.3 Statistical Properties of T-TIGE Family

This section focuses on the statistical properties of the T-TIGE family. These include: quantile functions, moments, moment generating function, incomplete moments, inequality measures, mean residual life, stochastic ordering and order statistics.

4.3.1 The Quantile Function

The quantile function which helps in generating other statistical properties was derived for further analyses. The quantile function is another way of describing a probability distribution. It can also be called the inverse CDF. It can be used to generate random samples for probability and thereby can serve as an alternative to the PDF.

Lemma 4.2. For a nonnegative continuous random variable X that follows the T-TIGE family of distributions, the quantile function $Q(u)$ for a unit interval, $u \in (0,1)$ is given by

$$x_{(u)} = H^{-1} \left[1 - \frac{1}{\lambda} \ln \left(\frac{(\gamma + 1) + \sqrt{(\gamma + 1)^2 - 4\gamma u}}{2\gamma} \right) \right]^{\frac{1}{\alpha}}, u \in [0,1]$$

where $H^{-1}(\cdot)$ is the inverse of the random variable X of the baseline CDF of T-TIGE family.



Proof. For any $u \in (0,1)$, where u follows a uniform distribution, the quantile function is obtained by solving $u = T(x)$, $x > 0$, with respect to x , which is

$$(1 + \gamma)e^{\lambda(1-H(x))^{-\alpha}} - \gamma e^{2\lambda(1-H(x))^{-\alpha}} = u, \text{ and this leads to}$$

$\gamma e^{2\lambda(1-H(x))^{-\alpha}} - (1 + \gamma)e^{\lambda(1-H(x))^{-\alpha}} + u = 0$. Using the concept of quadratic equation gives

$$e^{\lambda(1-H(x))^{-\alpha}} = \frac{(\gamma + 1) + \sqrt{(\gamma + 1)^2 - 4\gamma u}}{2\gamma}.$$

Expressing $H(x)$ in terms of λ, μ, γ and α gives

$$H(x) = \left[1 - \frac{1}{\lambda} \ln \left(\frac{(\gamma + 1) + \sqrt{(\gamma + 1)^2 - 4\gamma u}}{2\gamma} \right) \right]^{-\frac{1}{\alpha}},$$

$$\text{Hence } x_{(u)} = H^{-1} \left[1 - \frac{1}{\lambda} \ln \left(\frac{(\gamma + 1) + \sqrt{(\gamma + 1)^2 - 4\gamma u}}{2\gamma} \right) \right]^{-\frac{1}{\alpha}}.$$

This completes the proof.

By using Lemma (4.2), the first quantile, median and upper quantile of the T-TIGE family are obtained when $u = 0.25$, $u = 0.5$ and $u = 0.75$ respectively.

4.3.2 Moments

The moment of a random variable X is the expectation of the r^{th} power of the random variable. The moment plays important roles when establishing the measures of central tendencies, measures of dispersion, and shapes of the



distribution of the random variable. The following proposition gives the r^{th} moment of the T-TIGE family.

Proposition 4.1. The r^{th} ordinary moment of a T-TIGE family of distributions is given

$$\text{by } \mu'_r = \lambda \alpha \sum_{i=0}^{\infty} \sum_{j=0}^{\infty} \sum_{k=0}^j C_{ijk} \int_{-\infty}^{\infty} x^r h(x) H(x)^k dx, \quad r = 1, 2, \dots.$$

where

$$C_{ijk} = \binom{\alpha(i+1)+j}{j} \binom{j}{k} \left(\frac{(1+\gamma)e^\lambda (-1)^i \lambda^i}{i!} - \frac{2\gamma e^{2\lambda} (-1)^i (2\lambda)^i}{i!} \right)$$

Proof. By definition, the r^{th} moment is given as

$$\mu'_r = E(X^r) = \int_{-\infty}^{\infty} x^r t(x) dx. \quad (4.3)$$

By substituting Lemma 4.1 into equation (4.3), and further simplification,

$$\text{yields } \mu'_r = \lambda \alpha \sum_{i=0}^{\infty} \sum_{j=0}^{\infty} \sum_{k=0}^j C_{ijk} \int_0^{\infty} x^r h(x) H(x)^k dx. \text{ This completes the proof.}$$

Setting $r = 1$ in equation (4.3) gives the mean of the random variable X .

4.3.3 Moment Generating Function

The moment generating function (MGF) is a very important statistical concept which is used among others to find moments of a given random variable.



Proposition 4.2. The MGF, of the T-TIGE family is given by

$$M_X(t) = \lambda\alpha \sum_{r=0}^{\infty} \sum_{i=0}^{\infty} \sum_{j=0}^{\infty} \sum_{k=0}^j \frac{C_{ijk}}{r!} \int_{-\infty}^{\infty} x^r h(x) H(x)^k dx.$$

where $C_{ijk} = \binom{\alpha(i+1)+j}{j} \binom{j}{k} \left(\frac{(1+\gamma)e^\lambda (-1)^i \lambda^i}{i!} - \frac{2\gamma e^{2\lambda} (-1)^i (2\lambda)^i}{i!} \right)$.

Proof. By definition, the MGF is given as:

$$M_X(t) = E[e^{tX}]. \tag{4.4}$$

Using the series expansion, $e^{tX} = 1 + tX + \frac{(tX)^2}{2!} + \frac{(tX)^3}{3!} + \dots + \frac{(tX)^n}{n!}$,

and substituting it into the equation (4.4), and with some algebraic

manipulation gives $M_X(t) = \sum_{r=0}^{\infty} \frac{t^r}{r!} \mu'_r$, which finally results to

$$M_X(t) = \lambda\alpha \sum_{r=0}^{\infty} \sum_{i=0}^{\infty} \sum_{j=0}^{\infty} \sum_{k=0}^j \frac{C_{ijk}}{r!} \int_{-\infty}^{\infty} x^r h(x) H(x)^k dx, \text{ which completes the proof.}$$

4.3.4 Incomplete Moment

The incomplete moment as a statistical property is a foundation for measuring inequalities. For instance, Income quantile and Lorenz as well as Bonferroni curves. Clearly these curves rely on the first incomplete moment of the distribution.

Proposition 4.3. The r^{th} incomplete moment of the T-TIGE family is given by

$$m_r(t) = \lambda\alpha \sum_{i=0}^{\infty} \sum_{j=0}^{\infty} \sum_{k=0}^j C_{ijk} \int_0^t x^r h(x) H(x)^k dx.$$



where $C_{ijk} = \binom{\alpha(i+1)+j}{j} \binom{j}{k} \left(\frac{(1+\gamma)e^\lambda (-1)^i \lambda^i}{i!} - \frac{2\gamma e^{2\lambda} (-1)^i (2\lambda)^i}{i!} \right)$.

Proof. The incomplete moment of a random variable X is defined as

$$m_r(t) = \int_0^t x^r t(x) dx. \tag{4.5}$$

Using the mixture representation of the PDF of the T-TIGE family, and substitute it into equation (4.5), yields

$$m_r(t) = \int_0^t x^r \lambda \alpha \sum_{i=0}^{\infty} \sum_{j=0}^{\infty} \sum_{k=0}^j C_{ijk} h(x) H(x)^k dx.$$

Thus, $m_r(t) = \lambda \alpha \sum_{i=0}^{\infty} \sum_{j=0}^{\infty} \sum_{k=0}^j C_{ijk} \int_0^t x^r h(x) H(x)^k dx$. This completes the proof.

4.3.5 Inequality Measures

The concept of inequality measure as a statistical property is concerned with disparity of a certain metric such as income level within a distribution. It is an important characteristic of non-negative distributions. An important application of the inequality curves is that they can be used to define some ordering. Such ordering allows the comparison of distributions in terms of inequality (Arcagni and Porro, 2014). The most popular measuring technique in literature for measuring the income inequality of a given distribution are the Lorez and Bonferroni curves (Nasiru, 2018b).



4.3.5.1 Lorenz Curve

Developed by Lorenz (1905), Lorenz curve $L_{G(t)}$ is a graphical representation of the cumulative income distribution. Thus, the Lorenz index shows the level of inequality in the wealth distribution.

The Lorenz curve of the T-TIGE family of distribution was developed by compounding the first moment and the PDF of each distribution.

Proposition 4.4. The Lorenz curve of the T-TIGE family is

$$L_{G(t)} = \frac{\lambda\alpha}{\mu} \sum_{i=0}^{\infty} \sum_{j=0}^{\infty} \sum_{k=0}^j C_{ijk} \int_{-\infty}^t x \cdot h(x) H(x)^k dx.$$

$$\text{where } C_{ijk} = \binom{\alpha(i+1)+j}{j} \binom{j}{k} \left(\frac{(1+\gamma)e^\lambda (-1)^i \lambda^i}{i!} - \frac{2\gamma e^{2\lambda} (-1)^i (2\lambda)^i}{i!} \right).$$

Proof. By definition, the Lorenz function is defined as

$$L_{G(t)} = \frac{1}{\mu} \int_{-\infty}^t x f(x) dx. \tag{4.6}$$

but $\int_{-\infty}^t x f(x) dx$ is the first incomplete moment, and using Lemma 4.2, yields

$$L_{G(t)} = \frac{\lambda\alpha}{\mu} \sum_{i=0}^{\infty} \sum_{j=0}^{\infty} \sum_{k=0}^j C_{ijk} \int_{-\infty}^t x \cdot h(x) H(x)^k dx. \quad \text{Thus, complete the proof.}$$

4.3.5.2 Bonferroni Curve

The Bonferroni curve of the T-TIGE family which is a graphical representation that compares the lower group with the total mean was derived by compounding the various elements and the CDF of the T-TIGE family of



distributions. The Bonferroni curve was proposed and studied by Bonferroni (1930) as a measure of income inequality based on partial means.

Proposition 4.5 If $X \sim T-TIGE(\alpha, \beta, \theta, \gamma, \lambda)$, then the Bonferroni index of

the T-TIGE family is given by $B_{F(t)} = \frac{\lambda\alpha}{\mu F(t)} \sum_{i=0}^{\infty} \sum_{j=0}^{\infty} \sum_{k=0}^j C_{ijk} \int_{-\infty}^t x h(x) H(x)^k dx$.

where $C_{ijk} = \binom{\alpha(i+1)+j}{j} \binom{j}{k} \left(\frac{(1+\gamma)e^\lambda (-1)^i \lambda^i}{i!} - \frac{2\gamma e^{2\lambda} (-1)^i (2\lambda)^i}{i!} \right)$.

Proof. Bonferroni index is by definition given as:

$$B_{F(t)} = \frac{L_{F(t)}}{F(t)}. \quad (4.7)$$

Substituting Proposition 4.4 into equation (4.7) yields

$$B_{F(t)} = \frac{\lambda\alpha}{\mu F(t)} \sum_{i=0}^{\infty} \sum_{j=0}^{\infty} \sum_{k=0}^j C_{ijk} \int_{-\infty}^t x h(x) H(x)^k dx. \quad \text{This completes the proof.}$$

4.3.6 Mean Residual Life

The mean residual life function is an important statistical property of interest. It indicates the average remaining survival time that a population (or an item) has survived beyond t . It has many applications in the field of applied statistics, for instance, its usage is relevant in the field of survival analysis, life insurance, quality control and so on.

Proposition 4.6. The mean residual life of the T-TIGE family is given as

$$\rho_x(t) = \frac{1}{S(t)} \left[\mu - \lambda\alpha \sum_{i=0}^{\infty} \sum_{j=0}^{\infty} \sum_{k=0}^j C_{ijk} \int_{-\infty}^t x \cdot h(x) H(x)^k dx \right] - t.$$



where $C_{ijk} = \binom{\alpha(i+1)+j}{j} \binom{j}{k} \left(\frac{(1+\gamma)e^\lambda (-1)^i \lambda^i}{i!} - \frac{2\gamma e^{2\lambda} (-1)^i (2\lambda)^i}{i!} \right)$.

Proof. By definition, the mean residual life is defined as

$$\begin{aligned} \rho_x(t) &= E[X - t / X > t] \\ &= \frac{\int_t^\infty (x-t) f(x) dx}{1-F(t)} \\ &= \frac{\mu'_t - \int_t^\infty xf(x) dx}{1-F(t)} - t, \quad t > 0. \end{aligned} \tag{4.8}$$

This leads to

$$\rho_x(t) = \frac{1}{S(t)} \left[\mu'_t - \int_{-\infty}^t xf(x) dx \right] - t.$$

and hence,

$$\rho_x(t) = \frac{1}{S(t)} \left[\mu - \lambda\alpha \sum_{i=0}^\infty \sum_{j=0}^\infty \sum_{k=0}^j C_{ijk} \int_{-\infty}^t x \cdot h(x) H(x)^k dx \right] - t.$$

This completes the proof.

4.3.7 Stochastic Ordering Property

This is a statistical concept that helps to quantify one random variable being bigger than another. It shows an ordering mechanism in lifetime distribution.

It is useful for comparison of probabilistic models in different areas such as reliability, survival analysis, risk management and finance. It is also an essential tool in the study of structural properties of complex stochastic



systems. Stochastic ordering thus provides important guide for decision making under uncertainty.

A random variable X_1 is said to be stochastically smaller than a random variable X_2 in the:

- i. stochastic order ($X_1 \leq_{st} X_2$) if the associated CDFs satisfy the following: $F_{X_1}(x) \geq F_{X_2}(x), \quad \forall x$
- ii. hazard rate order ($X_1 \leq_{hrt} X_2$) if the associated hazard rates satisfy the following: $h_{X_1}(x) \geq h_{X_2}(x), \quad \forall x$
- iii. likelihood ratio order ($X_1 \leq_{lr} X_2$) if the associated PDFs given by $\frac{f_{X_1}(x)}{f_{X_2}(x)}$ decreases in x .

This study considered the likelihood ratio order (\leq_{lr}), stochastic order (\leq_{st}), hazard rate order (\leq_{hr}) and mean residual life order (\leq_{mlr}). This can be written in a general terms as $X \leq_{lr} Y, \Rightarrow X \leq_{hr} Y, \Rightarrow X \leq_{mlr} Y, \Rightarrow X \leq_{st} Y$. For a comprehensive literature on the stochastic ordering, refer to Shaked and Shanthikumar (1994) or Bakouch et al. (2017) or Nasiru (2018a).

A random variable X_1 is less than another random variable X_2 in likelihood order if $\frac{f_{X_1}(x)}{f_{X_2}(x)}$ is a decreasing function of x .

Proposition 4.7. Let $X_1 \sim T-TIGE(\lambda, \alpha, \beta, \gamma)$, and $X_2 \sim TIGE(\lambda, \alpha, \beta)$, then X_1 is less than X_2 in likelihood ratio order $X_1 \leq_{lr} X_2$, if $\lambda > 0$.



Proof. Let
$$\frac{t_1(x)}{t_2(x)} = \frac{\lambda\alpha h(x)H(x)^{-(\alpha+1)} e^{\lambda(1-H(x))^{-\alpha}} \left[(1+\gamma) - 2\gamma e^{\lambda(1-H(x))^{-\alpha}} \right]}{\lambda\alpha h(x)H(x)^{-(\alpha+1)} e^{\lambda(1-H(x))^{-\alpha}}}$$

which gives $\frac{t_1(x)}{t_2(x)} = (1+\gamma) - 2\gamma e^{\lambda(1-H(x))^{-\alpha}}$, and differentiating it with respect

to x yields $\frac{d}{dx} \left(\frac{t_1(x)}{t_2(x)} \right) = -2\gamma\alpha h(x)H(x)^{-(\alpha+1)} e^{\lambda(1-H(x))^{-\alpha}}$.

Since $\frac{d}{dx} \left(\frac{t_1(x)}{t_2(x)} \right) < 0$ and $\gamma > 0$ it implies that $X_1 \leq_{lr} X_2$ is in likelihood

ratio order, and this completes the proof.

4.3.8 Distribution of Order Statistics

Order statistics have been employed in many areas of both statistical theory and applied statistics.

Proposition 4.8. The q^{th} order statistics of the T-TIGE family is

$$t_{q:n}(x) = \frac{n!\lambda\alpha}{(q-1)!(n-q)!} \sum_{m=0}^{n-q} (-1)^i \binom{n-q}{m} \left[e^{\lambda(1-H(x))^{-\alpha}} \left(1 + \gamma(1 - e^{\lambda(1-H(x))^{-\alpha}}) \right) \right]^{p+m-1} \sum_{i=0}^{\infty} \sum_{j=0}^{\infty} \sum_{k=0}^j C_{ijk} h(x) H(x)^k.$$

where
$$C_{ijk} = \binom{\alpha(i+1)+j}{j} \binom{j}{k} \left(\frac{(1+\gamma)e^{\lambda}(-1)^i \lambda^i}{i!} - \frac{2\gamma e^{2\lambda}(-1)^i (2\lambda)^i}{i!} \right).$$

Proof. Consider $X_1, X_2, X_3, \dots, X_n$, to be a random sample of size n having the T-TIGE family of distributions, and $X_{1:n} < X_{2:n} < X_{3:n} < \dots < X_{n:n}$ are order statistics derived from the sample. The PDF, $t_{q:n}(x)$ of the q^{th} order statistics, say $X_{q:n}$ is given by



$$t_{q:n}(x) = \frac{n!}{(q-1)!(n-q)!} \sum_{m=0}^{n-q} (-1)^i \binom{n-q}{m} [T(x)]^{p+m-1} t(x). \quad (4.9)$$

Substituting the Lemma 4.1 and CDF of the T-TIGE family into equation (4.9) yields

$$t_{q:n}(x) = \frac{n!\lambda\alpha}{(q-1)!(n-q)!} \sum_{m=0}^{n-q} (-1)^i \binom{n-q}{m} \left[e^{\lambda(1-H(x))^{-\alpha}} (1 + \gamma(1 - e^{\lambda(1-H(x))^{-\alpha}})) \right]^{p+m-1} \sum_{i=0}^{\infty} \sum_{j=0}^{\infty} \sum_{k=0}^j C_{ijk} h(x) H(x)^k.$$

$$\text{where } C_{ijk} = \binom{\alpha(i+1)+j}{j} \binom{j}{k} \left(\frac{(1+\gamma)e^{\lambda}(-1)^i \lambda^i}{i!} - \frac{2\gamma e^{2\lambda}(-1)^i (2\lambda)^i}{i!} \right).$$

Proposition 4.9. The r^{th} non-central moment of the q^{th} order statistic is given by

$$\mu_r^{(q:n)} = \int_0^{\infty} x^r \frac{n!\lambda\alpha}{(q-1)!(n-q)!} \sum_{m=0}^{n-q} (-1)^i \binom{n-q}{m} \left[e^{\lambda(1-H(x))^{-\alpha}} (1 + \gamma(1 - e^{\lambda(1-H(x))^{-\alpha}})) \right]^{p+m-1} \sum_{i=0}^{\infty} \sum_{j=0}^{\infty} \sum_{k=0}^j C_{ijk} h(x) H(x)^k dx.$$

$$\text{where } C_{ijk} = \binom{\alpha(i+1)+j}{j} \binom{j}{k} \left(\frac{(1+\gamma)e^{\lambda}(-1)^i \lambda^i}{i!} - \frac{2\gamma e^{2\lambda}(-1)^i (2\lambda)^i}{i!} \right).$$

Proof. By definition the r^{th} non-central moment of the q^{th} order statistic of a random variable X is defined as:

$$\mu_r^{(q:n)} = \int_0^{\infty} x^r t_{q:n}(x) dx. \quad (4.10)$$



Substituting equation (4.9) into equation (4.10), yields,

$$\mu_r^{(q;n)} = \int_0^\infty x^r \frac{n! \lambda \alpha}{(q-1)!(n-q)!} \sum_{m=0}^{n-q} (-1)^i \binom{n-q}{m} \left[e^{\lambda(1-H(x))^{-\alpha}} \left(1 + \gamma(1 - e^{\lambda(1-H(x))^{-\alpha}}) \right) \right]^{p+m-1} \sum_{i=0}^\infty \sum_{j=0}^\infty \sum_{k=0}^j C_{ijk} h(x) H(x)^k dx.$$

This completes the proof.



4.4 Estimators of the T-TIGE Family

The method of maximum likelihood method was used to develop the estimators of the parameters T-TIGE family. This was the fulfillment of the third objective of this study.

Let us consider $x_1, x_2, x_3, \dots, x_n$ to be observed values from the T-TIGE family with parameters $(\boldsymbol{\theta}) = (\alpha, \lambda, \gamma, \xi)^T$. The total log-likelihood function is

$$L(\boldsymbol{\theta}) = n \ln \lambda + n \ln \alpha + \sum_{i=1}^n \ln h(x_i; \boldsymbol{\varphi}) - (\alpha + 1) \sum_{i=1}^n \ln H(x_i; \boldsymbol{\varphi}) + \lambda \sum_{i=1}^n [1 - H(x_i; \boldsymbol{\varphi})]^{-\alpha} + \sum_{i=1}^n \ln [1 + \gamma - 2\gamma e^{\lambda [1 - H(x_i; \boldsymbol{\varphi})]^{-\alpha}}]. \quad (4.11)$$

By differentiating equation (4.11) with respect to the parameters, the score functions are derived as follows:

$$\frac{\partial L(\boldsymbol{\theta})}{\partial \lambda} = \frac{n}{\lambda} + \sum_{i=1}^n (1 - H(x_i; \boldsymbol{\varphi})^{-\alpha}) - 2\gamma \sum_{i=1}^n \left[\frac{(1 - H(x_i; \boldsymbol{\varphi})^{-\alpha}) e^{\lambda (1 - H(x_i; \boldsymbol{\varphi})^{-\alpha})}}{1 + \gamma - 2\gamma e^{\lambda (1 - H(x_i; \boldsymbol{\varphi})^{-\alpha})}} \right]. \quad (4.12)$$

$$\frac{\partial L(\boldsymbol{\theta})}{\partial \gamma} = \sum_{i=1}^n \left[\frac{1 - 2e^{\lambda (1 - H(x_i; \boldsymbol{\varphi})^{-\alpha})}}{1 + \gamma - 2\gamma e^{\lambda (1 - H(x_i; \boldsymbol{\varphi})^{-\alpha})}} \right]. \quad (4.13)$$

$$\begin{aligned} \frac{\partial L(\boldsymbol{\theta})}{\partial \alpha} &= \frac{n}{\alpha} - \sum_{i=1}^n \ln H(x_i; \boldsymbol{\varphi}) + \gamma \sum_{i=1}^n H(x_i; \boldsymbol{\varphi})^{-\alpha} \\ &+ \ln H(x_i; \boldsymbol{\varphi}) - 2\lambda \sum_{i=1}^n \frac{(e^{\lambda [1 - H(x_i; \boldsymbol{\varphi})^{-\alpha}]}) ((H(x_i; \boldsymbol{\varphi})^{-\alpha} \ln H(x_i; \boldsymbol{\varphi}))}{1 + \gamma - 2\gamma e^{\lambda (1 - H(x_i; \boldsymbol{\varphi})^{-\alpha})}}. \end{aligned} \quad (4.14)$$

$$\frac{\partial L(\boldsymbol{\theta})}{\partial \boldsymbol{\varphi}} = \sum_{i=1}^n \frac{1}{x_i} + \lambda \alpha \sum_{i=1}^n H(x_i; \boldsymbol{\varphi})^{-(\alpha+1)} + 2\gamma \lambda \sum_{i=1}^n \left[\frac{e^{\lambda (1 - H(x_i; \boldsymbol{\varphi}))} H'(x_i; \boldsymbol{\varphi})}{1 + \gamma (1 - 2e^{\lambda (1 - H(x_i; \boldsymbol{\varphi}))})} \right] - (1 + \alpha) \sum_{i=1}^n \left[\frac{H'(x_i; \boldsymbol{\varphi})}{H(x_i; \boldsymbol{\varphi})} \right]. \quad (4.15)$$



where

$$h'_r(x_i; \varphi) = \frac{\partial}{\partial \varphi_r} [h(x_i; \varphi)], H'_r(x_i; \varphi) = \frac{\partial}{\partial \varphi_r} [H(x_i; \varphi)].$$

Setting the nonlinear system of equations to zero and solving them simultaneously yields the maximum likelihood estimates of $\hat{\boldsymbol{\theta}} = (\hat{\alpha}, \hat{\lambda}, \hat{\gamma}, \hat{\varphi})^T$.

The observed information matrix $I(\boldsymbol{\theta})$ is used to construct the confidence interval for the estimated parameters. The observed information matrix for the T-TIGE family is given by

$$I(\boldsymbol{\theta}) = - \begin{bmatrix} \frac{\partial^2 L(\boldsymbol{\theta})}{\partial \alpha^2} & \frac{\partial^2 L(\boldsymbol{\theta})}{\partial \alpha \partial \lambda} & \frac{\partial^2 L(\boldsymbol{\theta})}{\partial \alpha \partial \gamma} & \frac{\partial^2 L(\boldsymbol{\theta})}{\partial \alpha \partial \varphi} \\ & \frac{\partial^2 L(\boldsymbol{\theta})}{\partial \lambda^2} & \frac{\partial^2 L(\boldsymbol{\theta})}{\partial \lambda \partial \gamma} & \frac{\partial^2 L(\boldsymbol{\theta})}{\partial \lambda \partial \varphi} \\ & & \frac{\partial^2 L(\boldsymbol{\theta})}{\partial \gamma^2} & \frac{\partial^2 L(\boldsymbol{\theta})}{\partial \gamma \partial \varphi} \\ & & & \frac{\partial^2 L(\boldsymbol{\theta})}{\partial \varphi^2} \end{bmatrix} \quad 4.16$$

Under standard regularity conditions when $n \rightarrow \infty$, the distribution of $(\hat{\boldsymbol{\theta}})$ can be approximated by a multivariate normal $N_p(\boldsymbol{\theta}, I(\hat{\boldsymbol{\theta}})^{-1})$ distribution to construct approximate confidence intervals for the parameters, and this apply to all the special distributions derived.



4.5 Special T-TIGE Distributions

A number of new models can be deduced as special models from the T-TIGE family. This section therefore focuses on the derivation of the five new special distributions of the from T-TIGE generator. These are T-TIGER, T-TIGEW, T-TIGEEEE, T-TIGEFr and the T-TIGEL distributions.

4.5.1 The T-TIGE Rayleigh Distribution

The Rayleigh model with positive single parameter has the following CDF and PDF respectively as

$$F(x) = 1 - \exp\left(-\frac{x^2}{2\theta^2}\right), \quad (4.17)$$

and

$$f(x) = \frac{x}{\theta^2} \exp\left(-\frac{x^2}{2\theta^2}\right) \quad (4.18)$$

Substuting equation (4.17) into equation (4.1) gives the the CDF of the Transmuted Type I General Exponential Rayleigh (T-TIGER) model as represented in equations (4.19) as:

$$T_R(x) = \left(1 + \gamma - \gamma \exp\left(\lambda \left(1 - \left(1 - \exp\left(-\frac{x^2}{2\theta^2}\right)\right)^{-\alpha}\right)\right)\right) \exp\left(\lambda \left(1 - \left(1 - \exp\left(-\frac{x^2}{2\theta^2}\right)\right)^{-\alpha}\right)\right) \quad (4.19)$$

Figure 4.1 depicts the various cumulative distribution functions of the T-TIGER.



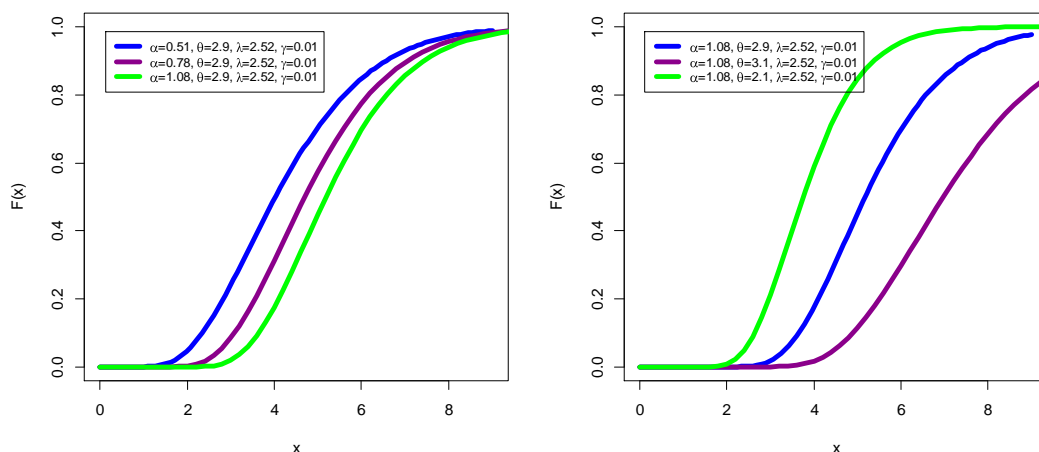


Figure 4.1: The CDF plots of the T-TIGER distribution

The corresponding PDF of the T-TIGER model was arrived at by differentiating equation (4.19) given by

$$t_R(x) = \frac{\lambda \alpha x}{\theta^2} \exp\left(-\frac{x^2}{2\theta^2}\right) \left(1 - \exp\left(-\frac{x^2}{2\theta^2}\right)\right)^{-(\alpha+1)} \exp\left(\lambda \left[1 - \left(1 - \exp\left(-\frac{x^2}{2\theta^2}\right)\right)^{-\alpha}\right]\right) A, \quad (4.20)$$

$$\text{where } A = \left[(1 + \gamma) - 2\gamma \exp\left(\lambda \left[1 - \left(1 - \exp\left(-\frac{x^2}{2\theta^2}\right)\right)^{-\alpha}\right]\right) \right].$$

The PDF plot of the T-TIGER distribution as shown in Figure 4.2 can be right skewed, left skewed. This indicates the flexibility nature of the T-TIGER family of distributions.



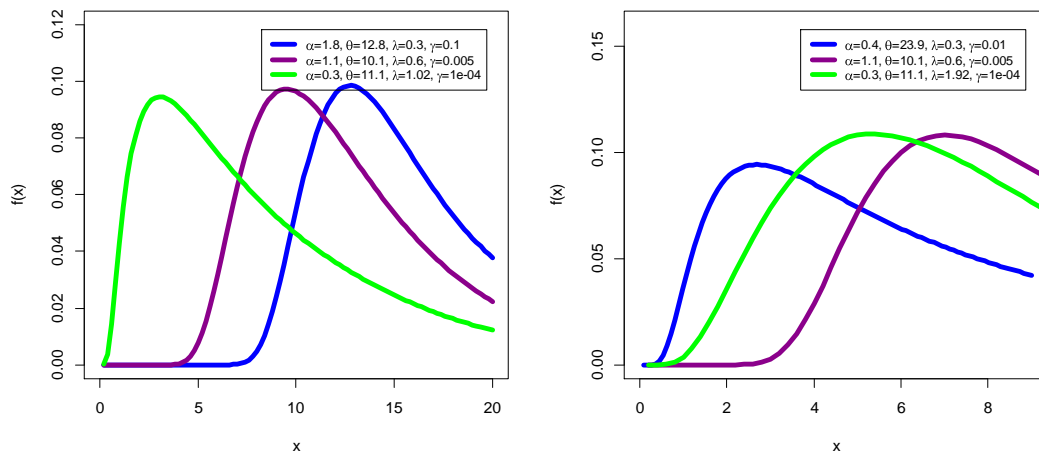


Figure 4.2: The PDF plots of T-TIGER distribution

The reliability (survival) function of the T-TIGER model is given as

$$S_R(x) = 1 - \left(1 + \gamma - \gamma \exp \left(\lambda \left(1 - \left(1 - \exp \left(-\frac{x^2}{2\theta^2} \right) \right)^{-\alpha} \right) \right) \right) \exp \left(\lambda \left(1 - \left(1 - \exp \left(-\frac{x^2}{2\theta^2} \right) \right)^{-\alpha} \right) \right) \quad 4.21$$

The graph representing the various survival function of the T-TIGER model is shown in Figure 4.3.

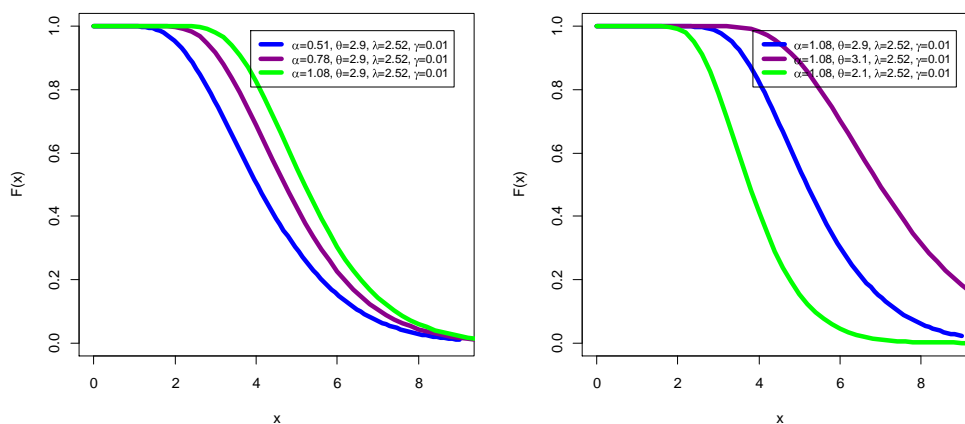


Figure 4.3. Survival function plots of T-TIGER model

The diagram representing the hazard rate function of the T-TIGER model is displayed in Figure 4.4. It could be deduced that the hazard rate function of the T-TIGER model as shown in Figure 4.4 exhibits different shapes such as bathtub, monotonically increasing or monotonically decreasing for various shapes of the hazard function. This further confirms the flexibility of the T-TIGE family.

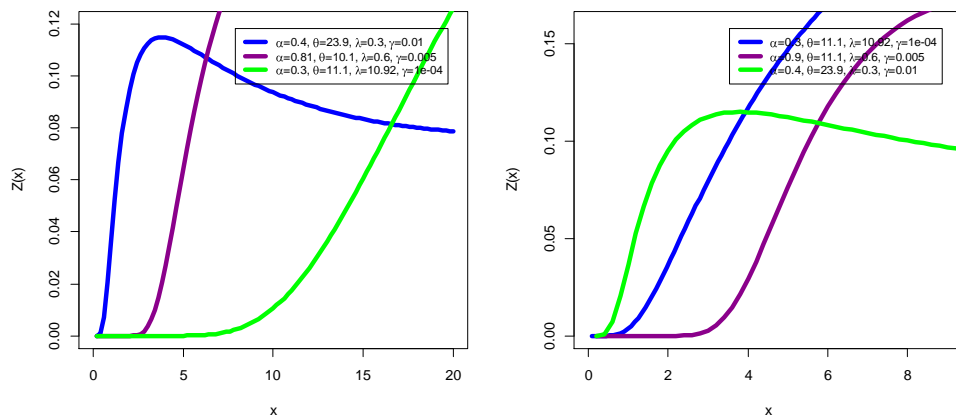


Figure 4.4: Hazard rate plots of T-TIGER distribution



4.5.2 The T-TIGE Weibull Distribution

The Weibull distribution with shape parameter $\beta > 0$ and scale parameter $\theta > 0$ has the following CDF and PDF respectively as:

$$F(x) = 1 - e^{-\theta x^\beta} \tag{4.22}$$

and

$$f(x) = \theta \beta x^{\beta-1} e^{-\theta x^\beta} \tag{4.23}$$

Compounding equations (4.22) and (4.1) yields the CDF of the Transmuted Type I General Exponential Weibull (T-TIGEW) model and this is represented in equation (4.24).

$$T_w(x) = \left[1 + \gamma - \gamma \exp\left(\lambda \left(1 - (1 - \theta x^\beta)^{-\alpha}\right)\right) \right] \left[\exp\left(\lambda \left(1 - (1 - \theta x^\beta)^{-\alpha}\right)\right) \right]. \tag{4.24}$$

The graph representing the CDF of T-TIGEW model is shown in Figure 4.5.

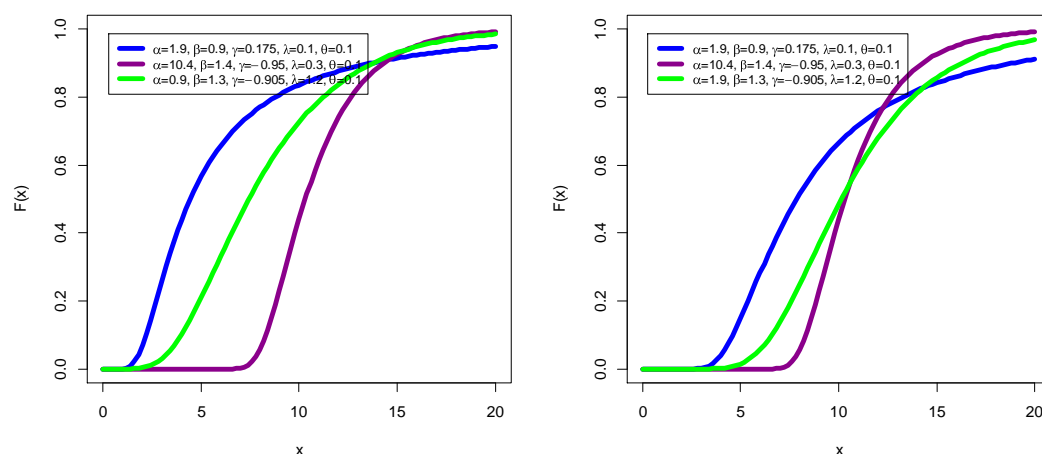


Figure 4.5: The CDF plots of T-TIGEW model



The corresponding PDF of the T-TIGEW model as shown in equation (4.25) was arrived at by differentiating equations (4.24):

$$t_w(x) = \lambda \alpha \theta \beta x^{\beta-1} e^{-\theta x^\beta} (1 - e^{-\theta x^\beta})^{-(\alpha+1)} e^{\lambda \left(1 - (1 - e^{-\theta x^\beta})^{-\alpha}\right)} \left(1 + \gamma - 2\gamma e^{\lambda \left(1 - (1 - e^{-\theta x^\beta})^{-\alpha}\right)}\right). \quad (4.25)$$

The diagram representing the PDF of T-TIGEW model as shown in Figure 4.6 indicates right skewed, left skewed. This indicates the flexibility of the T-TIGE family.

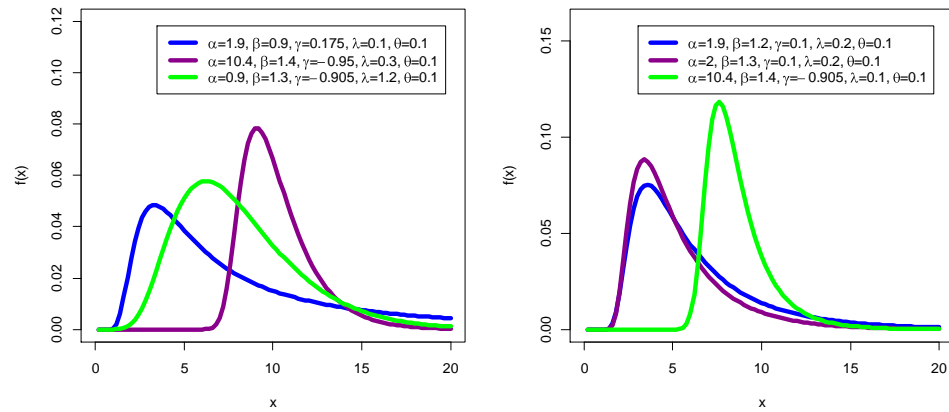


Figure 4.6: The PDF plots of T-TIGEW distribution

The reliability function of the T-TIGEW model is given as:

$$S_w(x) = 1 - \left[1 + \gamma - \gamma \exp\left(\lambda \left(1 - (1 - \theta x^\beta)^{-\alpha}\right)\right)\right] \left[\exp\left(\lambda \left(1 - (1 - \theta x^\beta)^{-\alpha}\right)\right)\right] \quad (4.26)$$

The Figure 4.7 represents the graph of the various survival function of the T-TIGEW model.



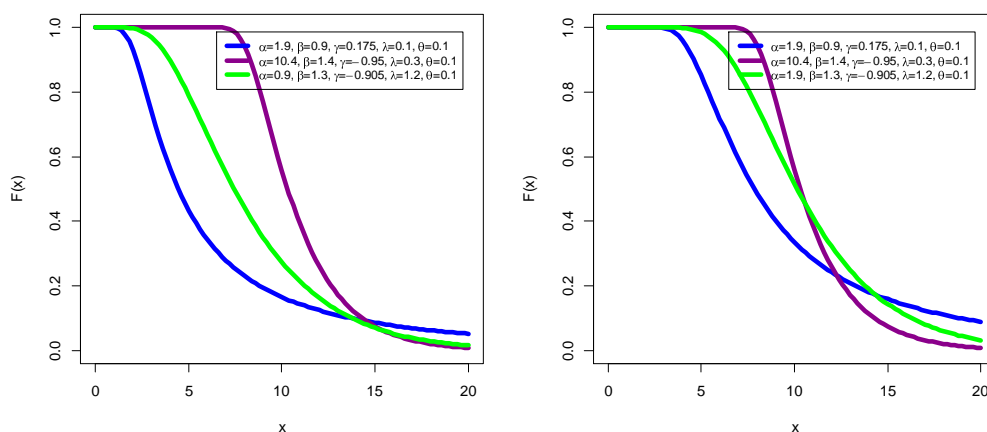


Figure 4.7: The Survival functions of T-TIGEW model

Also, the hazard rate function of the T-TIGEW distribution is given as:

$$Z_w(x) = \frac{W \left(1 + \gamma - \gamma \exp \left(\lambda \left(1 - \left(1 - e^{-\theta x^\beta} \right)^{-\alpha} \right) \right) \right)}{1 - \left[1 + \gamma - \gamma \exp \left(\lambda \left(1 - \left(1 - \theta x^\beta \right)^{-\alpha} \right) \right) \right] \left[\exp \left(\lambda \left(1 - \left(1 - \theta x^\beta \right)^{-\alpha} \right) \right) \right]} \quad (4.27)$$

where

$$W = \alpha \lambda \theta \beta x^{\beta-1} \exp(-\theta x \beta) \left(1 - \exp(-\theta x \beta) \right)^{-(\alpha+1)} \left(\exp \left(\lambda \left(1 - \left(1 - e^{-\theta x^\beta} \right)^{-\alpha} \right) \right) \right)$$

The Figure 4.8 shows the graph of the hazard rate function of the T-TIGEW model. It could be deduced that the hazard rate function of the distribution as shown in Figure 4.8 also exhibits different shapes such as bathtub, monotonically increasing or monotonically decreasing for various shapes of the hazard function. This further confirms the flexibility of the T-TIGE family.



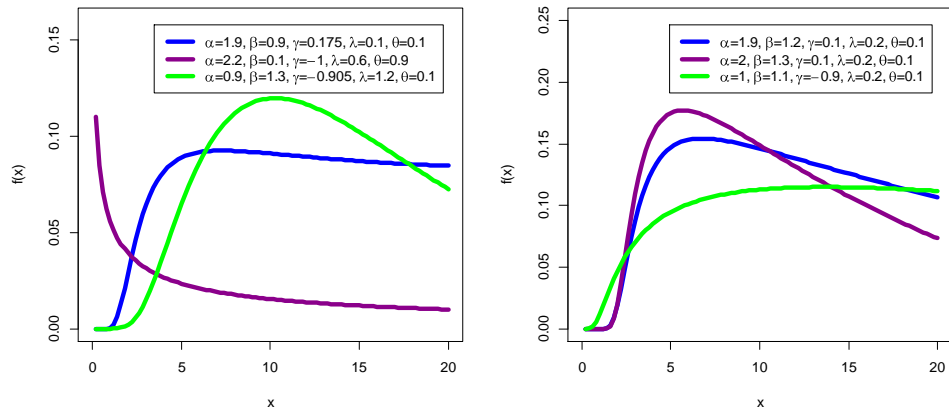


Figure 4.8: Hazard rate plots of T-TIGEW distribution



4.5.3 The T-TIGE Fréchet Distribution

The Fréchet model with two positive parameters α and β has the following CDF and PDF respectively as:

$$F(x) = e^{-(\theta/x)^\beta} \tag{4.28}$$

and

$$f(x) = \beta\theta^\beta x^{(\beta+1)} e^{-(\theta/x)^\beta}, \alpha > 0, \beta > 0, x > 0. \tag{4.29}$$

The CDF of the Transmuted Type I General Exponential Fréchet (T-TIGEFr) model, as defined in equation (4.30) was arrived at as a result of compounding equation (4.28) and the CDF of the T-TIGE family..

$$T_{Fr}(x) = \exp\left(\lambda\left(1 - \left(e^{-(\theta/x)^\beta}\right)^{-\alpha}\right)\right)\left(1 + \gamma - \gamma \exp\left(\lambda\left(1 - \left(e^{-(\theta/x)^\beta}\right)^{-\alpha}\right)\right)\right). \tag{4.30}$$

The plots of the cumulation function of the T-TIGEFr model are shown in Figure 4.9.

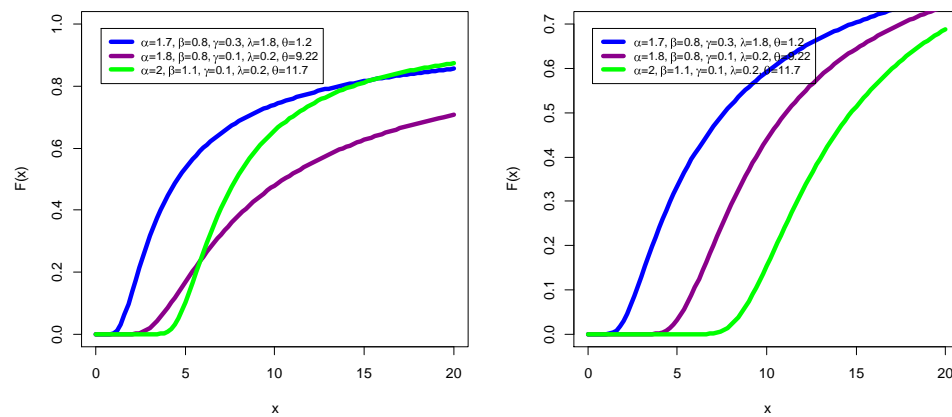


Figure 4.9: The CDF plots of T-TIGEFr distribution



The PDF of the T-TIGEFr model as represented in equation (4.31) was arrived at as the first differential of equation (4.30).

$$t_{Fr}(x) = \lambda \alpha \beta \theta^\beta x^{(\beta+1)} \left(\exp\left(-(\theta/x)^\beta\right) \right)^{-\alpha} \exp\left(\lambda \left(1 - \left(e^{-(\theta/x)^\beta}\right)^{-\alpha}\right)\right) \times \left(1 + \gamma - 2\gamma \exp\left(\lambda \left(1 - \left(e^{-(\theta/x)^\beta}\right)^{-\alpha}\right)\right)\right). \quad (4.31)$$

The graphs of density function of the T-TIGEFr model are displayed in Figure 4.10. It could be observed that the T-TIGEFr model exhibits both the right skewed and left skewed. This furthermore shows the flexibility of the T-TIGE generator.

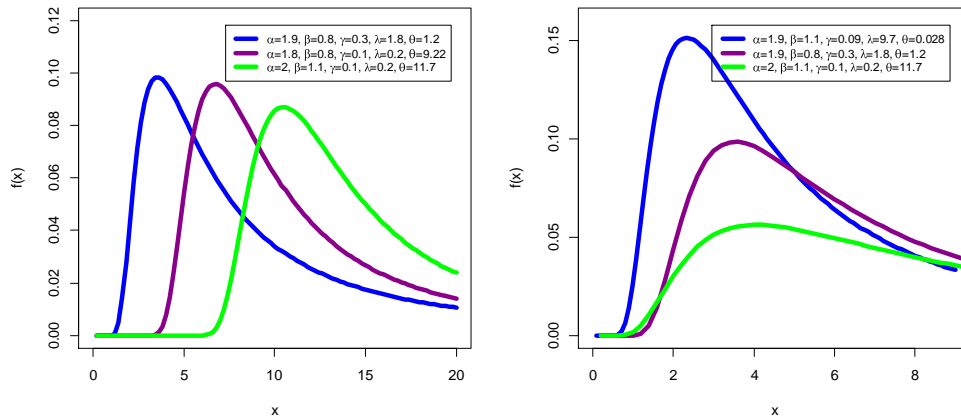


Figure 4.10: The PDF plots of T-TIGEFr distribution

The survival function of the T-TIGEFr model is defined as:

$$S_{Fr}(x) = 1 - \exp\left(\lambda \left(1 - \left(e^{-(\theta/x)^\beta}\right)^{-\alpha}\right)\right) \left(1 + \gamma - \gamma \exp\left(\lambda \left(1 - \left(e^{-(\theta/x)^\beta}\right)^{-\alpha}\right)\right)\right). \quad (4.32)$$

The Figure 4.11 displayed the various survival functions of the T-TIGEFr model.



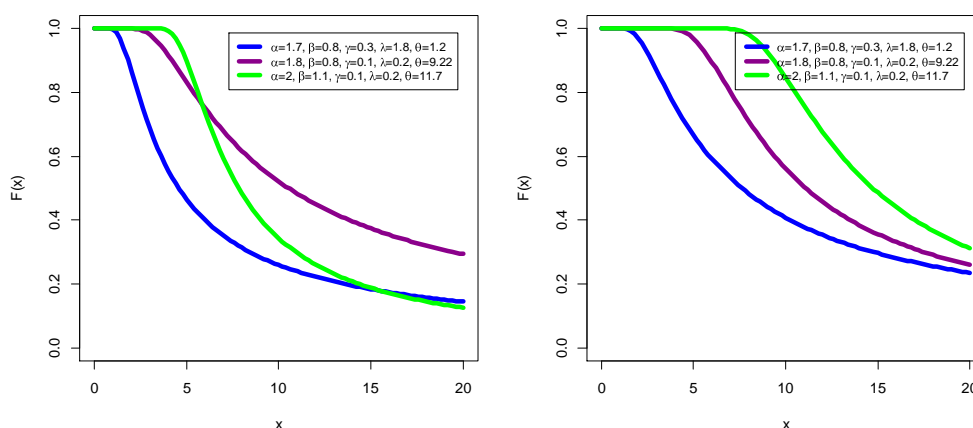


Figure 4.11: The survival plots of T-TIGEFr distribution

Also, the hazard rate function of the T-TIGEFr model is given as:

$$Z_{fr}(x) = \frac{\lambda \alpha \beta \theta^\beta x^{(\beta+1)} \left(\exp(-(\theta/x)^\beta) \right)^{-\alpha} \exp\left(\lambda \left(1 - \left(e^{-(\theta/x)^\beta} \right)^{-\alpha} \right) \right) \left(1 + \gamma - 2\gamma \exp\left(\lambda \left(1 - \left(e^{-(\theta/x)^\beta} \right)^{-\alpha} \right) \right) \right)}{1 - \exp\left(\lambda \left(1 - \left(e^{-(\theta/x)^\beta} \right)^{-\alpha} \right) \right) \left(1 + \gamma - \gamma \exp\left(\lambda \left(1 - \left(e^{-(\theta/x)^\beta} \right)^{-\alpha} \right) \right) \right)} \quad (4.33)$$

Figure 4.12 depicts the graphical representation of the hazard rate function of the T-TIGEFr model. It could be deduced that the hazard rate function of the T-TIGEFr model as shown in Figure 4.12 exhibits different shapes such as bathtub, monotonically increasing or monotonically decreasing for various shapes of the hazard function. This further confirms the flexibility of the T-TIGE family and therefore, could be used to model diverse nature of datasets.



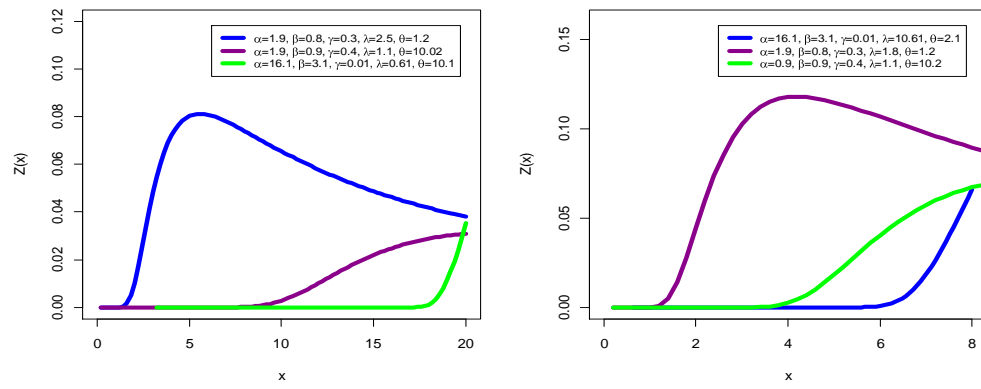


Figure 4.12: Hazard rate plots of T-TIGEFr model



4.5.4 The T-TIGE Exponentiated Exponential Distribution

Exponentiated Exponential model with positive parameters has the following CDF and PDF respectively as:

$$F(x) = (1 - \exp(-\theta x))^\beta \quad (4.34)$$

and

$$f(x) = \beta\theta \exp(-\theta x) (1 - \exp(-\theta x))^{\beta-1}. \quad (4.35)$$

Substituting the CDF of the Exponentiated Exponential distribution into the CDF of the T-TIGE generator yields the new special model known as the T-TIGE Exponentiated Exponential (T-TIGEEEE) model which is defined as

$$T_{EE}(x) = \exp\left(\lambda \left(1 - \left((1 - \exp(-\theta x))^\beta\right)^{-\alpha}\right)\right) \left(1 + \gamma - \gamma \exp\left(\lambda \left(1 - \left((1 - \exp(-\theta x))^\beta\right)^{-\alpha}\right)\right)\right). \quad (4.36)$$

The corresponding PDF of T-TIGEEEE model was derived by differentiating the equation (4.36) which gives:

$$t_{EE}(x) = \lambda\alpha\beta\theta \exp(-\theta x) (1 - \exp(-\theta x))^{\beta-1} \left((1 - \exp(-\theta x))^\beta\right)^{-(\alpha+1)} \times \exp\left(\lambda \left(1 - \left((1 - \exp(-\theta x))^\beta\right)^{-\alpha}\right)\right) \left(1 + \gamma - 2\gamma \exp\left(\lambda \left(1 - \left((1 - \exp(-\theta x))^\beta\right)^{-\alpha}\right)\right)\right). \quad (4.37)$$

The Figure 4.13 shows the graph representation of the CDF of T-TIGEEEE model.



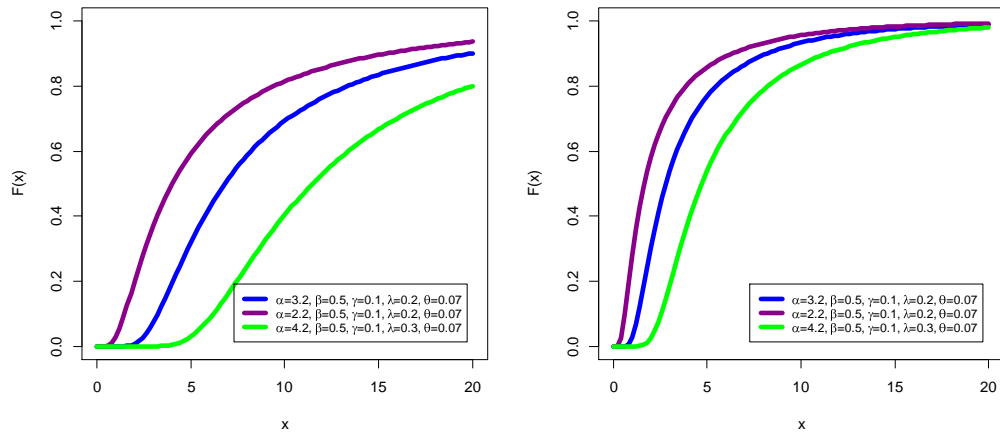


Figure 4.13: The CDF plots of T-TIGEE distribution

The PDF plots of the T-TIGEE model as shown in Figure 4.14 exhibit right skewed and left skewed.

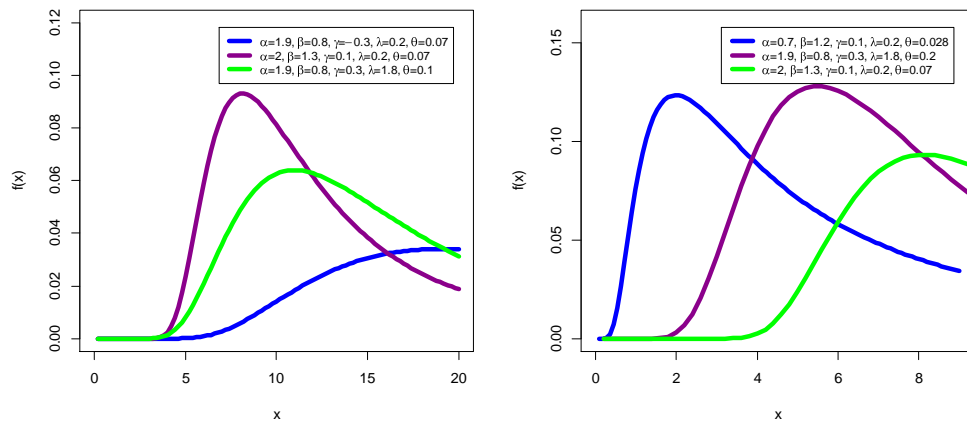


Figure 4.14: The PDF plots of T-TIGEE distribution

The survival (reliability) function of the T-TIGEEE model is defined in equation (4.38).

$$S_{EE}(x) = 1 - \exp\left(\lambda\left(1 - \left((1 - \exp(-\theta x))^\beta\right)^{-\alpha}\right)\right)\left(1 + \gamma - \gamma \exp\left(\lambda\left(1 - \left((1 - \exp(-\theta x))^\beta\right)^{-\alpha}\right)\right)\right). \quad (4.38)$$

The plots representing the survival functions of the T-TIGEEE model is shown in Figure 4.15

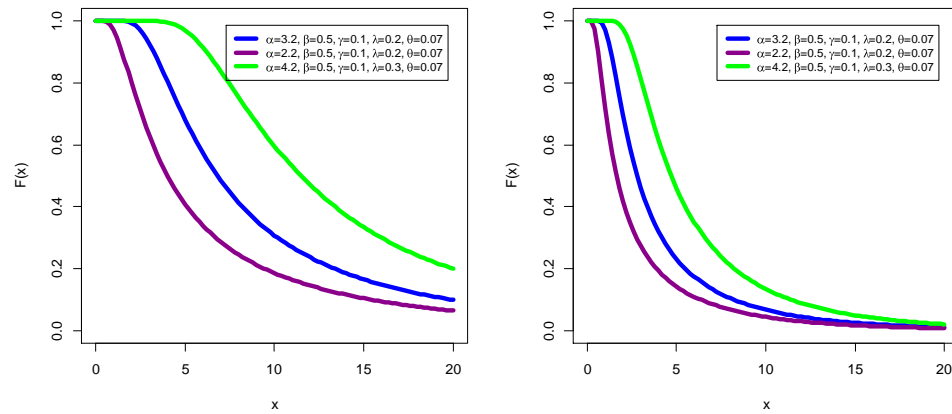


Figure 4.15: The survival plots of T-TIGEEE distribution

The hazard rate function of the T-TIGEEE model is shown graphically in Figure 4.16 with different values of parameters. It could be deduced that the hazard rate function of the T-TIGEEE model as shown in Figure 4.16 exhibits different shapes such as bathtub, monotonically increasing or monotonically decreasing for various shapes of the hazard function. This further confirms the flexibility of the T-TIGEE family.



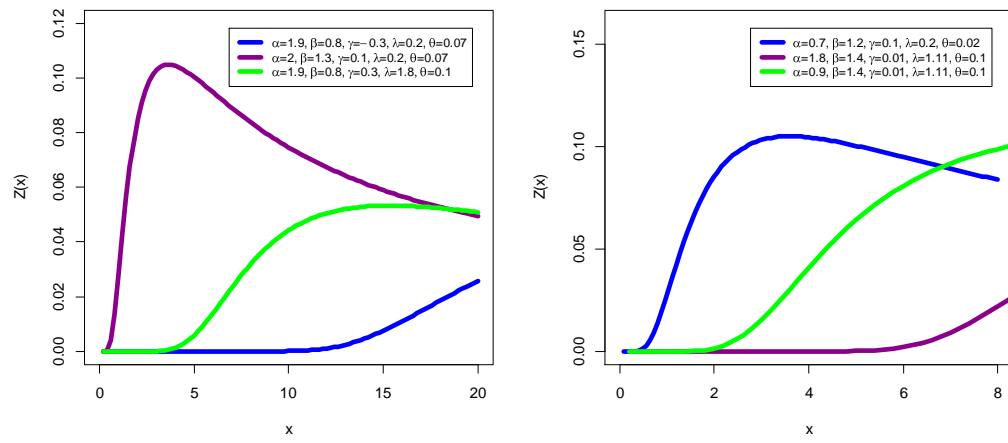


Figure 4.16: Hazard rate plots of T-TIGEEE model

4.5.5 The T-TIGE Lomax Distribution

Another special model derived from the T-TIGE generator is that of the Transmuted Type I General Exponential Lomax (T-TIGEL) model. Consider the Lomax model with shape parameter $\beta > 0$ and scale parameter $\theta > 0$ which has the following CDF and PDF respectively as:

$$F(x) = 1 - \left(1 + \frac{x}{\theta}\right)^{-\beta}, \quad x > 0, \beta, \theta > 0 \quad (4.39)$$

and

$$f(x) = \frac{\beta}{\theta} \left(1 + \frac{x}{\theta}\right)^{-(\beta+1)} \quad (4.40)$$

Compounding equations (4.39) and (4.1) yields the cumulative function of the T-TIGEL model as:

$$T_L(x) = \exp \lambda \left[1 - \left(1 - \left(1 + \frac{x}{\theta} \right)^{-\beta} \right)^{-\alpha} \right] \left[1 + \gamma - \gamma \exp \lambda \left[1 - \left(1 - \left(1 + \frac{x}{\theta} \right)^{-\beta} \right)^{-\alpha} \right] \right], \quad (4.41)$$

for $\alpha, \beta, \theta, \lambda > 0, |\gamma| \leq 1, x > 0$.

The Figure 4.17 graphically displayed the CDF of T-TIGEL model.



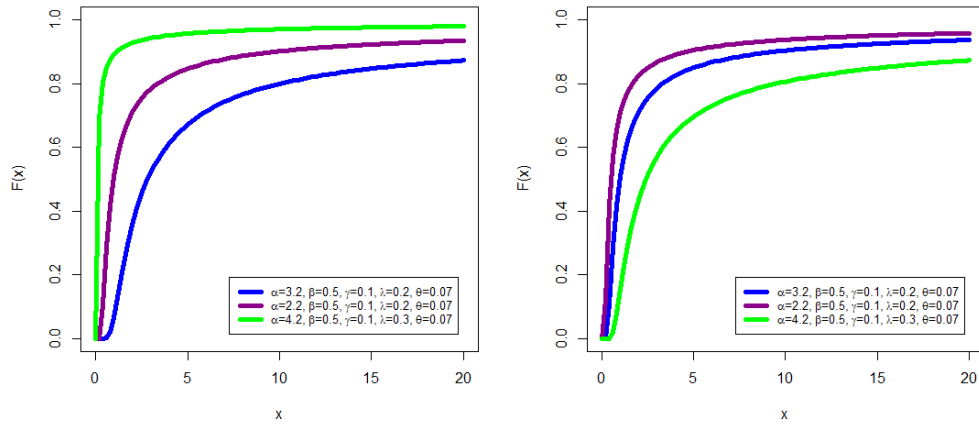


Figure 4.17: The CDF plots of T-TIGEL model

The corresponding PDF of the T-TIGEL model as shown in equation (4.42) was arrived at by differentiating equations (4.41), which gives:

$$t_l(x) = \lambda \alpha \left(\frac{\beta}{\theta} \left(1 + \frac{x}{\theta} \right)^{-(\beta+1)} \right) \left(1 - \left(1 + \frac{x}{\theta} \right)^{-\beta} \right)^{-(a+1)} \exp \lambda \left[1 - \left(1 - \left(1 + \frac{x}{\theta} \right)^{-\beta} \right)^{-a} \right] \left[1 + \gamma - 2\gamma \lambda \left[1 - \left(1 - \left(1 + \frac{x}{\theta} \right)^{-\beta} \right)^{-a} \right] \right]. \quad (4.42)$$

The graph of the PDF of T-TIGEL model as shown in Figure 4.18 indicates right skewed and left skewed. This indicates the flexibility of the T-TIGE family.



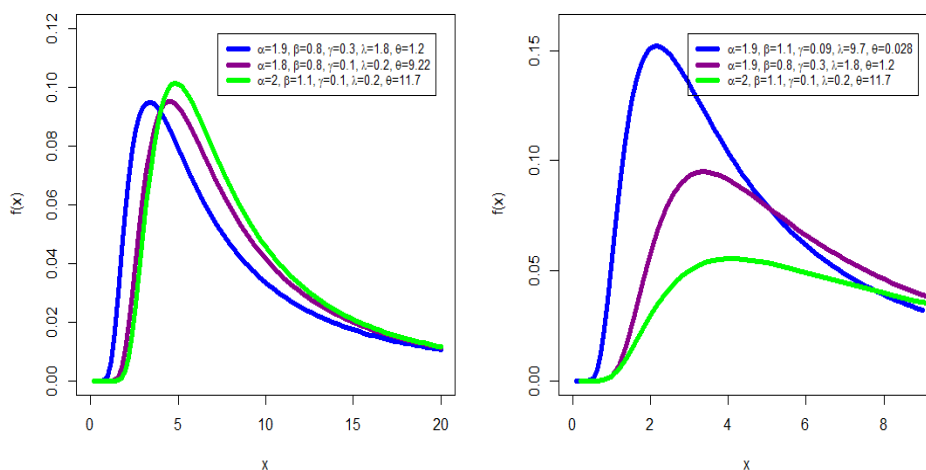


Figure 4.18: The PDF of T-TIGEL model

The survival function of the T-TIGEL model is given as:

$$S_L(x) = 1 - \exp\lambda \left[1 - \left(1 - \left(1 + \frac{x}{\theta} \right)^{-\beta} \right)^{-\alpha} \right] \left[1 + \gamma - \gamma \exp\lambda \left[1 - \left(1 - \left(1 + \frac{x}{\theta} \right)^{-\beta} \right)^{-\alpha} \right] \right] \quad (4.43)$$

The graph of the various survival functions of the T-TIGEL model is shown in

Figure 4.19.

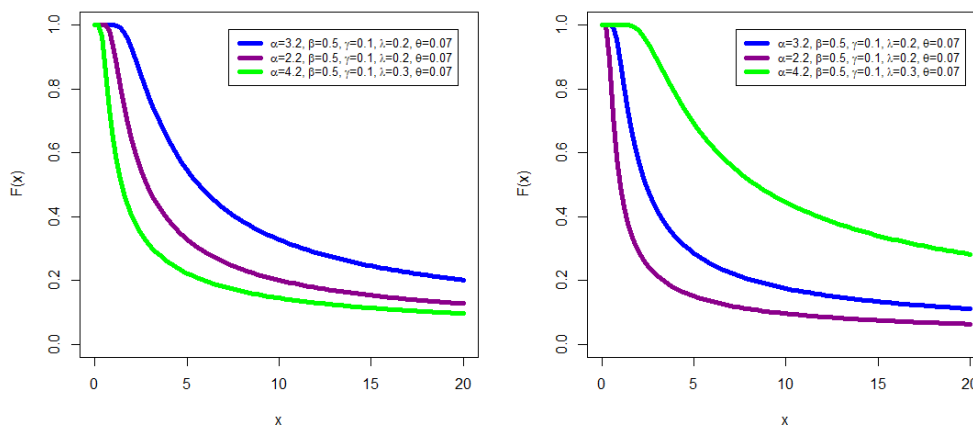


Figure 4.19: The survival plots of T-TIGEL distribution

Also, the hazard rate function of the T-TIGEL model is given as:

$$Z_L(x) = \frac{\lambda \alpha \left(\frac{\beta}{\theta} \left(1 + \frac{x}{\theta} \right)^{-(\beta+1)} \right) \left(1 - \left(1 + \frac{x}{\theta} \right)^{-\beta} \right)^{-(\alpha+1)} \exp \lambda \left[1 - \left(1 - \left(1 + \frac{x}{\theta} \right)^{-\beta} \right)^{-\alpha} \right] \left(1 + \gamma - 2\gamma \lambda \left[1 - \left(1 - \left(1 + \frac{x}{\theta} \right)^{-\beta} \right)^{-\alpha} \right] \right)}{1 - \exp \lambda \left[1 - \left(1 - \left(1 + \frac{x}{\theta} \right)^{-\beta} \right)^{-\alpha} \right] \left(1 + \gamma - \gamma \exp \lambda \left[1 - \left(1 - \left(1 + \frac{x}{\theta} \right)^{-\beta} \right)^{-\alpha} \right] \right)} \quad (4.44)$$

The hazard rate function of the T-TIGEL model is graphically shown in Figure 4.20. It could be deduced that the hazard rate function of the distribution as shown in Figure 4.20 also exhibits different shapes such as bathtub, monotonically increasing or monotonically decreasing for various shapes of the hazard function. This further confirms the flexibility of the T-TIGE family.

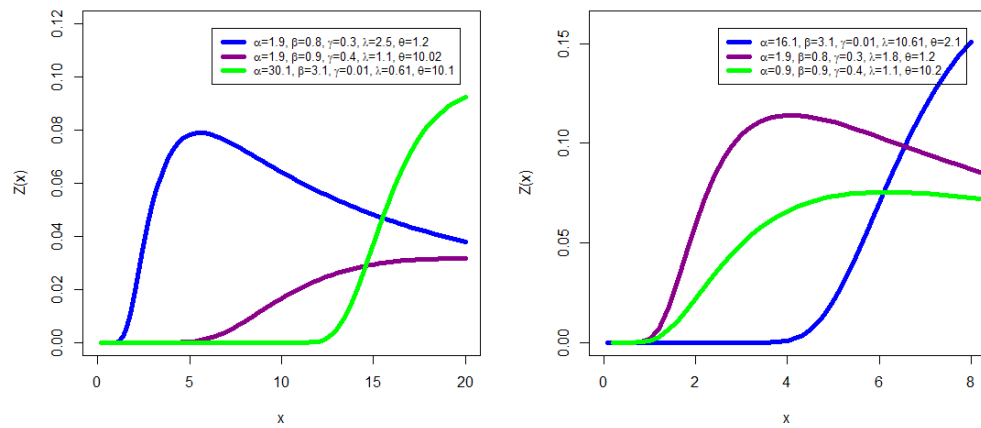


Figure 4.20: Hazard rate plots of T-TIGEL model



4.6 The Monte Carlo Simulation Studies

The estimators of the various special model derived were examined using the Monte Carlo Simulation technique. This section therefore is a response to the fifth objective of the study.

The Root Mean Square Errors (RMSE) and the Average Biases (AB) are presented in Tables 4.1 to 4.10. The quantile functions of these special distributions were used to generate the random samples of these distributions.

The simulation experiment was repeated for $N = 1,000$ times for each model with various sample sizes of $n = 25, 50, 75, 100$ and different parameter values.

Tables 4.1 and 4.2 respectively show the RMSE and AB of the maximum likelihood estimators of $(\alpha, \theta, \lambda, \gamma, \beta)$ for $n = 25, 50, 75, 100$ for the T-TIGEW model. From Tables 4.3 to Table 4.7, it could be noticed that the estimates are quite stable and close to the true value of the parameters for the various sample sizes. Thus, estimators of the parameters of both the RMSE and AB decrease as the sample size (n) increases.



Table 4.1: The RMSE of the MLE of T-TIGEW distribution

RMSE of estimated parameters						
$(\alpha, \theta, \lambda, \gamma, \beta)$	n	$\hat{\alpha}$	$\hat{\theta}$	$\hat{\lambda}$	$\hat{\gamma}$	$\hat{\beta}$
(0.3,0.2,0.1, 0.2,0.1)	25	0.2324	103.701	3.85755	0.32133	0.07436
	50	0.4803	7.78242	1.77892	0.31385	0.06089
	75	0.4609	4.22556	1.37040	0.27569	0.05694
	100	0.4405	3.05633	0.65330	0.26870	0.05320
(0.2,0.2,0.1, 0.2,0.1)	25	0.1595	52.8412	3.00442	0.27481	0.04831
	50	0.3071	104.732	1.31964	0.30210	0.05023
	75	0.3745	7.52802	0.66610	0.28028	0.04916
	100	0.3383	3.51450	0.39636	0.27985	0.04644
(0.3,0.2,0.1, 0.2,0.1)	25	0.2246	64.3763	3.34755	0.32106	0.07572
	50	0.4852	46.7850	1.92911	0.31784	0.06271
	75	0.4685	5.33141	1.44544	0.28902	0.05732
	100	0.4869	3.04859	0.63031	0.27185	0.05198
(0.3,0.1,0.2, 0.2,0.3)	25	0.2550	11.0378	4.50751	0.32283	0.23527
	50	0.3677	1.84995	2.21065	0.33224	0.17495
	75	0.3073	1.56504	1.70797	0.31002	0.15656
	100	0.2507	1.28587	1.17212	0.31493	0.15082



Table 4.2: The AB of the MLE of T-TIGEW distribution

Average biases of estimated parameters						
$(\alpha, \theta, \lambda, \gamma, \beta)$	n	$\hat{\alpha}$	$\hat{\theta}$	$\hat{\lambda}$	$\hat{\gamma}$	$\hat{\beta}$
(0.3,0.2,0.1, 0.2,0.1)	25	0.2495	17.4786	1.5916	0.0599	0.0079
	50	0.2074	3.80391	0.7566	0.0039	0.0193
	75	0.2064	2.61030	0.4065	0.0620	0.0108
	100	0.1731	2.13732	0.2285	0.0547	0.0081
(0.2,0.2,0.1, 0.2,0.1)	25	0.0240	15.0605	0.8180	0.0260	0.0036
	50	0.1235	10.2954	0.4226	0.0196	0.0198
	75	0.1821	3.00904	0.2385	0.0449	0.0263
	100	0.1695	2.14472	0.1440	0.0404	0.0267
(0.3,0.2,0.1, 0.2,0.1)	25	-0.0010	14.6331	1.5028	0.0637	0.0076
	50	0.1792	6.13051	0.7807	0.0022	0.0136
	75	0.1920	2.70515	0.4475	0.0367	0.0119
	100	0.1827	2.09262	0.2321	0.0546	0.0086
(0.3,0.1,0.2, 0.2,0.3)	25	0.0081	2.61592	1.8572	0.0409	0.0157
	50	0.0988	1.39632	0.7665	0.0248	0.0206
	75	0.0713	1.10649	0.4728	-0.0134	0.0004
	100	0.0487	0.87921	0.3105	0.00244	0.0126



Tables 4.3 and show the RMSE and AB of the maximum likelihood estimators of $(\alpha, \theta, \lambda, \gamma, \beta)$ for $n=25, 50, 75, 100$ for the T-TIGER model. The estimators RMSE and average biases reduce as the sample size increases.

Table 4.3: The RMSE of the MLE of T-TIGER distribution

$(\alpha, \theta, \lambda, \gamma)$	n	RMSE of estimated parameters			
		$\hat{\alpha}$	$\hat{\theta}$	$\hat{\lambda}$	$\hat{\gamma}$
(0.1,0.2,0.1,0.2)	25	0.02796	0.03330	0.07817	0.22014
	50	0.02167	0.02594	0.05567	0.21398
	75	0.01930	0.02365	0.05688	0.22206
	100	0.01769	0.02034	0.04261	0.19794
(0.2,0.2,0.1,0.2)	25	0.04801	0.14195	0.21146	0.22095
	50	0.03587	0.11282	0.10825	0.23065
	75	0.03121	0.09845	0.09535	0.26361
	100	0.02809	0.08722	0.08182	0.26187
(0.2,0.3,0.1,0.2)	25	0.04701	0.21390	0.18183	0.21450
	50	0.03614	0.16905	0.11198	0.24155
	75	0.03057	0.14845	0.09738	0.26329
	100	0.02842	0.12623	0.08634	0.26281
(0.1,0.2,0.3,0.2)	25	0.04451	0.10898	0.65800	0.24701
	50	0.02701	0.06208	0.37940	0.28544
	75	0.02007	0.03907	0.26067	0.28453
	100	0.01805	0.03212	0.22673	0.26197



Table 4.4 depicts the AB of the maximum likelihood estimators of $(\alpha, \theta, \lambda, \gamma, \beta)$ for $n = 25, 50, 75, 100$ for the T-TIGER model. The estimators of the parameters of the AB decrease as the sample size increases.

Table 4.4: The AB of the MLE of T-TIGER distribution

Average biases of estimated parameters					
$(\alpha, \theta, \lambda, \gamma)$	n	$\hat{\alpha}$	$\hat{\theta}$	$\hat{\lambda}$	$\hat{\gamma}$
(0.1,0.2,0.1,0.2)	25	0.01540	-0.02248	-0.01026	-0.07580
	50	0.01445	0.01839	0.01907	0.07298
	75	0.01335	-0.01653	-0.01811	-0.07749
	100	0.01360	0.01514	0.02374	0.10647
(0.2,0.2,0.1,0.2)	25	0.00487	0.04690	0.08417	0.03650
	50	0.00510	0.02226	0.03630	0.0111
	75	0.00075	0.00822	0.03397	0.02247
	100	0.00126	0.00138	0.02760	0.03247
(0.2,0.3,0.1,0.2)	25	0.00860	0.05078	0.06365	0.03693
	50	0.00185	0.02835	0.04092	0.00204
	75	-0.00258	0.01609	0.03737	0.02689
	100	-0.00228	0.00906	0.03053	0.03393
(0.1,0.2,0.3,0.2)	25	0.24701	0.07226	0.17209	-0.06112
	50	0.00012	0.02363	0.12245	0.01178
	75	0.00211	0.00976	0.08357	0.03015
	100	0.00146	0.00912	0.06630	0.00777



Tables 4.5 and 4.6 respectively show the RMSE and AB of the maximum likelihood estimators of $(\alpha, \theta, \lambda, \gamma, \beta)$ for $n = 25, 50, 75, 100$ for the T-TIGEFr model. The estimators of the parameters of both the RMSE and average biases decrease as the sample size increases. It is observed that the estimates are quite stable and are closer to the true value of the parameters for these sample sizes.

Table 4.5: The RMSE of the MLE of T-TIGEFr distribution

		RMSE of estimated parameters				
$(\alpha, \theta, \lambda, \gamma, \beta)$	n	$\hat{\alpha}$	$\hat{\theta}$	$\hat{\lambda}$	$\hat{\gamma}$	$\hat{\beta}$
$(0.4, 0.3, 0.5, 0.6, 0.7)$	25	0.57927	0.16397	1.45527	0.49062	0.26949
	50	0.60841	0.16392	1.78301	0.44909	0.24993
	75	0.57236	0.15712	0.81421	0.43901	0.24106
	100	0.50602	0.15703	0.55377	0.41412	0.23919
$(0.4, 0.3, 0.5, 0.1, 0.7)$	25	0.50241	0.15564	7.19286	0.21166	0.27103
	50	0.44747	0.13301	5.76043	0.23754	0.20969
	75	0.42737	0.12438	2.02787	0.24345	0.18855
	100	0.43401	0.11372	1.12418	0.24306	0.17997
$(0.4, 0.3, 0.5, 0.2, 0.7)$	25	0.49334	0.15377	4.68342	0.22784	0.26807
	50	0.44716	0.13242	3.01534	0.24396	0.20898
	75	0.46388	0.14301	1.88564	0.22611	0.19534
	100	0.43075	0.12091	1.10347	0.21351	0.18732
$(0.3, 0.3, 0.5, 0.3, 0.7)$	25	0.40807	0.16268	3.00771	0.28203	0.25894
	50	0.44555	0.16261	2.91197	0.29253	0.21488
	75	0.40613	0.15319	2.03833	0.27398	0.19750
	100	0.40474	0.14690	0.88844	0.23998	0.18942



Table 4.6: The AB of the MLE of T-TIGEFr distribution

Average biases of estimated parameters						
$(\alpha, \theta, \lambda, \gamma, \beta)$	n	$\hat{\alpha}$	$\hat{\theta}$	$\hat{\lambda}$	$\hat{\gamma}$	$\hat{\beta}$
(0.4,0.3,0.5,0.6,0.7)	25	0.20360	0.06566	-0.01821	0.41213	0.05481
	50	0.22405	0.06279	0.06164	0.30782	0.02375
	75	0.21015	0.05839	0.00384	0.29092	0.02094
	100	0.20305	0.06193	0.03089	0.25492	0.00697
(0.4,0.3,0.5,0.1,0.7)	25	0.17770	0.04058	1.36938	0.01041	0.02409
	50	0.13436	0.02184	0.94084	0.03315	0.00581
	75	0.14091	0.02936	0.31583	0.04211	-0.0140
	100	0.13708	0.02622	0.21189	0.03753	0.01675
(0.4,0.3,0.5,0.2,0.7)	25	0.15563	0.03427	0.89543	0.08444	0.04014
	50	0.13589	0.03287	0.48752	0.06682	0.01056
	75	0.16742	0.04484	0.22475	0.03688	0.02029
	100	0.14142	0.03304	0.16243	0.02635	-0.01146
(0.3,0.3,0.5,0.30.7)	25	0.12970	0.04153	0.53333	0.17356	0.04425
	50	0.16216	0.05234	0.29310	0.12087	0.00345
	75	0.15263	0.05202	0.16013	0.09506	0.01357
	100	0.15213	0.05218	0.05776	0.08788	0.02192

Tables 4.7 and 4.8 depict the RMSE and average biases of the maximum likelihood estimators of $(\alpha, \theta, \lambda, \gamma, \beta)$ for $n = 25, 50, 75, 100$ for the T-TIGEEEE model. The estimators of the parameters of the AB decrease as the sample size increases.



Table 4.7: The RMSE of the MLE of T-TIGEEE distribution

RMSE of estimated parameters						
$(\alpha, \theta, \lambda, \gamma, \beta)$	n	$\hat{\alpha}$	$\hat{\theta}$	$\hat{\lambda}$	$\hat{\gamma}$	$\hat{\beta}$
(0.3,0.4,0.5,0.4,0.3)	25	0.10446	4.81254	0.84594	0.35467	0.10473
	50	0.06969	1.80140	0.47129	0.34628	0.06561
	75	0.05679	0.85361	0.35039	0.32772	0.06004
	100	0.04951	0.63861	0.34638	0.31934	0.04951
(0.2,0.4,0.5,0.4,0.3)	25	0.05883	0.57029	2.09409	0.39704	0.08621
	50	0.04708	0.10369	0.57585	0.38848	0.06644
	75	0.04178	0.07177	0.32432	0.37673	0.06889
	100	0.04254	0.05809	0.28631	0.36898	0.05828
(0.2,0.3,0.5,0.4,0.3)	25	0.05868	0.53320	0.81674	0.39381	0.07141
	50	0.04842	0.08515	0.50382	0.38456	0.06176
	75	0.05048	0.05908	0.30905	0.37296	0.05670
	100	0.07460	0.07215	0.29143	0.37078	0.06378
(0.4,0.5,0.5,0.4,0.3)	25	0.11372	1.67242	0.54711	0.35362	0.08543
	50	0.08048	0.86935	0.33850	0.34706	0.05625
	75	0.06775	0.57119	0.28776	0.33681	0.04821
	100	0.063097	0.47708	0.27901	0.33004	0.04340



Table 4.8: The average biases (AB) of the MLE of T-TIGEEE distribution

Average biases of estimated parameters						
$(\alpha, \theta, \lambda, \gamma, \beta)$	n	$\hat{\alpha}$	$\hat{\theta}$	$\hat{\lambda}$	$\hat{\gamma}$	$\hat{\beta}$
(0.3,0.4,0.5,0.4,0.3)	25	0.04418	1.65370	0.04437	0.26819	0.04732
	50	0.03001	0.74922	-0.00321	0.19855	0.02787
	75	0.02043	0.35702	-0.00845	0.15128	0.01983
	100	0.01477	0.24408	0.00190	0.12811	0.01457
(0.2,0.4,0.5,0.4,0.3)	25	0.02819	0.12617	0.06744	-0.18077	0.03558
	50	0.02918	0.04689	-0.09463	-0.19448	0.03666
	75	0.02915	0.03333	-0.14783	-0.21272	0.04112
	100	0.03229	0.03122	-0.17897	-0.23299	0.04094
(0.2,0.3,0.5,0.4,0.3)	25	0.03002	0.10691	-0.00890	-0.16728	0.03224
	50	0.03114	0.04313	-0.11643	0.20334	0.03757
	75	0.03143	0.03430	-0.15319	0.21281	0.03836
	100	0.03372	0.03590	-0.17692	0.23718	0.04172
(0.4,0.5,0.5,0.4,0.3)	25	0.04604	0.74500	-0.03149	0.25766	0.03731
	50	0.03264	0.36680	-0.04623	0.18739	0.02141
	75	0.02524	0.20908	-0.05343	0.16164	0.01976
	100	0.02009	0.16644	-0.04067	0.14187	0.01720

The estimators for the parameters of the T-TIGEL model were also examined via the Monte Carlo technique. The root mean square root (RMSE) and average bias (AB) of the parameters were observed and displayed in Table 4.9 and Table 4.10 respectively. The AB for the estimators also exhibits similar patterns as displayed in Table 4.10.



Table 4.9: The RMSE of the MLE of T-TIGEL distribution

$(\alpha, \theta, \lambda, \gamma, \beta)$	n	RMSE of estimated parameters				
		$\hat{\alpha}$	$\hat{\theta}$	$\hat{\lambda}$	$\hat{\gamma}$	$\hat{\beta}$
(0.13, 0.01, 0.12, 0.02, 0.03)	25	0.0319	0.2193	0.0808	0.2659	0.4551
	50	0.0241	0.1462	0.0779	0.3109	0.0951
	75	0.0216	0.1597	0.0760	0.3385	0.0681
	100	0.0198	0.1845	0.0754	0.3421	0.0722
(0.12, 0.011, 0.12, 0.02, 0.03)	25	0.0330	0.1676	0.0828	0.2348	0.1253
	50	0.0278	0.1588	0.0832	0.2739	0.0935
	75	0.0269	0.1721	0.0820	0.3169	0.0833
	100	0.0251	0.1611	0.0822	0.2951	0.0932
(0.125, 0.011, 0.12, 0.02, 0.06)	25	0.0353	0.1742	0.0865	0.2198	0.1212
	50	0.0278	0.1440	0.0842	0.2824	0.1017
	75	0.026	0.1584	0.0835	0.2961	0.0946
	100	0.0252	0.1562	0.0834	0.2978	0.1001
(0.13, 0.01, 0.12, 0.02, 0.04)	25	0.0329	0.1666	0.0827	0.2252	0.1089
	50	0.0262	0.1657	0.0801	0.3071	0.1175
	75	0.0228	0.1605	0.0789	0.3077	0.0872
	100	0.0219	0.1602	0.0785	0.3222	0.0797



Table 4.10: The AB of the MLE of T-TIGEL distribution

		Average biases of estimated parameters				
$(\alpha, \theta, \lambda, \gamma, \beta)$	n	$\hat{\alpha}$	$\hat{\theta}$	$\hat{\lambda}$	$\hat{\gamma}$	$\hat{\beta}$
	25	0.016	0.1288	-0.0696	0.1411	0.0853
(0.13, 0.01,	50	0.013	0.1049	-0.0699	0.1805	0.0594
0.12,0.02,	75	0.011	0.1081	-0.0679	0.1986	0.0511
0.03)	100	0.010	0.1114	-0.0685	0.2097	0.0488
	25	0.022	0.1048	-0.0756	0.1237	0.0678
(0.12, 0.011,	50	0.021	0.0929	-0.0777	0.1413	0.0557
0.12,0.02,	75	0.020	0.0968	-0.0752	0.1688	0.0502
0.03)	100	0.019	0.0915	-0.0769	0.1493	0.0501
	25	0.023	0.1219	-0.0798	0.0959	0.0724
(0.125, 0.011,	50	0.019	0.1041	-0.0777	0.1295	0.0582
0.12,0.02,	75	0.018	0.1087	-0.0773	0.1334	0.0574
0.06)	100	0.018	0.1075	-0.0773	0.1342	0.0612
	25	0.019	0.1240	-0.0745	0.1107	0.0731
(0.13, 0.01,	50	0.014	0.1207	-0.0715	0.1696	0.0674
0.12,0.02,	75	0.013	0.1146	-0.0719	0.1662	0.0596
0.04)	100	0.012	0.1142	-0.0716	0.1753	0.0564



CHAPTER FIVE

EMPIRICAL RESULTS AND APPLICATIONS

5.1 Introduction

This chapter presents the results of the sixth stated objective of this study. That is, the special models derived from the T-TIGE family are applied to different real datasets to assess the dynamism of the T-TIGE family of distributions.

5.2 The Application of the T-TIGER Distribution

This section demonstrates how the application of the T-TIGER model works in practice by using three (3) different real datasets. The T-TIGER model fitness was compared with different models namely the Exponentiated Transmuted Generalized Rayleigh (ETGR) by Afify et al. (2015), Weibull-Fréchet (WFr) by Afify et al. (2016), Transmuted Rayleigh (TR) distribution by Merovci (2013c), the General Exponential (GE) model by Gupta and Kundu (1999), the Generalized Rayleigh (GR) by Raqab et al. (2017), the Weibull (W) distribution by Weibull (1951), the Exponential (E) and the Rayleigh (R) model.

For these analyses, the following datasets were used; the tax revenue data (Appendix A1), the Kiamo Blowhole (Appendix A2) and Applied Analysis data (Appendix A3).

The descriptive statistics of the tax revenue data is presented in Table 5.1. It could be observed from the Table 5.1 that the first, second and third quarters of the tax revenue data were 8.45, 10.60 and 16.85 respectively. The minimum and maximum of the tax revenue were 4.10 and 39.20 Egyptian pounds respectively. The average tax revenue was 13.49 Egyptian pounds per month.

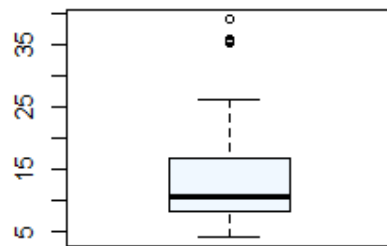


The coefficient of skewness of 1.57 and excess kurtosis of 2.08 indicated that the tax revenue data was skewed and more peak than the normal curve. The descriptive statistics of the tax revenue dataset is further presented in Figure 5.1.

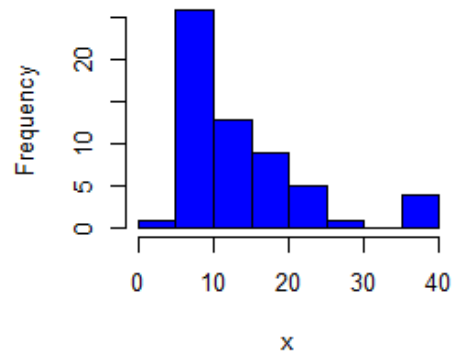
Table 5.1: Descriptive statistic of the tax revenue data

Min	1 st Q	Median	Mean	Sd	3 rd Q	Max	Skewness	Kurtosis
4.10	8.45	10.60	13.49	8.05	16.85	39.20	1.57	2.08

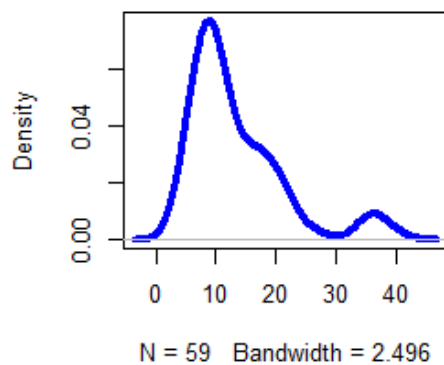
Boxplot of Tax Revenue Dataset



Histogram of x



density.default(x = x)



Normal Q-Q Plot

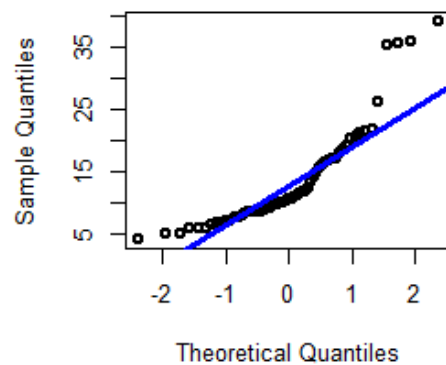


Figure 5.1: A graphical summary of the tax revenue dataset



In order to determine the shape of the most appropriate hazard function for modeling, graphical analysis of the data become more useful. As shown in Figure 5.2, the tax revenue data set has an increasing failure rate as indicated by the TTT-transform plot which has a concave shape since the curve shown is above the 45⁰.line as shown in Figure 5.2.

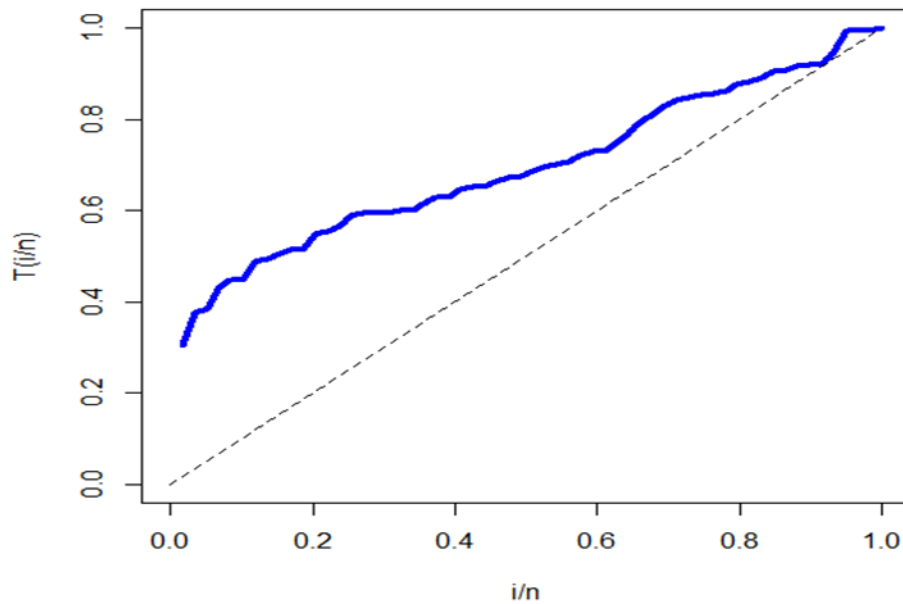


Figure 5.2: The TTT-transform plot for tax revenue data

The estimated parameters of the fitted models with their respective standard are estimated by maximum likelihood are presented in Table 5.2. The values of most of the fitted distributions are significant at the 5% significant level. This can be verified by using the standard error test which states that for a parameter to be significant at the 5% significant level, the standard error should be less than half the parameter value. For instance, for the T-TIGER model, the parameters for alpha and theta were significant at the 10% and 1% significant levels respectively.



Table 5.2: The MLE estimates using the tax revenue data

Model	Estimate	Standard error	z-value	P-value
T-TIGER	$\hat{\alpha} = 0.9325$	3.36×10^{-1}	2.7739	5.5×10^{-3}
	$\hat{\theta} = 18.002$	5.19×10^0	3.4662	5.0×10^{-4}
	$\hat{\lambda} = 11.891$	5.03×10^0	2.3641	4.6×10^{-11}
	$\hat{\gamma} = 0.1793$	3.07×10^{-2}	5.8404	3.2×10^{-3}
WFr	$\hat{\alpha} = 15.045$	7.51×10^0	2.0043	4.5×10^{-2}
	$\hat{\beta} = 1.8730$	7.55×10^{-1}	2.4795	1.3×10^{-2}
	$\hat{\theta} = 1.6320$	1.39×10^0	1.1717	2.4×10^{-1}
	$\hat{\lambda} = 0.5360$	1.43×10^{-1}	3.7487	1.8×10^{-3}
GTR	$\hat{\alpha} = 1.4660$	2.57×10^{-1}	5.7009	1.2×10^{-8}
	$\hat{\beta} = 0.1050$	2.37×10^{-1}	0.4429	6.6×10^{-3}
	$\hat{\theta} = 12.490$	1.48×10^0	8.4154	$< 2.2 \times 10^{-16}$
	$\hat{\lambda} = 10.265$	2.42×10^1	0.4237	6.7×10^{-1}
ETGR	$\hat{\alpha} = 0.1978$	7.32×10^{-2}	2.7025	6.9×10^{-3}
	$\hat{\beta} = 12.204$	7.05×10^0	1.7318	8.3×10^{-2}
	$\hat{\theta} = 0.0520$	7.30×10^{-3}	7.1440	9.1×10^{-13}
	$\hat{\lambda} = 0.9070$	7.00×10^{-2}	12.9483	$< 2.2 \times 10^{-16}$
EWE	$\hat{\alpha} = 1.0010$	3.60×10^{-4}	2.7526	$< 2.2 \times 10^{-16}$
	$\hat{\beta} = 0.6051$	4.00×10^{-2}	12.4788	$< 2.2 \times 10^{-16}$
	$\hat{\theta} = 1.8925$	3.90×10^{-4}	4.8059	$< 2.2 \times 10^{-16}$
	$\hat{\lambda} = 0.0128$	1.90×10^{-3}	6.7433	1.5×10^{-11}



Table 5.2: The MLE estimates using the tax revenue data (Cont'd)

TR	$\hat{\theta}=13.1342$	1.30×10^1	9.8498	$< 2.2 \times 10^{-16}$
	$\hat{\gamma}=0.6426$	2.40×10^{-1}	2.6932	7.0×10^{-3}
GE	$\hat{\alpha}=5.5301$	1.40×10^1	3.8557	1.2×10^{-4}
	$\hat{\beta}=0.1787$	2.30×10^{-2}	7.6727	1.7×10^{-14}
GR	$\hat{\alpha}=1.0311$	1.80×10^{-1}	5.5894	2.3×10^{-8}
	$\hat{\theta}=0.0645$	5.70×10^{-3}	11.3315	$< 2.2 \times 10^{-16}$
R	$\hat{\theta}=11.083$	7.20×10^{-1}	15.362	$< 2.2 \times 10^{-16}$
	$\hat{\beta}=1.8020$	1.70×10^{-1}	10.4463	$< 2.2 \times 10^{-16}$
W	$\hat{\theta}=0.0070$	3.90×10^{-4}	1.8732	$6. \times 10^{-2}$
E	$\hat{\theta}=0.0740$	9.60×10^{-3}	7.6811	1.6×10^{-14}

The inverse of the Hessian matrix of the T-TIGER model is given by

$$I^{-1} = \begin{bmatrix} 1.13 \times 10^{-1} & 6.5 \times 10^{-2} & -8.0 \times 10^{-2} & -2.3 \times 10^{-1} \\ 6.5 \times 10^{-2} & 2.7 \times 10^1 & -5.3 \times 10^{-1} & 8.6 \times 10^{-1} \\ -8.0 \times 10^{-2} & -5.3 \times 10^{-1} & 6.8 \times 10^{-2} & 1.6 \times 10^{-1} \\ -2.3 \times 10^{-1} & 8.6 \times 10^{-1} & 1.6 \times 10^{-1} & 6.5 \times 10^{-1} \end{bmatrix}$$

The approximately 95% CI for α, θ, λ , and γ are displayed in Table 5.3.

Table 5.3: Confidence Interval for the model parameters

CI	α	θ	λ	γ
95%	(0.2736, 1.5914)	(7.822, 28.1811)	(0.1, 0.6984)	(-0.4013, 0.8599)

It can be observed from the Table 5.3 that all the confidence intervals contained their respective point estimates. It must be noted the values of the gamma, γ ranges from -1 to +1, hence the confidence interval of the gamma doe indicates that it is significant. The estimates of the T-TIGER model were significant at 5% significant level.

The model selection was carried out using the values of log-likelihood function, AIC, AICc, HQ, BIC, A*, W* and K-S as explained earlier in the methodology. Table 5.4 gives the rest of the statistics. It could be deduced from the Table 5.4 that the T-TIGER provides a better fit than the comparative models. That is the T-TIGER distribution leads to better fit compared to the other ten models.

Table 5.4: The negative log-likelihood, information criteria and goodness of fit statistics for tax revenue data

Model	-L	AIC	AICc	BIC	HQ	A*	W*	K-S
T-TIGER	187.62	383.23	383.98	391.54	386.48	0.24	0.037	0.05
WFr	191.79	386.37	386.31	399.88	396.82	0.52	0.063	0.09
GTR	194.53	397.05	397.79	405.36	400.29	1.47	0.235	0.15
ETGR	191.42	390.84	391.58	399.15	394.08	0.95	0.155	0.12
EWE	189.85	387.71	388.44	396.01	390.95	0.65	0.109	0.10
TR	195.71	395.42	395.63	399.57	397.04	1.61	0.257	0.13
GE	191.22	386.44	386.66	390.60	398.07	0.87	0.144	0.12
R	197.71	397.42	397.49	399.49	398.23	1.99	0.312	0.17
W	197.32	398.63	398.85	402.79	400.25	1.83	0.288	0.14
E	212.51	427.01	427.08	429.09	427.82	1.21	0.194	0.30



The plots of empirical density and densities of the fitted models are presented in Figure 5.3. The dash line with the blue colour represents the T-TIGER distribution. It can be observed that the fitted T-TIGER distribution mimics the empirical density of the tax revenue data, hence the T-TIGER distribution provides a better fit.

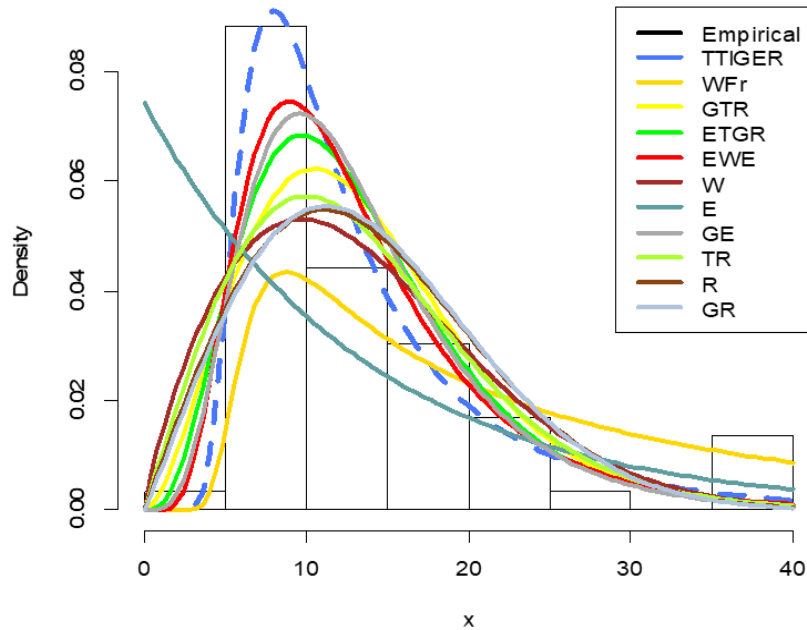


Figure 5.3: Plots of empirical density and densities of the fitted models.

The second dataset relates to the waiting times between sixty-five consecutive eruptions of a blowhole, called the Kiamo Blowhole (Pinho et al., 2012) was also used to demonstrate the usefulness of the T-TIGER model. The Kiamo Blowhole is a tourist attraction located nearly 120km to the south of Sydney, Australia. The data set are given in an Appendix A2.

The descriptive statistics of the Kiamo Blowhole dataset are presented in Table 5.5. It could be observed from the Table 5.5 that the first, second and third quarters of the Kiamo Blowhole data were 14.75, 28.00 and 60.00



respectively. The minimum and maximum values of the dataset were 7.00 and 169.00 respectively.

The dataset has an average value of 39.83. The coefficient of skewness of 1.51 and excess kurtosis of 2.59 indicated that the Kiamo Blowhole dataset was positively skewed and the kurtosis value indicates that the model has relatively a flatter peak than the normal distribution.

The descriptive statistic of the Kiamo Blowhole dataset is further presented in figure 5.4.

Table 5.5: Descriptive statistic of Kiamo Blowhole Data

Min	1 st Q	Mean	Std dev	3 rd Q	Max	skewness	Kurtosis
7.00	14.75	39.83	33.75	60.00	169.00	1.51	2.59



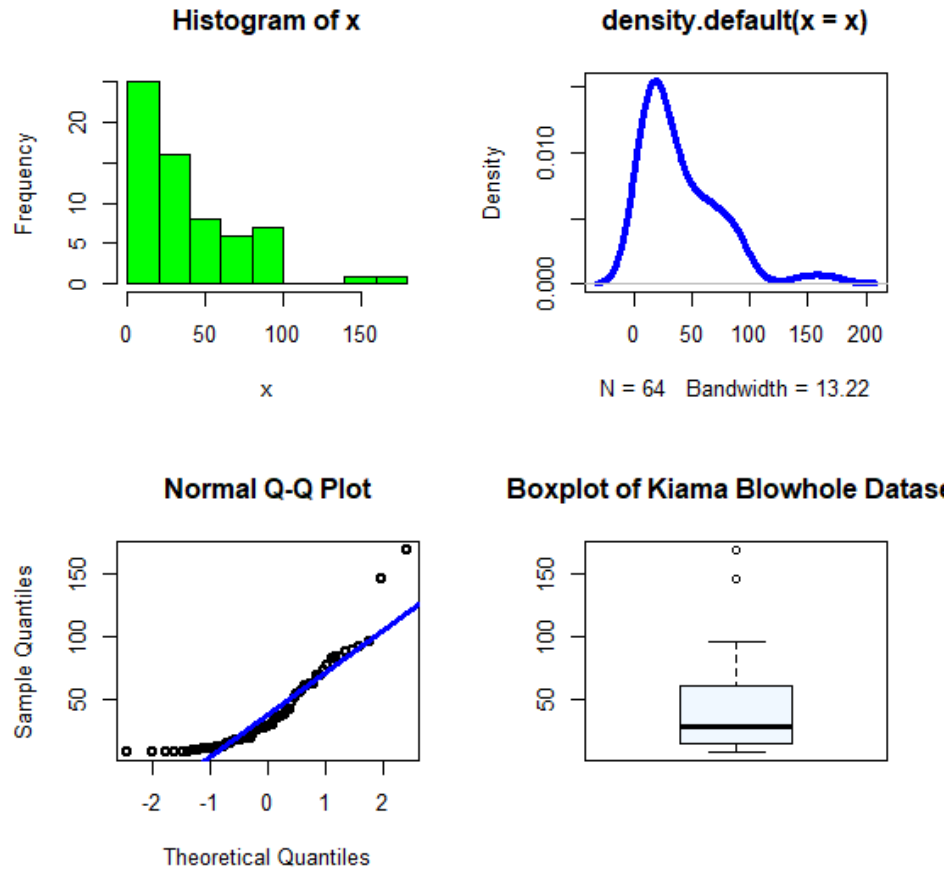


Figure 5.4: A graphical summary of the Kiamo Blowhole dataset

In order to determine the shape of the most appropriate hazard function for modeling, graphical analysis of the data become more useful. As shown in Figure 5.5, the Kiamo Blowhole data set has an increasing failure rate as indicated by the TTT-transform plot which has a concave shape.



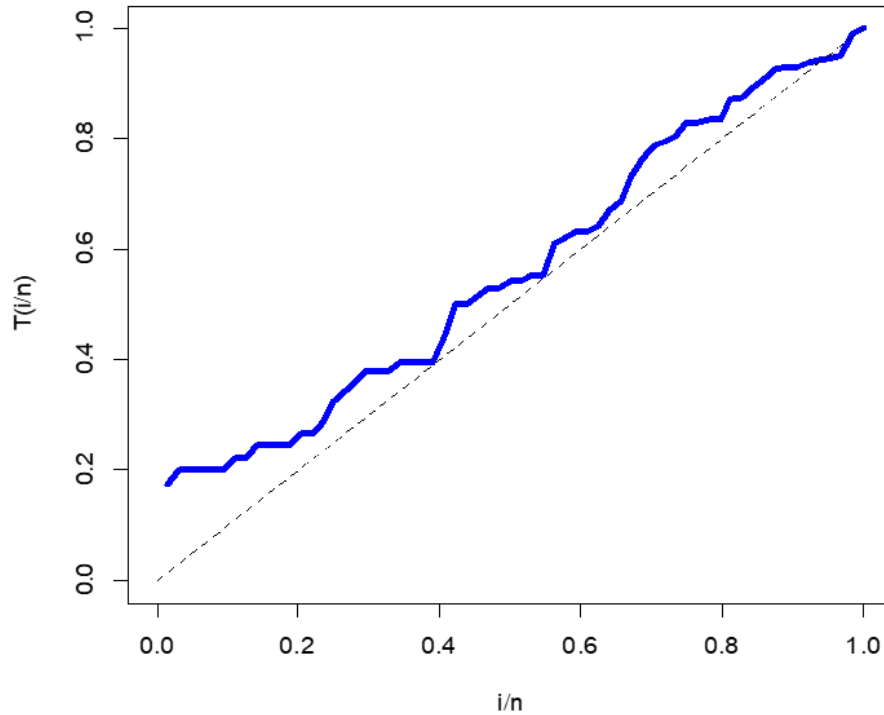


Figure 5.5: The TTT-transform plot for Kiamo Blowhole data

The fitted models with their respective standard errors were estimates were presented in Table 5.6. The parameters of most fitted distributions are significant at the 5% significant level. This can be verified by using the standard error test which states that for a parameter to be significant at the 5% significant level, the standard error should be less than half the parameter value.



Table 5.6: The maximum likelihood estimates of parameters of the

Kiamo Blowhole data

Model	Estimate	Std error	z-value	P-value
T-TIGER	$\hat{\alpha} = 0.4899$	0.1284	3.8149	1.2×10^{-4}
	$\hat{\theta} = 69.4916$	16.676	4.1672	3.1×10^{-5}
	$\hat{\lambda} = 0.5270$	0.2276	2.3154	2.6×10^{-2}
	$\hat{\gamma} = -0.8340$	0.2514	-3.3174	$8. \times 10^{-3}$
ETGR	$\hat{\alpha} = 11.3488$	0.0145	781.986	$< 2.2 \times 10^{-16}$
	$\hat{\beta} = 0.04512$	0.0068	6.6733	2.5×10^{-11}
	$\hat{\theta} = 0.0151$	0.0017	9.0576	$< 2.2 \times 10^{-16}$
	$\hat{\lambda} = -0.0031$	0.6505	-0.0047	9.9×10^{-1}
EWE	$\hat{\alpha} = 4.1602$	1.3562	1.3562	2.2×10^{-3}
	$\hat{\beta} = 0.3505$	0.0565	6.2048	5.5×10^{-10}
	$\hat{\theta} = 14.5165$	0.0470	308.7835	$< 2.2 \times 10^{-16}$
	$\hat{\lambda} = 0.0116$	0.0074	1.5648	1.2×10^{-1}
TR	$\hat{\theta} = 42.6897$	3.9890	10.7018	$< 2.2 \times 10^{-16}$
	$\hat{\gamma} = 0.6562$	0.2007	3.2701	1.1×10^{-3}
GE	$\hat{\alpha} = 1.7326$	0.3201	5.4129	6.2×10^{-8}
	$\hat{\beta} = 0.0351$	0.0051	6.8523	7.3×10^{-12}
GR	$\hat{\alpha} = 0.51234$	0.0767	6.6826	2.348×10^{-11}
	$\hat{\theta} = 0.0151$	0.0015	9.8573	$< 2.2 \times 10^{-16}$
R	$\hat{\theta} = 36.7939$	2.2996	16.0000	$< 2.2 \times 10^{-16}$
W	$\hat{\beta} = 1.2584$	0.1221	10.3053	$< 2.2 \times 10^{-16}$
	$\hat{\theta} = 0.0088$	0.0046	1.9223	5.5×10^{-2}
E	$\hat{\theta} = 0.02511$	0.0032	8.0000	1.2×10^{-15}

The variance-covariance matrix for the estimated parameters of the T-TIGER

model is given by

$$I^{-1} = \begin{bmatrix} 1.65 \times 10^{-2} & 8.72 \times 10^{-1} & -2.76 \times 10^{-3} & -3.09 \times 10^{-2} \\ 8.72 \times 10^{-1} & 2.78 \times 10^2 & -2.27 \times 10^0 & 4.61 \times 10^{-2} \\ -2.76 \times 10^{-3} & -2.27 \times 10^0 & 5.18 \times 10^{-2} & 6.01 \times 10^{-2} \\ -3.09 \times 10^{-2} & 4.61 \times 10^{-2} & 6.01 \times 10^{-2} & 1.81 \times 10^{-1} \end{bmatrix}$$



Thus, Table 5.7 displayed the approximately 95% confidence interval for the parameters $\alpha, \theta, \lambda,$ and γ .

Table 5.7: Confidence Interval for the model parameters

CI	α	θ	λ	γ
95%	(0.238, 0.7426)	(36.807, 102.1765)	(0.1, 0.7031)	(-0.916, 0.7498)

It can be observed that all the confidence intervals contained their respective point estimates. Thus all the estimated parameters of the T-TIGER distribution using the Kiamo Blowhole dataset were significant at the 5% significant level. Hence the estimated parameters can be relied upon.

The appropriate distribution was selected using the log-likelihood functions, AIC, AICc, HQ, BIC, A*, W* and K-S as explained earlier in the methodology. It could be deduced from the Table 5.8 that the T-TIGER model provides a better fit than the comparative models. Table 5.8 gives the rest of the statistics.



Table 5.8: The negative log-likelihood, information criteria and goodness of fit statistics for the Kiamo Blowhole data

Model	-L	AIC	AICc	BIC	HQ	A*	W*	K-S
T-TIGER	291.63	591.26	591.94	599.89	594.67	0.61	0.07	0.08
ETGR	299.75	607.49	608.17	616.13	610.89	1.29	0.19	0.14
EWE	293.78	595.56	596.24	604.19	598.96	0.73	0.10	0.11
TR	306.66	617.31	617.51	621.63	619.01	1.18	0.18	0.26
GE	295.67	595.33	595.53	599.65	597.03	0.90	0.13	0.12
GR	299.75	603.49	603.69	607.81	605.19	1.29	0.19	0.14
R	311.38	624.75	624.82	626.91	625.60	1.29	0.19	0.28
W	296.91	597.82	598.02	602.14	599.52	1.03	0.15	0.11
E	299.81	601.63	601.69	603.78	602.48	0.92	0.13	0.17

Figure 5.6 shows the empirical density and the fitted densities of the distributions based on the Kiamo Blowhole dataset. The dashed blue density represents the T-TIGER model, which best fitted the dataset as compared with other competing models.



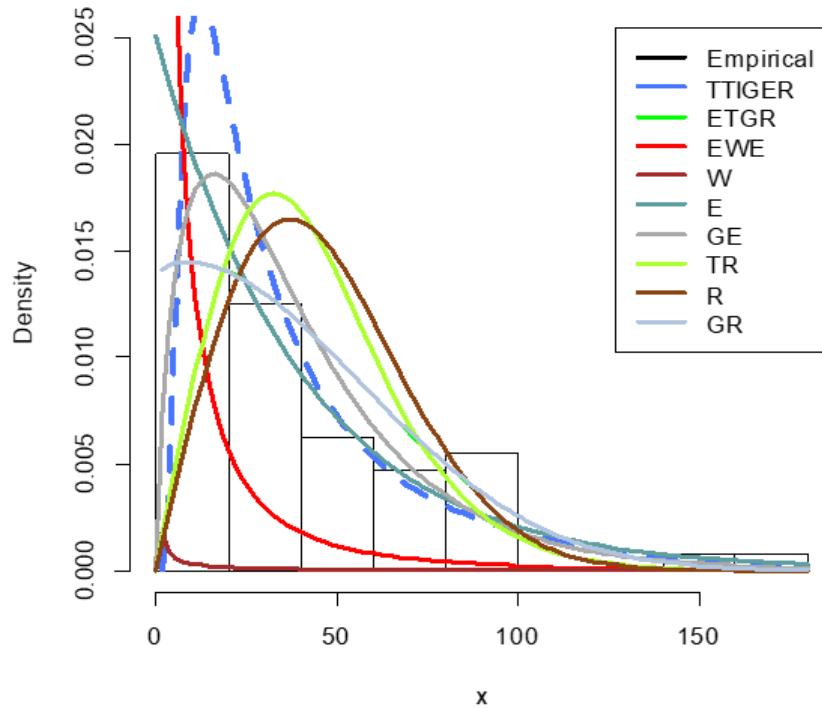


Figure 5.6: Empirical and densities plots of the fitted models.

The T-TIGER model was also applied to the third dataset as shown in Appendix A3. The descriptive summary of the dataset is given in Table 5.9. It could be seen that the dataset of the Applied Life Analysis is positively skewed with a coefficient of 2.19 and a kurtosis of 4.33.

Table 5.9: The descriptive summary of the Applied Life Data

Min	1 st Q	Median	Mean	Sd	3 rd Q	Max	Skewness	Kurtosis
0.19	2.97	6.50	14.36	18.88	21.91	72.89	2.19	4.33

The descriptive statistic of the Applied Analysis dataset is further depicts in figure 5.7.

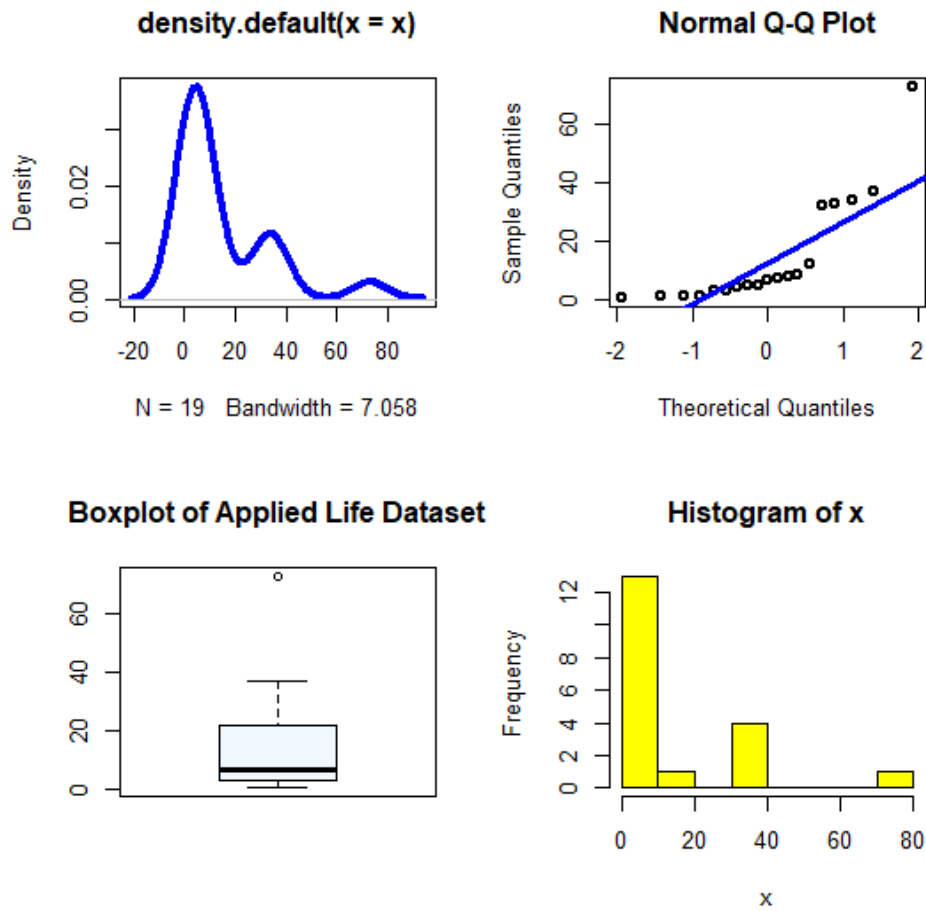


Figure 5.7: A graphical summary of the applied life dataset

Also, in order to determine the shape of the most appropriate hazard function for modeling, graphical analysis of the data become more useful. As shown in Figure 5.8, the applied life data set has an increasing failure rate as indicated by the TTT transform plot which has a concave shape.



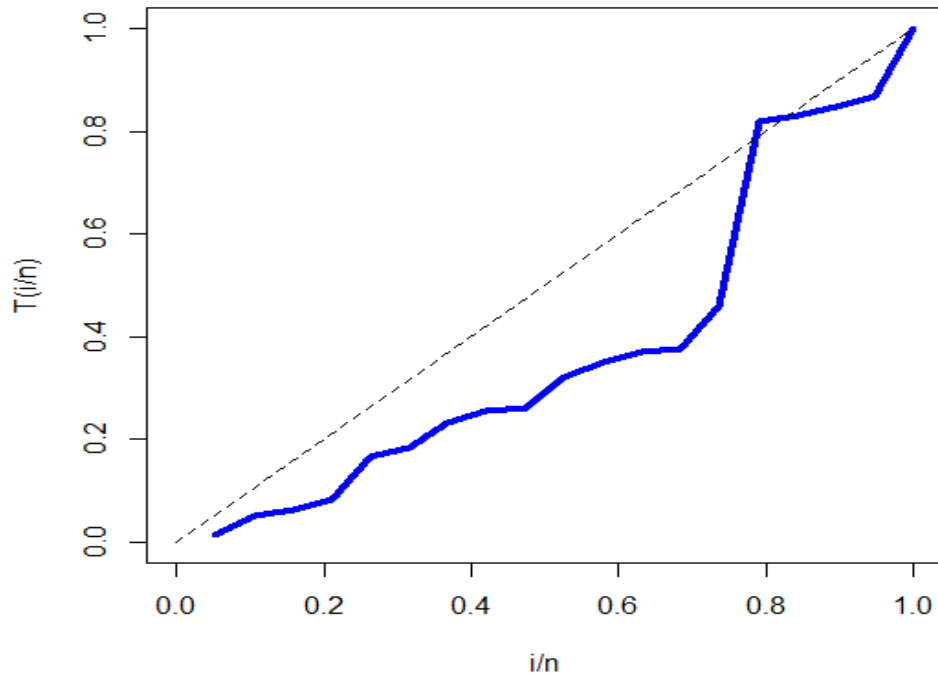


Figure 5.8: The TTT-transform plot for applied life data

The estimates of the fitted models and their respective standard errors are presented in Table 5.10. The parameters of most of the fitted distributions were significant at the 5% significant level. This can be verified by using the standard error test which states that for a parameter to be significant at the 5% significant level, the standard error should be less than half the parameter value.

For instance, for the T-TIGER model, the parameters for alpha and theta were significant at the 10% and 1% significant levels respectively.



Table 5.10: The MLE estimates of the applied life data

Model	Estimate	Std error	z-value	P-value
T-TIGER	$\hat{\alpha} = 0.767$	0.1338	5.7364	9.7×10^{-9}
	$\hat{\theta} = 38.157$	17.522	2.1777	2.9×10^{-2}
	$\hat{\lambda} = 0.795$	1.6340	0.4865	6.3×10^{-6}
	$\hat{\gamma} = 0.693$	0.2514	2.7578	5.8×10^{-3}
ETGR	$\hat{\alpha} = 0.167$	0.1523	1.0959	2.7×10^{-1}
	$\hat{\beta} = 0.457$	0.0503	9.0918	$< 2.2 \times 10^{-16}$
	$\hat{\theta} = 0.012$	0.0029	4.0912	4.3×10^{-5}
	$\hat{\lambda} = 2.522$	3.0297	0.8325	4.1×10^{-1}
TR	$\hat{\theta} = 18.32$	2.5868	7.0813	1.4×10^{-12}
	$\hat{\gamma} = 0.209$	1.3278	0.1573	8.7×10^{-1}
R	$\hat{\theta} = 16.491$	1.8916	8.7179	$< 2.2 \times 10^{-16}$

Table 5.11 gives the rest of the statistics of the log-likelihood function, AIC, AICc, HQ, BIC, A, W* and K-S. It could be deduced from the Table 5.11 that the T-TIGER provides a better fit than the competing models.



Table 5.11: The negative log-likelihood, information criteria and goodness of fit statistics for the applied life dataset

Model	-L	AIC	AICc	BIC	HQ	A	W*	K-S
T-TIGER	67.69	143.38	146.23	147.15	144.02	0.30	0.05	0.13
ETGR	69.21	146.428	149.48	150.2057	147.81	0.69	0.15	0.45
TR	88.61	181.23	181.98	183.12	181.55	0.70	0.13	0.53
R	91.56	185.13	185.36	186.07	185.28	0.75	0.14	0.57

The variance-covariance matrix for the T-TIGER model using the applied life data is given by

$$I^{-1} = \begin{bmatrix} 2.32 \times 10^{-2} & -3.58 \times 10^{-1} & -2.45 \times 10^{-1} & -1.66 \times 10^{-1} \\ -3.58 \times 10^{-1} & 3.07 \times 10^2 & 3.04 \times 10^2 & 1.01 \times 10^1 \\ -2.45 \times 10^{-1} & 3.04 \times 10^2 & 2.67 \times 10^0 & 1.87 \times 10^0 \\ -1.66 \times 10^{-1} & 1.01 \times 10^1 & 1.87 \times 10^0 & 1.76 \times 10^0 \end{bmatrix}$$

The approximately 95% CI for α , θ , λ and γ are presented in Table 5.12

Table 5.12: Confidence Interval for the model parameters

CI	α	θ	λ	γ
95%	(0.000, 0.4653)	(3.8141, 72.500)	(0, 3.9980)	(-1.0, 1.0)

The plots of empirical density and densities of the fitted models are presented in Figure 5.9. It can be seen that the T-TIGER model mimic the empirical density and CDF of the applied life dataset.



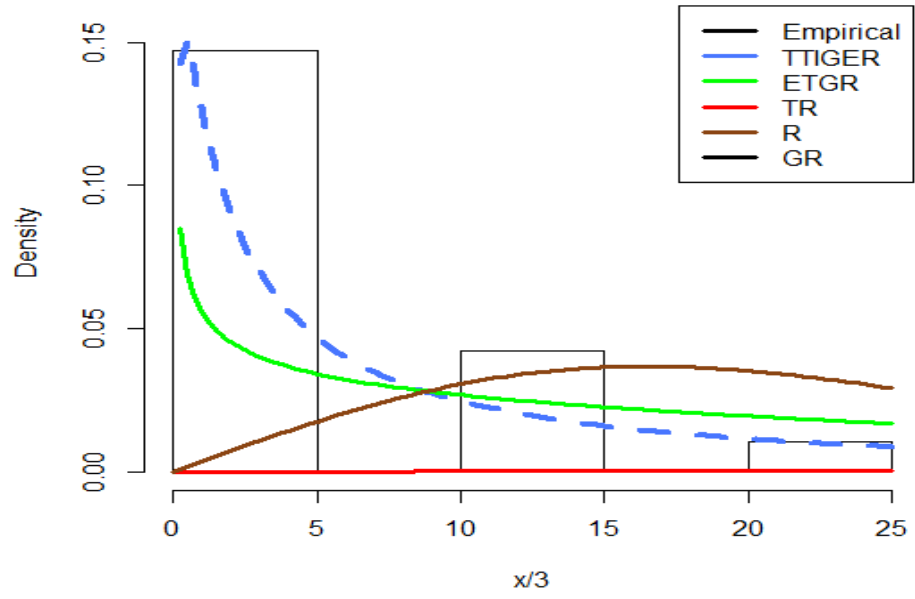


Figure 5.9: Plots of empirical and densities of the fitted models



5.3 The Application of the T-TIGEW distribution

In this section the application of the T-TIGEW model was demonstrated using real datasets, namely the aircraft windshield failure data set. These dataset is represented in Appendix B

The descriptive summary of the aircraft windshield failure data are represented in Table 5.13. It could be observed from the Table 5.13 that the first, second and third quantile (Q) of the aircraft windshield data were 1.866, 2.385 and 3.376 respectively. The minimum and maximum of the aircraft windshield data were 0.04 and 4.663 respectively. The average value of the data set was 2.563. The coefficient of skewness of 0.09 and excess kurtosis was -0.69.

The descriptive statistic of the windshield failure dataset is further presented in figure 5.10.

Table 5.13: Descriptive statistic of the Aircraft Windshield data

Min	1 st Q	Median	Mean	Sd	3 rd Q	Max	Skewness	Kurtosis
0.040	1.866	2.385	2.563	1.110	3.376	4.663	0.09	-0.69



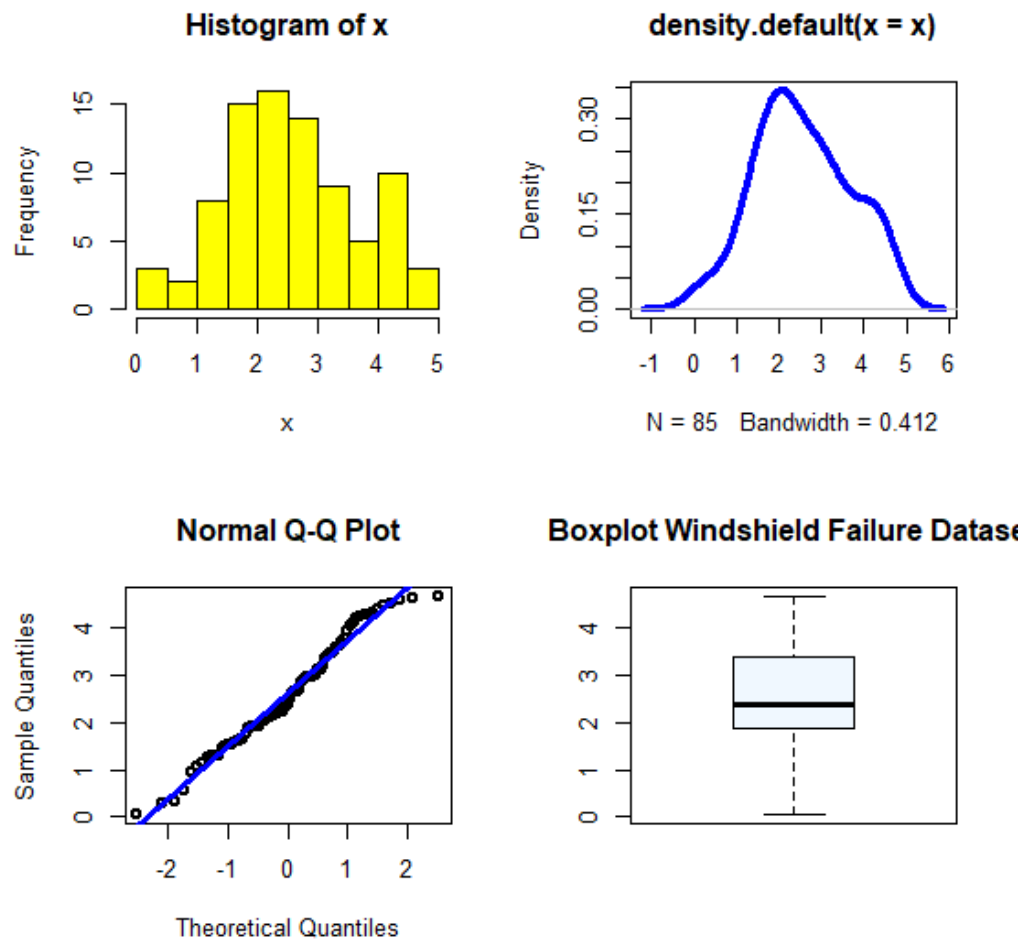


Figure 5.10: A graphical summary of the windshield failure dataset

In order to determine the shape of the most appropriate hazard function for modeling, graphical analysis of the data become more useful. As shown in Figure 5.11, the aircraft windshield data set has an increasing failure rate as indicated by the TTT-transform plot which has a concave shape.

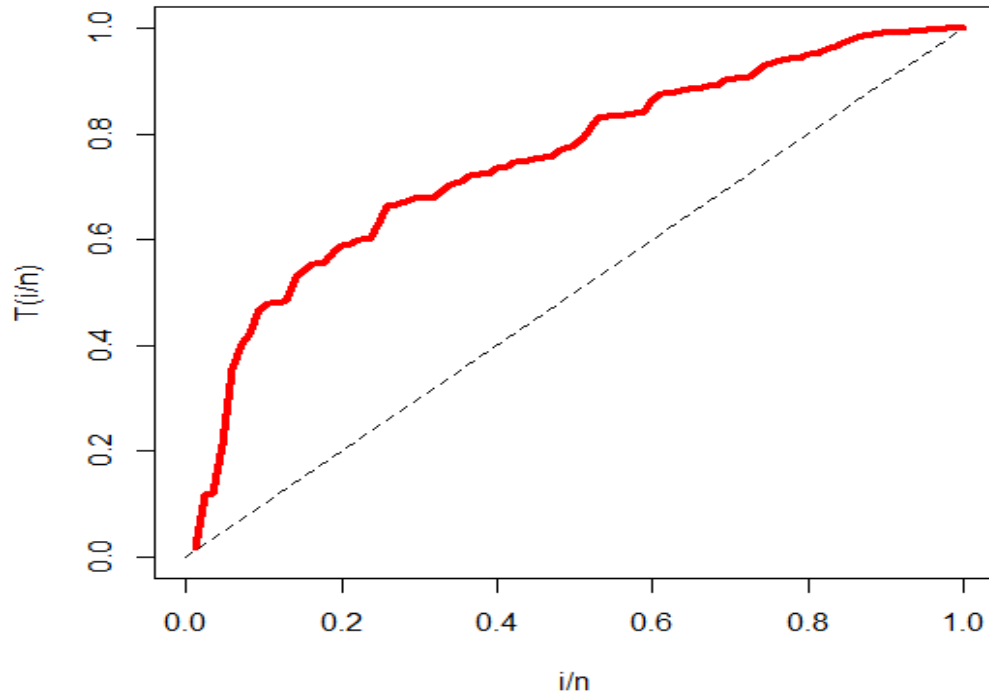


Figure 5.11: The TTT-transform plot for windshield failure data

The estimated parameters of the fitted models and their respective standard errors were presented in Table 5.14. The parameters of most of the fitted models were significant at the 5% significant level. This can be verified by using the standard error test which states that for a parameter to be significant at the 5% significant level, the standard error should be less than half the parameter value.



Table 5.14: The MLE estimates of the aircraft windshield data

Model	Estimate	Std error	z-value	P-value
T-TIGEW	$\hat{\alpha} = 0.0059$	0.0037	1.5807	1.1×10^{-10}
	$\hat{\beta} = 4.2792$	1.7602	2.4312	1.5×10^{-2}
	$\hat{\theta} = 1.0128$	0.0973	10.4044	$< 2.2 \times 10^{-16}$
	$\hat{\lambda} = 41.961$	0.0020	20697	$< 2.2 \times 10^{-16}$
	$\hat{\gamma} = -0.8391$	0.2015	-4.1639	3.13×10^{-5}
TEMW	$\hat{\alpha} = 65.564$	145.52	0.4505	6.5×10^{-1}
	$\hat{\beta} = 0.0093$	0.0237	0.3904	6.9×10^{-1}
	$\hat{\theta} = 0.0042$	0.0113	0.3573	7.2×10^{-1}
	$\hat{\lambda} = 2.5958$	2.1721	1.1951	2.3×10^{-1}
	$\hat{\gamma} = -0.7144$	0.2245	-3.1814	1.5×10^{-3}
TIGEW	$\hat{\alpha} = 0.0229$	0.0111	2.0562	3.9×10^{-2}
	$\hat{\beta} = 4.1659$	1.5650	2.6619	7.8×10^{-3}
	$\hat{\theta} = 0.0043$	0.0106	0.4047	6.9×10^{-1}
	$\hat{\lambda} = 16.9747$	0.0752	225.8121	$< 2.2 \times 10^{-16}$
TW	$\hat{\beta} = 1.9713$	0.2541	7.7572	8.7×10^{-15}
	$\hat{\theta} = 0.1759$	0.0669	2.6304	8.5×10^{-3}
	$\hat{\gamma} = -0.6599$	0.2599	-2.5389	1.1×10^{-1}



Table 5.14: The MLE estimates of the aircraft windshield data (cont'd)

Model	Estimate	Std error	z-value	P-value
WFr	$\hat{\alpha} = 0.0866$	2.76×10^{-2}	3.1401	1.6×10^{-2}
	$\hat{\beta} = 0.0871$	7.50×10^{-3}	11.5555	$< 2.2 \times 10^{-16}$
	$\hat{\theta} = 5.2134$	1.7×10^{-4}	3.01×10^4	$< 2.2 \times 10^{-16}$
	$\hat{\lambda} = 19.043$	5.48×10^{-4}	3.54×10^4	$< 2.2 \times 10^{-16}$
W	$\hat{\beta} = 2.3932$	2.10×10^{-1}	11.3887	$< 2.2 \times 10^{-16}$
	$\hat{\theta} = 0.0803$	2.22×10^{-2}	3.6162	2.9×10^{-4}
E	$\hat{\theta} = 0.3902$	4.23×10^{-2}	9.2195	$< 2.2 \times 10^{-16}$

The performance of the T-TIGEW model was compared with different models using the log-likelihood functions .AIC, AICc, HQ, BIC, A*, W* and K-S. Table 5.15 gives the rest of the statistics. It could be deduced from the Table 5.15 that the T-TIGEW model provides a better fit compared with the competing models.



Table 5.15: The negative log-likelihood, information criteria and goodness of fit statistics for the Aircraft windshield failure data

Model	-L	AIC	AICc	BIC	HQ	A*	W*	K-S
T-TIGEW	128.18	266.36	267.12	278.58	271.28	0.64	0.039	0.008
TIGEW	133.97	276.94	286.44	297.71	291.87	0.86	0.097	0.074
TEMW	131.77	273.54	274.29	285.75	278.45	0.66	0.057	0.069
WFr	131.96	271.92	272.42	281.69	275.85	0.69	0.064	0.060
TW	130.35	276.70	276.99	279.03	279.65	0.92	0.048	0.058
W	131.29	276.58	276.72	281.46	286.54	0.86	0.058	0.054
E	164.99	331.98	332.02	334.42	332.96	1.34	0.167	0.303

The Hessian matrix for the estimates of T-TIGEW model is given by

$$I^{-1} = \begin{bmatrix} 1.37 \times 10^{-5} & -6.17 \times 10^{-3} & 4.01 \times 10^{-5} & -7.08 \times 10^{-6} & 3.57 \times 10^{-4} \\ -6.17 \times 10^{-3} & 3.10 \times 10^0 & -0.02 \times 10^0 & 3.60 \times 10^{-3} & 9.14 \times 10^{-2} \\ 4.01 \times 10^{-5} & -2.00 \times 10^{-2} & 1.28 \times 10^{-4} & -2.29 \times 10^{-5} & 6.12 \times 10^{-4} \\ -7.08 \times 10^{-6} & 3.60 \times 10^{-3} & -2.29 \times 10^{-5} & 4.11 \times 10^{-6} & -1.00 \times 10^{-4} \\ 3.57 \times 10^{-4} & 9.14 \times 10^{-2} & 6.12 \times 10^{-4} & -1.00 \times 10^{-4} & 4.06 \times 10^{-2} \end{bmatrix}$$

The approximate 95% CI for α , β , θ , λ , and γ are given in Table 5.16.

Table 5.16: Confidence Interval for the model parameters

CI	α	β	θ	λ	γ
95%	(0.01,0.13)	(0.83, 7.73)	(0.01, 1.98)	(41.94, 41.98)	(-1.0, -0.44)

It can be observed that all the confidence intervals contained their respective point estimates, which indicating that some parameters of the T-TIGEW



model were significant at 5% significance level. The plots of empirical density and densities of the fitted model are presented in Figure 5.12.

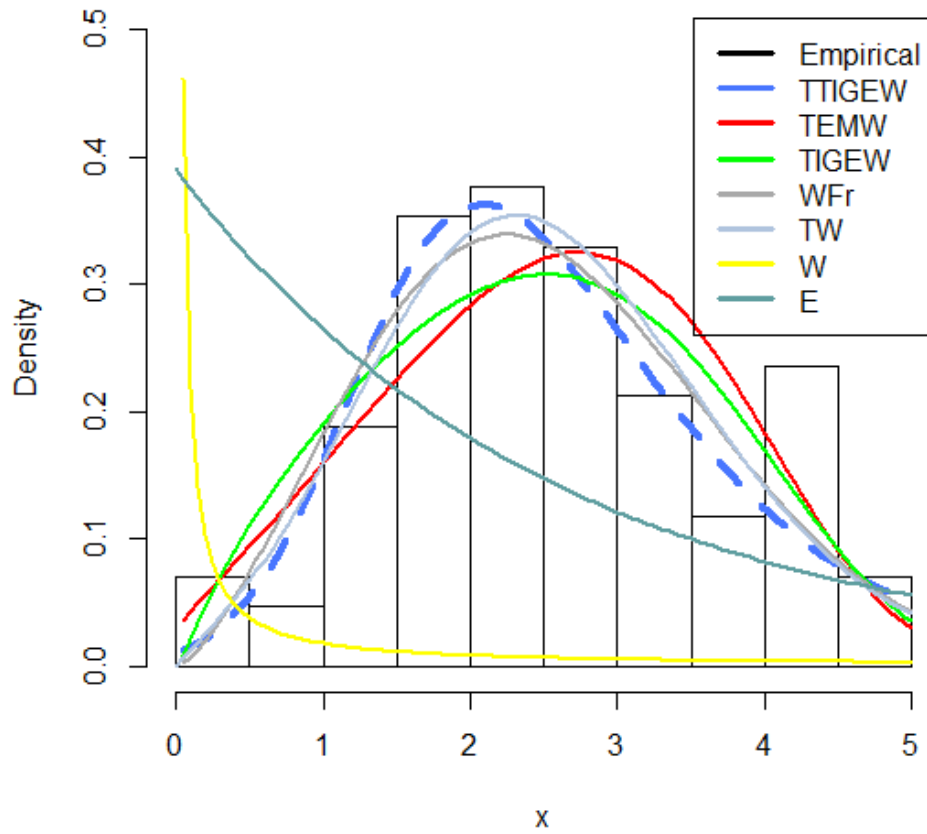


Figure 5.12: Plots of empirical and densities of the fitted models



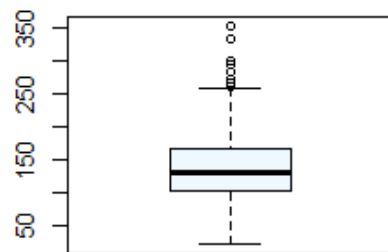
5.4 The Application of the T-TIGEFr Distribution

This section presents the application of the T-TIGEFr model. The rainfall datasets (Appendix C1) was used to evaluate the performance of the proposed model. The descriptive summary of the data is shown in Table 5.17.

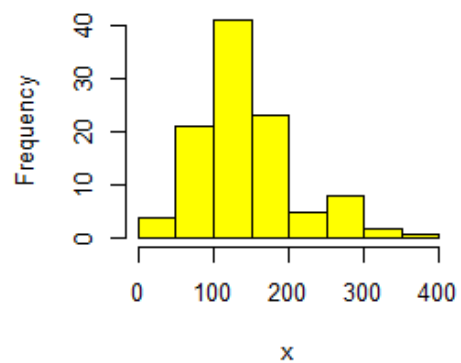
Table 5.17: Descriptive statistic of the rainfall data

Min	1 st Q	Median	Mean	Sd	3 rd Q	Max	Skewness	Kurtosis
20.7	101.6	131.6	144.6	66.18	165.5	354.7	0.93	0.73

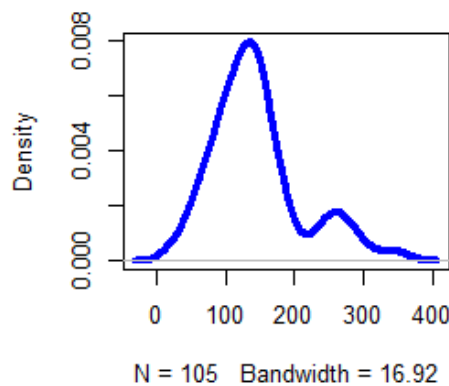
Boxplot of Rainfall Data



Histogram of x



density.default(x = x)



Normal Q-Q Plot

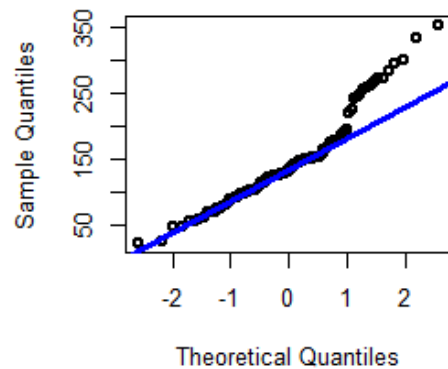


Figure 5.13: A graphical summary of the rainfall data



In order to determine the shape of the most appropriate hazard function for modeling, graphical analysis of the data become more useful. In this context, the TTT-transform plot is very useful. As shown in Figure 5.23, the data set illustrated by the TTT-transform plot has a concave shape which provides evidence that the data set an increasing failure rate as indicated by the TTT-transform plot which has a concave shape.

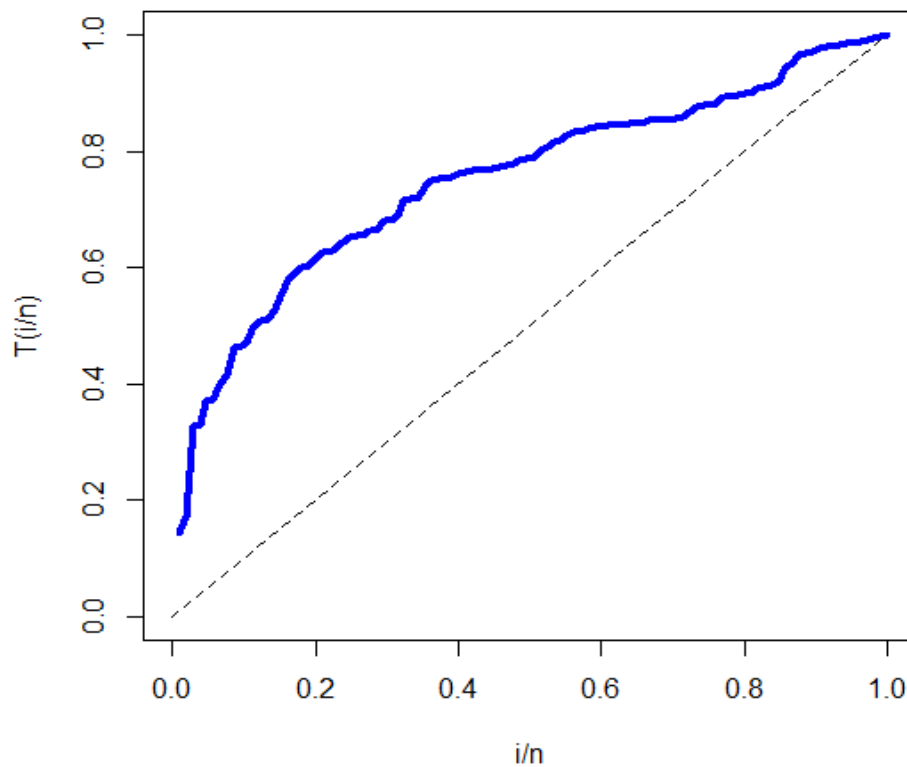


Figure 5.14: The TTT-transform plot for rainfall dataset

The Table 5.18 presents the estimated parameters of the fitted distributions with their respective standard errors were estimated by maximum likelihood. The parameters of most of the fitted distributions were significant at the 5% significant level. This can be verified by using the standard error test which states that for a parameter to be significant at the 5% significant level, the standard error should be less than half the parameter value.



Table 5.18. The MLE estimates of parameters of the rainfall data

Model	Estimate	Std error	z-value	P-value
T-TIGEFr	$\hat{\alpha} = 0.3761$	7.90×10^0	0.0476	9.6×10^{-11}
	$\hat{\beta} = 1.833$	1.13×10^{-1}	16.1132	$< 2.0 \times 10^{-16}$
	$\hat{\theta} = 0.5980$	8.79×10^{-3}	67.9953	$< 2.2 \times 10^{-16}$
	$\hat{\lambda} = 141.247$	1.67×10^2	0.8475	3.9×10^{-11}
	$\hat{\gamma} = -0.8725$	9.07×10^{-2}	-9.6189	$< 2.0 \times 10^{-16}$
GTFr	$\hat{\alpha} = 1.65038$	1.03×10^{-1}	15.9941	$< 2.2 \times 10^{-16}$
	$\hat{\beta} = 41.0956$	1.08×10^1	3.7936	1.5×10^{-4}
	$\hat{\theta} = 48.5427$	9.17×10^1	5.2916	1.2×10^{-7}
	$\hat{\lambda} = 0.0011$	3.75×10^{-1}	0.0003	9.9×10^{-1}
	$\hat{\gamma} = 8.3270$	9.59×10^1	0.0867	9.3×10^{-1}
Fr	$\hat{\beta} = 1.6497$	1.03×10^{-1}	15.995	$< 2.2 \times 10^{-16}$
	$\hat{\theta} = 99.934$	6.29×10^2	15.881	$< 2.2 \times 10^{-16}$
E	$\hat{\theta} = 0.0069$	6.70×10^{-4}	10.247	$< 2.2 \times 10^{-16}$

Table 5.19 gives the statistics of log-likelihood function, AIC, AICc, HQ, BIC, A*, W* and K-S. It could be deduced from the Table 5.22 that the T-TIGEFr provides a better fit than the competing models.



Table 5.19: The negative log-likelihood, information criteria and goodness of fit statistics for the Rainfall dataset

Model	-L	AIC	AICc	BIC	HQ	A*	W*	K-S
T-TIGEFr	602.6	1215.1	1215.7	1228.4	1220.5	3.4	0.59	0.13
GTFr	608.6	1227.2	1227.8	1240.5	1232.6	4.1	0.71	0.15
Fr	608.6	1221.2	1221.3	1226.5	1223.4	4.1	0.71	0.15
E	627.3	1256.5	1256.5	1259.2	1257.6	0.9	0.75	0.30

The inverse Hessian matrix for the estimates of the T-TIGEFr model using the Rainfall dataset is given by

$$I^{-1} = \begin{bmatrix} 6.245 \times 10^1 & -1.055 \times 10^{-3} & -7.574 \times 10^2 & -2.532 \times 10^1 & 3.008 \times 10^{-5} \\ -1.055 \times 10^{-3} & 1.280 \times 10^{-2} & 3.514 \times 10^{-2} & 3.310 \times 10^0 & -2.369 \times 10^{-4} \\ -7.574 \times 10^2 & 3.514 \times 10^{-2} & 9.214 \times 10^3 & -5.455 \times 10^2 & -8.577 \times 10^{-4} \\ -2.532 \times 10^1 & 3.310 \times 10^0 & -5.455 \times 10^2 & 2.778 \times 10^4 & 5.820 \times 10^{-1} \\ 3.008 \times 10^{-5} & -2.369 \times 10^{-4} & -8.577 \times 10^{-4} & 5.820 \times 10^{-1} & 8.227 \times 10^{-3} \end{bmatrix}$$

The approximate 95% CI for the $\alpha, \beta, \theta, \lambda,$ and γ are represented in Table 5.20.

Table 5.20: Confidence Interval for the model parameters

CI	α	β	θ	λ	γ
95%	(0, 5.274)	(1.602, 2.045)	(0, 19.64)	(148.54, 341.61)	(-0.93, 0.238)



It can be observed that all the confidence intervals contained their respective point estimates. The plots of empirical and densities of the fitted models are presented in Figure 5.24

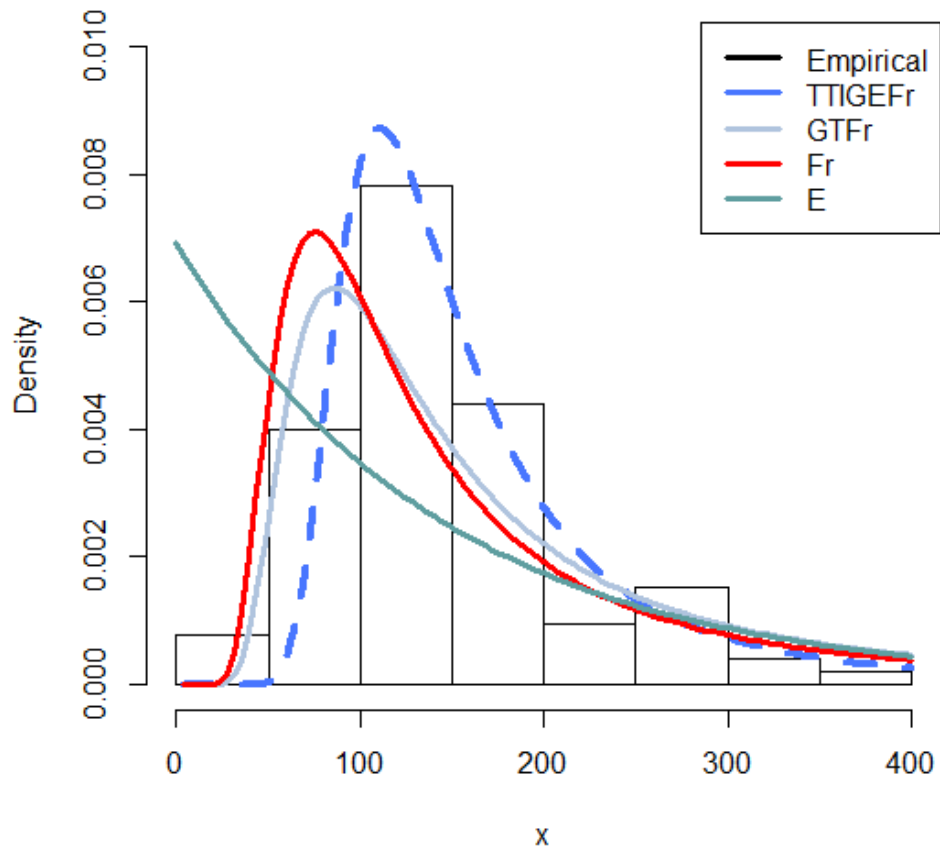


Figure 5.15: Plots of empirical and densities of the fitted model

The second dataset used to assess the flexibility of the T-TIGEFr model is the breaking strength dataset. This is uncensored data set from the work of Nichols and Padgett (2006) and displayed in Appendix C2. This dataset is recently used by Mahmoud and Mandouh (2013).

The descriptive statistics of the breaking stress of carbon fibers dataset is presented in Table 5.21, and it could be observed that the first, second and



third quantile of the Breaking stress dataset are respectively 1.302, 1.544 and 1.814. The minimum and maximum of breaking stress of carbon fibers dataset are 0.920 and 5.306 respectively. The average value of the data set is 1.658. The coefficient of skewness of 3.13 and excess kurtosis was 14.08.

Table 5.21: Descriptive statistic of the breaking stress data

Min	1 st Q	Median	Mean	Sd	3 rd Q	Max	Skewness	Kurtosis
0.920	1.302	1.544	1.658	0.6	1.814	5.306	3.13	14.08

Further descriptive of the Breaking stress of carbon fibers dataset is presented in Figure 5.25

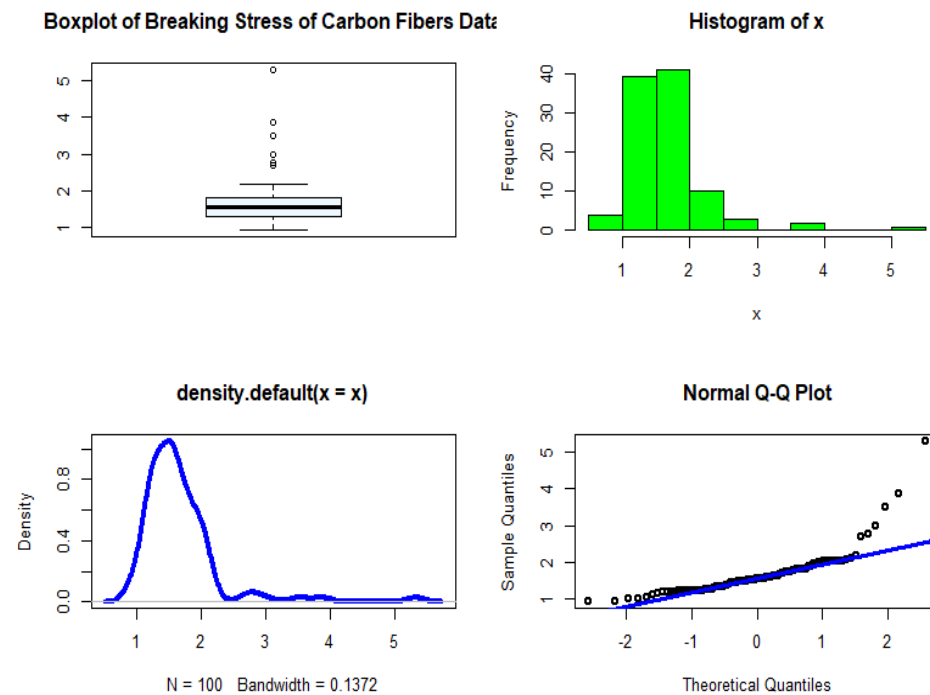


Figure 5.16: A graphical summary of the breaking stress data



Figure 5.17 represented the breaking stress of carbon fibers dataset which was illustrated by the TTT transform plot and has a concave shape which provides evidence that the data set an increasing failure rate as indicated by the TTT transform plot which has a concave shape.

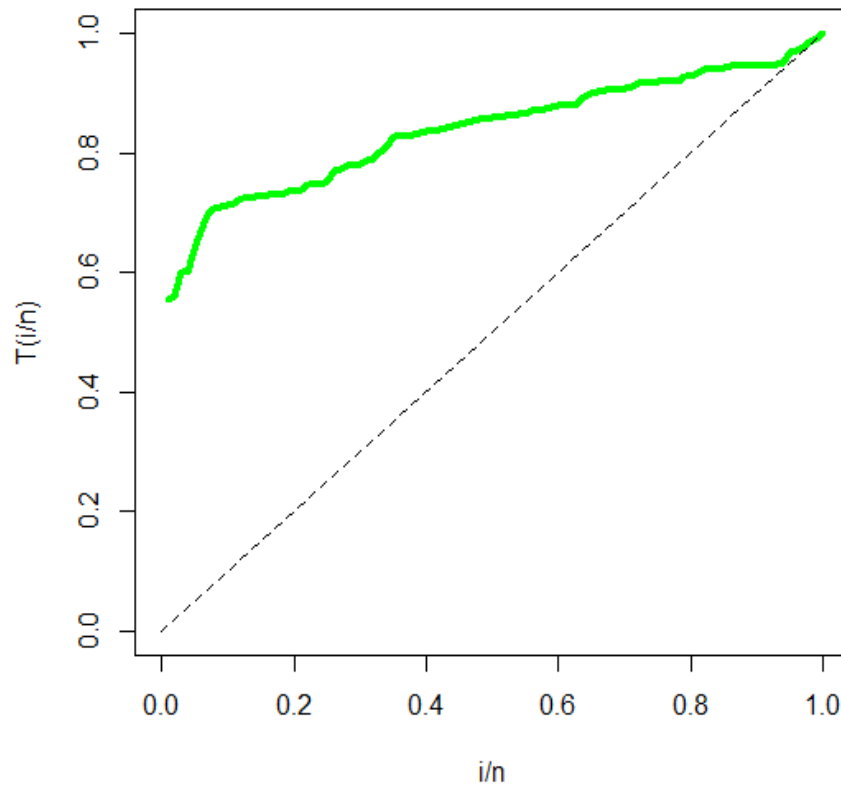


Figure 5.17: The TTT-transform plot for breaking stress data

The Table 5.22 presents the maximum likelihood estimates of the fitted models. All the estimates are significant at the five per cent (5%) significant level, except that of the parameter α .



Table 5.22. The MLE estimates of the breaking stress dataset

Model	Estimate	Stand error	z-value	P-value
T-TIGEFr	$\hat{\alpha} = 0.7692$	2.67×10^0	0.2879	7.7×10^{-6}
	$\hat{\beta} = 3.2186$	3.82×10^{-1}	8.4325	$< 2.2 \times 10^{-16}$
	$\hat{\theta} = 0.0519$	7.30×10^{-3}	7.1440	9.1×10^{-13}
	$\hat{\lambda} = 0.0128$	1.9×10^{-3}	6.7433	1.5×10^{-11}
	$\hat{\gamma} = 0.8819$	$0.1.62 \times 10^{-1}$	5.4277	5.7×10^{-8}
EGFr	$\hat{\alpha} = 2.1706$	2.63×10^0	0.8238	4.1×10^{-1}
	$\hat{\beta} = 4.4313$	1.85×10^1	0.2364	8.1×10^{-1}
	$\hat{\theta} = 1.1957$	8.88×10^{-1}	1.3469	1.8×10^{-1}
	$\hat{\lambda} = 2.5505$	2.82×10^0	0.9034	3.7×10^{-1}
BXFr	$\hat{\alpha} = 0.1091$	2.00×10^{-2}	5.4485	5.1×10^{-8}
	$\hat{\beta} = 0.0373$	2.60×10^{-2}	1.4225	$< 2.2 \times 10^{-16}$
	$\hat{\theta} = 9.7962$	3.20×10^{-5}	3.0×10^6	$< 2.2 \times 10^{-16}$
TFr	$\hat{\beta} = 4.7123$	3.66×10^{-1}	12.883	$< 2.0 \times 10^{-16}$
	$\hat{\theta} = 1.2656$	5.79×10^{-2}	21.8705	$< 2.0 \times 10^{-16}$
	$\hat{\gamma} = -0.7169$	2.61×10^{-1}	-2.7445	6.1×10^{-3}
Fr	$\hat{\beta} = 4.3726$	3.28×10^{-1}	13.34	$< 2.2 \times 10^{-16}$
	$\hat{\theta} = 1.3968$	3.37×10^{-2}	41.45	$< 2.2 \times 10^{-16}$
E	$\hat{\theta} = 0.6032$	6.03×10^{-2}	10.0000	$< 2.2 \times 10^{-16}$
R	$\hat{\theta} = 1.2458$	6.23×10^{-2}	20.0000	$< 2.2 \times 10^{-16}$



The model selection was carried out to determine the most appropriate model. The test statistic of log-likelihood, AIC, AICc, BIC, HIQ, A*, W* and K-S were used. It could be deduced from the Table 5.23 that the T-TIGEFr model exhibits a better fit in modeling the breaking stress data compared with its competing distributions.

Table 5.23: The negative log-likelihood, information criteria and goodness of fit statistics for the Breaking Stress dataset

Model	-L	AIC	AICc	BIC	HQ	A*	W*	K-S
T-TIGEF	51.250	105.010	109.648	118.036	114.282	0.4173	0.0593	0.0616
EGFr	52.889	113.779	114.201	124.201	117.997	0.6091	0.0799	0.0755
WFr	51.609	111.218	111.639	121.639	115.435	0.4507	0.0627	0.0657
BXFr	55.269	116.537	116.787	124.353	119.701	0.8426	0.1039	0.0833
TFr	52.699	111.398	111.648	119.214	114.562	0.6209	0.0871	0.0782
Fr	53.692	111.383	111.507	116.593	113.492	0.7658	0.1090	0.0875
E	150.55	303.103	303.144	305.708	304.157	2.6556	0.3811	0.4439
R	102.61	207.220	207.261	209.825	208.275	4.0769	0.6237	0.3019

The variance-covariance matrix for the estimates of the T-TIGEFr model using the breaking stress dataset is given by

$$I^{-1} = \begin{bmatrix} 7.1 \times 10^1 & -5.7 \times 10^{-2} & -1.7 \times 10^1 & -1.3 \times 10^1 & 1.1 \times 10^{-2} \\ -5.7 \times 10^{-2} & 1.5 \times 10^{-1} & -1.8 \times 10^{-2} & 8.7 \times 10^1 & -4.2 \times 10^{-2} \\ -1.7 \times 10^1 & -1.8 \times 10^{-2} & 4.4 \times 10^{-1} & -8.4 \times 10^1 & 1.1 \times 10^{-3} \\ -1.3 \times 10^1 & 8.7 \times 10^1 & -8.4 \times 10^1 & 2.2 \times 10^3 & -1.4 \times 10^1 \\ 1.1 \times 10^{-2} & -4.2 \times 10^{-2} & 1.1 \times 10^{-3} & -1.4 \times 10^1 & 2.6 \times 10^{-2} \end{bmatrix}$$

The approximate 95% CI for $\alpha, \beta, \theta, \lambda,$ and γ are displayed in Table 5.24.



Table 5.24: Confidence Interval for the model parameters

CI	α	β	θ	λ	γ
95%	(0, 6.001)	(2.47, 3.967)	(0, 1.903)	(0, 121.72)	(0.564, 1.00)

Figure 5.18 shows the empirical density and the fitted densities of the distributions.

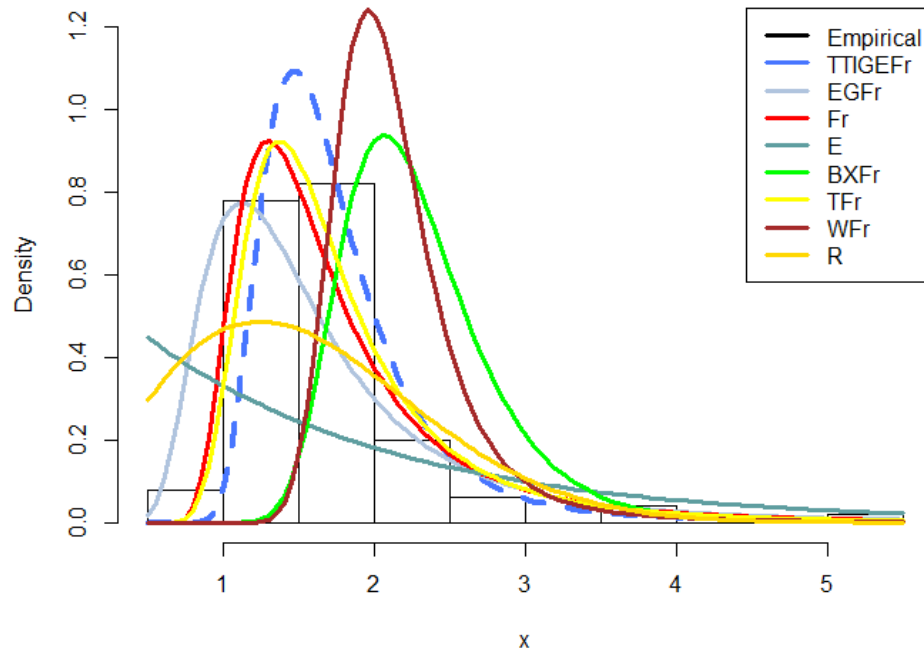


Figure 5.18: Empirical and densities plots of the fitted



5.5 The Application of the T-TIGEEE Distribution

The T-TIGEEE model was subjected to the fibre strength dataset as represented in Appendix D. This dataset was taken from the work of Selim and Badar (2016). The data was first considered by Badar and Priest (1982).

The descriptive summary of the dataset is given in Table 5.25. It could be seen that the dataset of the Fibre Strength is positively skewed with a coefficient of 0.62 and a kurtosis value of 0.18.

Table 5.25: Descriptive statistic of the fibre strength data

Min	1 st Q	Median	Mean	Sd	3 rd Q	Max	Skewness	Kurtosis
1.90	2.55	2.99	3.06	0.62	3.421	5.02	0.62	0.18

The descriptive statistics of the dataset is further displayed in Figure 5.19.

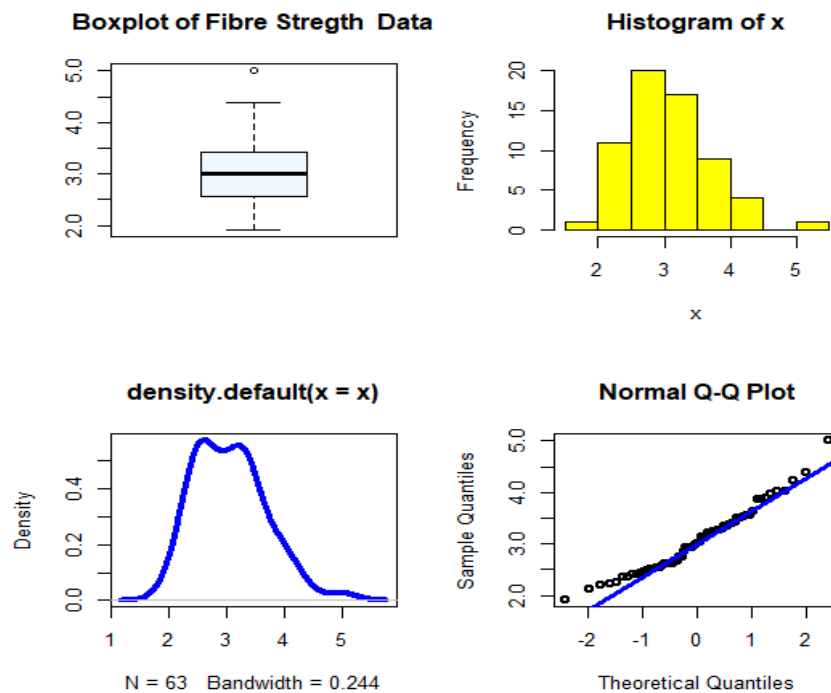


Figure 5.19: A graphical summary of the fibre strength data



The TTT-transform plot which is displayed in Figure 5.20 revealed that the Machine data set has an increasing failure rate since the TTT-transform plot in the Figure 5.20 which has a convex shape

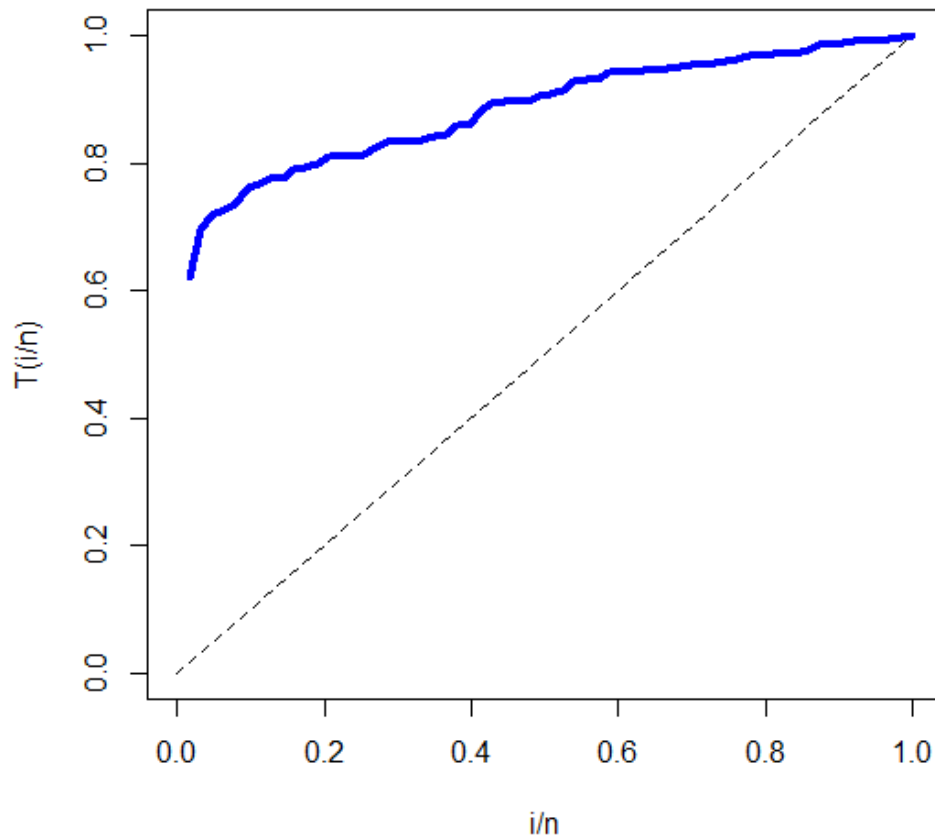


Figure 5.20: The TTT-transform plot for fibre strength data

The maximum likelihood estimates, standard errors of the estimate for the parameters of the T-TIGEEE model and the competitive models using the fibre strength dataset are represented in Table 5.26.



Table 5.26: The MLE estimates of models using the fibre strength data

Model	Estimate	Std error	z-value	P-value
T-TIGEEE	$\hat{\alpha}=5.41$	0.003	1.90×10^3	$< 2.0 \times 10^{-16}$
	$\hat{\beta}=1.18$	47.12	0.0251	9.8×10^{-10}
	$\hat{\theta}=1.99$	0.27	7.3744	1.6×10^{-13}
	$\hat{\lambda}=23.52$	108.15	0.2175	8.3×10^{-16}
	$\hat{\gamma}=0.832$	0.148	5.621×10^1	$< 2.2 \times 10^{-16}$
GTFr	$\hat{\alpha}=5.43$	0.51	10.6999	$< 2.2 \times 10^{-16}$
	$\hat{\beta}=30.92$	0.83	37.4304	$< 2.2 \times 10^{-16}$
	$\hat{\theta}=7.45$	3.42	2.1758	2.9×10^{-2}
	$\hat{\gamma}=0.09$	0.02	4.4485	8.6×10^{-6}
	$\hat{\lambda}=3.7 \times 10^{-4}$	5.36	-0.0001	9.9×10^{-1}
EE	$\hat{\beta}=2.1 \times 10^3$	9.0×10^6	2.3×10^8	$< 2.2 \times 10^{-16}$
	$\hat{\theta}=-0.29$	0.69	-0.4258	6.7×10^{-1}
E	$\hat{\theta}=3.2 \times 10^{-1}$	4.0×10^{-2}	7.9373	2.0×10^{-15}

The model selection was performed using the log-likelihood function, AIC, AICc, HQ, BIC, A*, W* and K-S statistics. It could be deduced from the Table 5.27 that the T-TIGEEE model with respect to the given data set provides a better fit than the comparative models.



Table 5.27: The negative log-likelihood, information criteria and goodness of fit statistics for the Fibre Strength data

Model	-L	AIC	AICc	BIC	HQ	A*	W*	K-S
T-TIGEEE	56.44	122.88	123.93	133.60	127.09	0.35	0.07	0.086
GTFr	58.90	127.80	128.62	138.52	133.47	0.39	0.09	0.13
EE	65.44	134.87	135.07	139.16	136.56	0.51	0.09	0.21
E	133.45	268.89	268.96	271.03	269.73	0.37	0.06	0.49

Figure 5.21 displayed the plots of empirical density and densities of the fitted models using the Fibre dataset

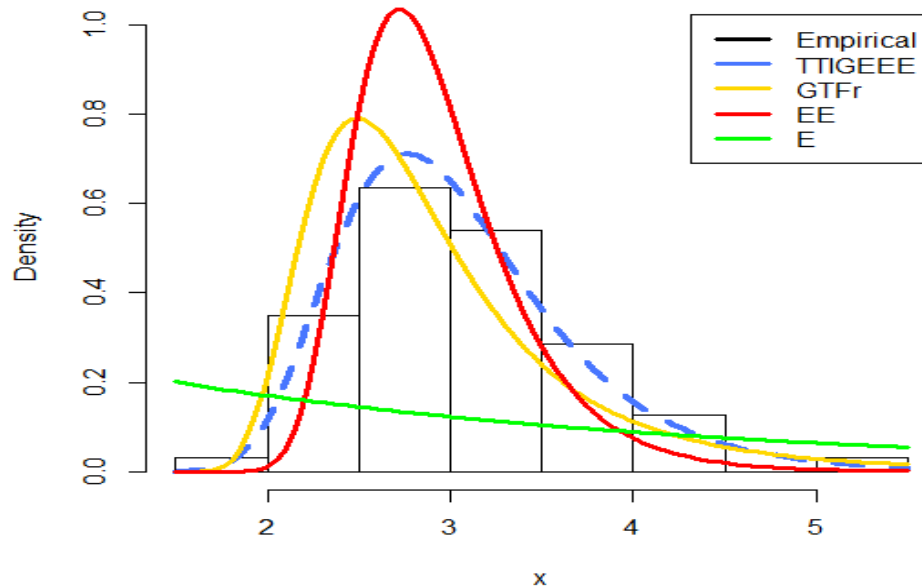


Figure 5.21: Empirical and densities plots of the fitted models



CHAPTER SIX

SUMMARY, CONCLUSIONS AND RECOMMENDATIONS

6.1 Introduction

This chapter presents the summary, conclusions and recommendations of the study in three different sections.

6.2 Summary

The lack of flexibility and tractability was identified in literature and the main objective of this study was to develop the Transmuted Type I General Exponential family of distributions to correct it. The relevant literature underpin this study were reviewed. Two different generators were compounded to develop the T-TIGE family. All the stated objectives of this study were successfully achieved. The results of this study were presented in two different fronts, namely theoretical and empirical fronts. Theoretical results include the development of the T-TIGE generator. Five special models were derived from the T-TIGE generator. The maximum likelihood estimators were developed for the unknown parameters of the T-TIGE family. The statistical properties of the T-TIGE family were derived. The behaviour of the estimators were examined using the Monte Carlo Simulation technique.

Results from the empirical perspective clearly indicate the usefulness of the special models of the T-TIGE family when applied to different real datasets.



6.3 Conclusions

The deficiency in the work of Hamedani et al. (2018) was corrected by the development of the T-TIGE generator. Skewness has been induced into the work of Hamedani et al. (2018) by adding a transmutation parameter. Clearly, this brings a new application of theory and empirical tools for data analyses onto the existing body of literature.

The statistical properties were derived and the maximum likelihood estimation technique was employed to develop the estimators of the parameters of T-TIGE family. These new statistical properties and the estimators derived are very important in statistical analyses and inferences.

The Monte Carlo Simulation was conducted to examine the estimators and it was concluded these estimators are stable and close to their true values. It can therefore be concluded the estimation technique used was appropriate.

This study generalized five new special models using the proposed generator. From the results of the this study, it was concluded that the proposed T-TIGE generator possesses bath-tub shaped curves, which serves the practical needs of for studying the monotone hazard rates and fitness of the parameters.

The usefulness and dynamism of the special models were demonstrated. From the results, it was found that the new special models of the T-TIGE family performed better than their competing models. It was therefore concluded that the ideas that originally motivated for this study indeed has its justification because the special models of the proposed generator have better fit and minimal loss of information with the different types of real datasets in modeling.



6.4 Recommendations

Based on the results from this study, the following are recommended:

- It is recommended that the T-TIGE family of distributions can be relied upon to model sets of given data.
- This study used the QRTM to generalize the TIGE class of distributions. It is recommended that other generalized families of distributions which should be different from QRTM can be used to generalize the work of Hamedani et al. (2018).
- The study uses the maximum likelihood method in estimating the parameters. It is recommended that further work consider more detail comparisons by using Bayesian estimation paradigm, in a future study.
- Five (5) special models were generalized using the T-TIGE generator, it is recommended that many more models be transformed using the proposed T-TIGE generator in further studies. This will therefore bring more innovations in addition to the existing models.
- This study focuses on univariate continuous distributions; it may be appropriate for a further study in terms of its extension to a bivariate models and subsequently multivariate set-up. This study therefore recommends bivariate extensions of the proposed generator. For instance, a parametric regression models may be developed to study the relationship between an output and input variables.
- Furthermore, this study recommends an analysis of the behaviour of the T-TIGE generator in the presence of censored data or observations, given the fact that the special models of the T-TIGE generator used uncensored data to demonstrate the flexibility of the T-TIGE family.



- From the finding of this study, it was established that the special models of the proposed T-TIGE family of distributions performed better than the competing models. It is therefore recommended that these special models of the proposed generator can be used as standard models to estimate a model that represents real life phenomenon when samples have different shapes and tails.

It is expected that this study will serve as a reference and help to advance future research in the area of applied statistics and other related disciplines.



REFERENCES

- Aarset, M.V.(1987). How to identify a bathtub hazard rate. *IEEE Transactions on Reliability*,**36**(1):106-108.
- Abbas, K., and Tang, Y. (2015). Analysis of Fréchet distribution using reference priors. *Communications in Statistics-Theory and Methods*, **44**(14), 2945-2956.
- Abd El-Monsef, M. M. E., Sweilam, N. H., and Sabry, M. A. (2020). The exponentiated power Lomax distribution and its applications. *Quality and Reliability Engineering International*.
- Abdul-Moniem, I. B. (2017). Order statistics from Power Lomax distribution. *International Journal of Innovative Science, Engineering and Technology*, **4**:1-4.
- Abouammoh, A. M., and Alshingiti, A. M. (2009). Reliability estimation of generalized inverted exponential distribution. *Journal of Statistical Computation and Simulation*, **79**(11), 1301-1315.
- Achieng, O. M., and No, I. (2010). Actuarial modeling for insurance claim severity in motor comprehensive policy using industrial statistical distributions. *In International Congress of Actuaries, Cape Town ;712*.



Adcock, C., Eling, M., and Loperfido, N. (2015). Skewed distributions in finance and actuarial science: a review. *The European Journal of Finance*, **21**(13-14), 1253-1281.

Afify, A.Z., Yousof, H.M. and Nadarajah, S. (2017). The beta transmuted-H family of distributions: properties and applications. *Statistics and its Inference*, **10**, 505-520.

Afify, A.Z., Hamedani, G.G., Indranil Ghosh and Mead, M.E. (2015). The Transmuted Marshall-Olkin Fréchet Distribution: Properties and applications. *International Journal of Statistics and Probability*; **4**(4):131-148

Afify, A. Z., Yousof, H. M., Cordeiro, G. M., Ortega, E. M., and Nofal, Z. M. (2016). The Weibull Fréchet distribution and its applications. *Journal of Applied Statistics*, **43**(14), 2608-2626.

Ahmad, Z., Mahmoudi, E., and Kharazmi, O. (2020). On modeling the earthquake insurance data via a new member of the TX family. *Computational intelligence and neuroscience*.

Akaike, A. (1973). Information theory and an extension of maximum likelihood principle. In *International Symposium on Information Theory, 2nd, Tsahkadsor, America SSR*, 267-281

Akaike, A. (1974). A new look at the statistical model identification. *IEEE Transactions on Automatic Control* **19**(6):716-723.



- Alexander, C., Cordeiro, G.M., Ortega, E.M., and Sarabia, J.M. (2012). Generalised beta-generated distributions. *Computational Statistics and Data Analysis*, **56**(6): 1880-1897.
- Alizadeh, M., Yousof, H. M., Afify, A. Z. , Cordeiro, G. M. Mansoor, M.(2018). The complementary generalized transmuted Poisson-G family of distributions, *Austrian Journal. Statist.*, **47** , 51–71. 1
- Alizadeh, M., Cordeiro, G. M., Pinho, L. G. B., and Ghosh, I. (2017). The Gompertz-G family of distributions. *Journal of Statistical Theory and Practice*, **11**(1), 179-207.
- Alizadeh, M., Merovci, F., and Hamedani, G. G. (2017). Generalized transmuted family of distributions: properties and applications. *Hacettepe Journal of Mathematics and Statistics*, **46**(4), 645-667.
- Almalki, S. J., and Yuan, J. (2013). A new modified Weibull distribution. *Reliability Engineering and System Safety*, **111**:164-170.
- Alshawarbeh, E., Lee, C., and Famoye F. (2012). The beta-Cauchy distribution. *Journal of Probability and Statistical Science*, **10**(1):41-57.
- Alzaatreh, A., Lee, C., and Famoye F. (2013). A new method for generating families of continuous distributions. *Metron*, **71**(1):63-79.
- Alzaatreh, A., and Ghosh, I. (2015). On the Weibull-X family of distributions. *Journal of Statistical Theory and Applications*, **14**(2), 169-183.



- Alzagal, A., Famoye F., and Lee, C. (2013). Exponentiated T-X family of distributions with some applications. *International Journal of Statistics and Probability*, **2**(3):31-49.
- Arcagni, A., and Porro, F. (2014). The graphical representation of inequality. *Revista Colombiana de estadística*, **37**(2), 419-437.
- Aryal, G. R., and Tsokos, C. P. (2009). On the transmuted extreme value distribution with application. *Nonlinear Analysis: Theory, Methods & Applications*, **71**(12), e1401-e1407.
- Aryal, G. R. and Tsokos, C.P. (2011). Transmuted Weibull distribution: A generalization of the Weibull probability distribution. *European journal of Pure and Applied Mathematics*. **4**(2):89-102
- Ashour, S. K., and Eltehiwy, M. A. (2013a). Transmuted lomax distribution. *American Journal of Applied Mathematics and Statistics*, **1**(6): 121-127.
- Ashour, S. K., and Eltehiwy, M. A. (2013b). Transmuted exponentiated Lomax distribution. *Australian Journal of Basic and Applied Sciences*, **7**(7):658-667.
- Athayde, E., Azevedo, C., Leiva, V., and Antonio, S. (2012). About Birnbaum-Sanders based on Johnson system. *Communication in Statistics-Theory and methods*, **41**(11):2061-2079.
- Azzalini, A. (1985). A class of distributions which includes the normal ones. *Scandinavian Journal of Statistics*, **12**(2):171-178



- Azzalini, A. (1986). Further results on class of distribution which includes the normal ones. *Statistica*, **46**(2):199-208.
- Bader, M. G., and Priest, A. M. (1982). Statistical aspects of fibre and bundle strength in hybrid composites. *Progress in science and engineering of composites*, 1129-1136.
- Bakouch, H.S., Jamal, F., Chesneau, C., and Nasir, A. (2017). A new transmuted family of distributions: Properties and estimation with applications.
- Barlow, R.E. and Doksum, K.A. (1972). Isotonic tests for convex orderings. In *Proceedings of the 6th Berkeley Symposium*, **1**:293-323.
- Bindu, P., and Sangita, K. (2015). Double lomax distribution and its applications. *Statistica*, **75**(3):331-432
- Birnbaum, Z.W. and Saunders, S.C. (1969). Estimation for a family of life distributions with applications to fatigue. *Journal of Applied Probability*, **6**:328-348.
- Blumenson, L.E., and Miller, K.S. (1963). Properties of generalised Rayleigh distributions. *Annals of Mathematical statistics*
- Boland, P. J. (2007). *Statistical and probabilistic methods in actuarial science*. CRC Press.
- Bolker, B. (2017). R Development Core Team. Package bbmle: Tools for general maximum likelihood estimation.



- Bonferroni, C.E. (1930). *Elementi di statistica generate*, Libreria Seber, Firenze.
- Bourguignon, M., Gosh, I., and Cordeiro, G.M. (2016). General results for the transmuted family of distributions and new models. *Journal of Probability and Statistics*,
- Burr, I.W. (1942). Cumulative frequency functions. *Annals of Mathematical Statistics*, **14**(2): 215-232.
- Brito, E., G. M. Cordeiro, H. M. Yousof, M. Alizadeh, and G. O. Silva. The Topp–Leone odd log-logistic family of distributions. *Journal of Statistical Computation and Simulation* **87**(15): 3040-3058.
- Broyden, C. G. (1970). The convergence of a class of double-rank minimization algorithms: The new algorithm. *IMA journal of applied mathematics*, **6**(3), 222-231.
- Carrasco, J. M., Ortega, E. M., and Cordeiro, G. M. (2008). A generalized modified Weibull distribution for lifetime modeling. *Computational Statistics and Data Analysis*, **53**(2): 450-462.
- Castillo, E., Hadi, A. S., Balakrishnan, N., and Sarabia, J. M. (2005). Extreme value and related models with applications in engineering and science.
- Chang, S.M. and Genton, M.G. (2007). Extreme value distributions for the skew-symmetric family of distributions. *Communications in Statistics-Theory and Methods*, **36** (9):1705-1717.



- Cordeiro, G.M. and de Castro, M. (2011). A new family of generalised distributions. *Journal of Statistical Computation and Simulation*, **81**(7):883-898.
- Cordeiro, G.M., Ortega, E.M.M. and Silva, G.O. (2012). The beta extended Weibull family. *Journal of probability and Statistical Science*, **10**(10):15-40.
- Cordeiro, G. M., Ortega, E. M., Popović, B. V., and Pescim, R. R. (2014). The Lomax generator of distributions: Properties, minification process and regression model. *Applied Mathematics and Computation*, **247**: 465-486.
- Coroni, C. (2002). The correct "ball bearing" data. *Lifetime Data Anal.*, to appear.
- Elbatal, I. (2013). Transmuted generalized inverted exponential distribution. *Stochastics and Quality Control*, **28**(2), 125-133.
- Elgarhy, M., and Shawki, M. R. A. (2016). Transmuted generalized Lindley distribution. *International Journal of Mathematics Trends and Technology*, **29**(2), 1-10.
- El-Monsef, M. M. E. A., Sweilam, N. H., and Sabry, M. A. (2020). The exponentiated power Lomax distribution and its applications. *Quality and Reliability Engineering International*.
- Embrechts, P., Frey, R., and McNeil, A. (2011). *Quantitative Risk Management*.



Eugene, N., Lee, C. and Famoye, F. (2002). The beta-normal distribution and its applications. *Communications in Statistics-Theory and Methods*, **31**(4): 497-512.

Famoye, F., Lee, C., and Olumolade, O. (2005). The beta-Weibull distribution. *Journal of Statistical Theory and Applications*, **4**(2):121-136.

Fernández, C. and Steel, M.F.J.(1998). On Bayesian modeling of fat tails and skewness. *Journal of American Statistical Association*, **93**(441): 359-371.

Ferreira, J.T.A.S. and Steel, M.F.J. (2006). A constructive representation of univariate skew distributions. *Journal of American Statistical Association*, **101**(474): 823-829.

Fletcher, R. (1970). A new approach to variable metric algorithms. *The computer journal*, **13**(3), 317-322.

Frees, E. W., Derrig, R. A., and Meyers, G. (Eds.). (2014). *Predictive modeling applications in actuarial science* (Vol. 1). Cambridge University Press

Goldfarb, D. (1970). A family of variable metric updates derived by variational means. *Mathematics of Computation*, **24**: 23-26.

Gomes-Silva, F., da Silva, R.V., Percontini, A., Ramos, M.W.A., and Cordeiro, G.M. (2017). An extended dagum distribution: Properties and applications. *International Journal of Applied mathematics and Statistics*, **56**(1):35-53.



- Guo, W. (2017). Development of a statistical oil spill model for risk assessment. *Environmental Pollution*, **230**: 945-953.
- Granzotto, D.C.T., Louzada, F. and Balakrishnan, N. (2017). Cubic rank transmuted distributions: inferential issues and applications. *Journal of Statistical Computation and Simulation*, **87**(14), 2760- 2778.
- Gray, R. J. and Pitts, S. M. (2012). *Risk modeling in general insurance: from principles to practice*. Cambridge University Press.
- Gupta, R. D., and Kundu, D. (2001). Exponentiated exponential distribution: An Alternative to gamma and Weibull distributions. *Biometrical Journal*, **43**(1): 117-130.
- Gupta, R.C., Gupta, P.L., and Gupta, R. D.(1998). Modeling failure time data by Lehman alternatives. *Communications in Statistics-Theory and Methods*, **27**(4):887-904
- Gupta, R. D., and Kundu, D. (1999). Generalised exponential distribution. *Australian and New Zealand Journal of statistics*,**41**(2): 173-188
- Hamedani,G.G., Yousof, H.M., Rasekhi,M., Alizadeh, M. and Najibi,S.M. (2018).Type I general exponential class of distributions. *Pakistan Journal of Statistics and Operational Research*, **14**(1):39-55.
- Hastings, J.C.,Mosteller, F., Tukey, J.W., and Windsor, C. (1947). Low moments for small samples: A comparative study of order statistics. *The Annals of Statistics*, **18**(3):413-426.



- Hazewinkel, M. (1994). *Exponential distribution, Encyclopedia of Mathematics*, Springer Science Business Media B.V. / Kluwer Academic Publishers, ISBN 978-1-55608-010-4
- Hurvich, C. M. and Tsai, C. L. (1989). Regression and time series model selection in small samples. *Biometrika*, **76**(2):297-307.
- Hussein, I, Abbas Z., and Ahmad, Z. (2018). Transmuted size-biased exponential distribution and its properties. *Pakistan Journal of Statistics*; **34**(2), 99-118.
- Ibrahim, N. A., Khaleel, M. A., Merovci, F., Kilicman, A., and Shitan, M. (2017). Weibull Burr X distribution properties and application. *Pakistan Journal of Statistics*, **33**(5).
- Ishak, K. J., Kreif, N., Benedict, A., and Muszbek, N. (2013). Overview of parametric survival analysis for health-economic applications. *Pharmacoeconomics*, **31**(8), 663-675.
- Jayakur, K., and Girish-Babu, M. (2017). T-transmuted X family of distribution. *Statistica annoLXXVII*, n.3.
- Johnson, N. L. (1949). System of frequency curves generated by methods of translation. *Biometrika*, **36**(2):149-176.
- Jones, M.C.(2004). Families of distributions arising from distribution of order statistics. *Test*, **13**(1):1-43.
- Jones, M.C.(2009). Kumaraswamy's distribution: A beta-type distribution with tractability advantages. *Statistical methodology*, **6**(1):70-81.



Kersey, J. H., Weisdorf, D., Nesbit, N.E., LeBien, T.W., Woods, W.G.,
McGlave, P.B., Tae Kim,

Khan, M., Pasha, G. R.S., and Pasha, A. H. (2008). Theoretical analysis of
Inverse Weibull distribution, *WSEAS Trans. Math., World Scientific
and Engineering Academy and Society* **7**: 30–38

Khan, M. S., and King, R. (2013). Transmuted modified Weibull distribution:
A generalization of the modified Weibull probability
distribution. *European Journal of Pure and Applied
Mathematics*, **6**(1):66-88.

Khan, M. S., and King, R. (2015). Transmuted modified inverse Rayleigh
distribution. *Austrian Journal of Statistics*, **44**(3), 17-29.

Khan, M.S., King, R. and Hudson, I. L. (2016). *Transmuted Weibull
distribution: Properties and Estimation*. *Communications in Statistics
Theory and Methods*. *Communications in Statistics - Theory and
Methods* **46**(11):5394-5418

Khan, M. S., King, R., and Hudson, I. L. (2017). Transmuted Kumaraswamy-
G family of distributions for modelling reliability data. *Journal of
Testing and Evaluation*, **45**(5), 1837-1848.

Khan, M. S., King, R., and Hudson, I. L. (2020). Transmuted Kumaraswamy
Weibull distribution with covariates regression modelling to analyze
reliability data. *Journal of Statistical Theory and Applications*.



- Klakattawi, H. S. (2019). The Weibull-gamma distribution: properties and applications. *Entropy*, **21**(5), 438.
- Kolmogorov, A.N. (1933). Sulla determinazione empirica di una legge di distribuzione. *Inst. Ital, Attari, Giorn.*, **4**:1-11.
- Krishna, E., Jose, K. K. and Ristić, M. M. (2013). Applications of Marshall-Olkin Fréchet Distribution, *Communications in Statistics - Simulation and Computation, Taylor and Francis* **42**, 76-89.
- Kumaraswamy, P. (1980). Generalised probability density function for double-bounded random processes. *Journal of Hydrology*, **46**:79-88.
- Lang, T. (2004). Twenty statistical errors even you can find in biomedical research articles
- Lawless, J.F. (1982). *Statistical models and methods for lifetime data*. New York: Wiley.
- Lee, C., Famoye, F., and Alzaatreh, A.Y. (2013). Methods for generating families of univariate continuous distributions in the recent decades, *WIRES Computational Statistics*, **5**: 219-238.
- Lieblein, J. and Zelen, M. (1956). Statistical investigation of the fatigue life of deep groove ball bearings. *J. Res. Nat. Bur Stand.*, **57**: 273-316.
- Lomax, K.S. (1954). Business failures: Another example of the analysis of failure data. *Journal of the American Statistical Association*, **49**:847-852.



- Louzada, F., and Granzotto, D. C. (2016). The transmuted log-logistic regression model: a new model for time up to first calving of cows. *Statistical Papers*, **57**(3), 623-640.
- Luguterah, A. and Nasiru, S. (2015). Transmuted exponential Pareto distribution. *Far East Journal of Theoretical Statistics* **50**(1):31-49
- Lorenz, M. O. (1905). Methods of measuring the concentration of wealth. *Publications of the American statistical association*, **9**(70), 209-219.
- Marshall, A.W. and Olkin, I. (1997). A new methods for adding a parameter to a family of distributions with application to the exponential and Weibull families. *Biometrika*. **84**: 641-652
- Mahmoud, M. R., and Mandouh, R. M. (2013). On the transmuted Fréchet distribution. *Journal of Applied Sciences Research*, **9**(10), 5553-5561.
- Marshall, A. W. and Olkin, I. (2007). *Life distributions*. Springer, New York.
- Mansour, M. M., Elrazik, E. M. A., Afify, A.Z., Ahsanullah, M, and Altund, (2019). The transmuted transmuted-G family: properties and applications. *Journal of Nonlinear Science. Applications.*, **12**: 217–229
- Mansoor, N., Vinknes, K. J., Veierød, M. B., and Retterstøl, K. (2016). Effects of low-carbohydrate diets v. low-fat diets on body weight and cardiovascular risk factors: a meta-analysis of randomised controlled trials. *British Journal of Nutrition*, **115**(3), 466-479.



- Morais, A.L., Cordeiro, G.M., and Cyseneiros, A.H.M.A. (2013). The beta generalised logistic distribution. *Brazilian Journal of Probability and Statistics*, **27**(2):185-200.
- Morgenthaler, S., and Tukey, J.W.(2000). Fitting quantile: doubling, HR,HQ, and HHH distributions. *Journal of Computational and Graphical Statistics*, **27**(2):180-195.
- Mudhokar, G.S. and Huston, A.D. (2000). The epsilon-skew normal distribution for analysing near normal data. *Journal of Statistical Planning and Inference*. **83**(2): 291-309.
- Mudhokar, G.S. and Srivastava, D.K. (1993). Exponentiated Weibull family for analysing bathtub failure rate data. *IEE Transactions on Reliability*, **42**: 299-302.
- Mahdavi, A., and Kundu, D. (2017). A new method for generating distributions with an application to exponential distribution. *Communications in Statistics-Theory and Methods*, **46**(13): 6543-6557.
- Mead, M. E. A. (2014). A note on Kumaraswamy Fréchet distribution, *Australian Journal of Basic and Applied Sciences* 8, 294-300
- Moolath, G. and Jayakumar,K. (2018) T-Transmuted X Family of Distributions, *Statistica* **77**:251–276.
- Merovci, F. (2013a). Transmuted exponentiated exponential distributions. *Mathematical Sciences And Applications E-Notes*,**1**(2):112-122.



- Merovci, F. (2013b). Transmuted Lindley distribution. *International Journal of Open problems in Computer Science and Mathematics*, **6**(2):63-72.
- Merovci, F. (2013c). Transmuted Rayleigh distribution. *Austrian Journal of Statistics*, **42**(1):21-31.
- Merovci, F., and Elbata, I. (2014). Transmuted Weibull-distribution and its applications. *School of Mathematics Northwest University Xian, Shaaxi, PR China*, **10**(1):68-82.
- Merovci, F. Alizadeh, M., Hamedani, M. G. G. (2016) Another generalized transmuted family of distributions: properties and applications, *Austrian Journal. Statist.*, **45**: 71–93.
- Merovci, F. Alizadeh, M., Yousof, H. M., Hamedani, G. G., (2017). The exponentiated transmuted-G family of distributions: theory and applications, *Comm. Statist. Theory Methods*, **46**: 10800–10822.
- Murthy, D.N.P., Xie, M. and Jiang, R. (2004). *Weibull Models*. Wiley publications.
- Nadarajah, S., and Kotz, S. (2006). The exponentiated type distribution. *Acta Applicande mathematica*, **92**(2):97-111.
- Nadarajah, S. and Kotz, S. (2013). The Exponentiated Frechet distribution, *Interstat Electronic Journal*, 1-7.
- Nadarajah, S. and Gupta, A. K. (2004). The beta Fréchet distribution, *Far East Journal of Theoretical Statistics* **14**:15-24.



- Nassar, M. M. and Nada, N. K. (2011). The beta generalized Pareto distribution. *Journal of Statistics: Advances in Theory and Applications*, **6**:1-17.
- Nasir, A., Yousof, H. M., Jamal, F., and Korkmaz, M. Ç. (2019). The Exponentiated Burr XII Power Series Distribution: Properties and Applications. *Stats*, **2**(1): 15-31
- Nasiru, S., Mwita, P.N., and Ngesa, O. (2017). Exponentiated generalised T-X family of distributions. *Journal of Statistical and Econometric Methods*, **6**(4):1-7.
- Nasiru, S., and Luguterah, A. (2015). The new Weibull-Pareto distribution. *Pakistan Journal of Statistics and Operation Research*, **11**:103-114.
- Nasiru, S., Luguterah, A., and Nantomah, K. (2018). The exponential Kumaraswamy linear exponential distribution: Theory and application. *Shag Journal of Mathematics, An international Journal*, **5**(1):1-8.
- Nasiru, S. (2018a). A new generalisation of transformed-transformer family of distributions. *Dotoral Thesis, Pan African University, Institute for Basic Sciences, Technology and Innovation*.
- Nasiru, S. (2018b). Extended odd Fréchet-G family of distributions, *Journal of Probability and Statistics*, 1-12
- Nasiru, S. (2018c). Serial Weibull-Rayleigh distribution: theory and application. *International Journal of Computing Science and Mathematics*. **7**, 239-244



- Nayak, T. K. (1987). Multivariate Lomax distribution: properties and usefulness in reliability theory. *Journal of Applied Probability*, **24**(1):170-177.
- Nichols, M. D., and Padgett, W. J. (2006). A bootstrap control chart for Weibull percentiles. *Quality and reliability engineering international*, **22**(2), 141-151.
- Nofal, Z.M., Afify, A.Z., Yousof, H.M. and Cordeiro, G.M. (2017). The generalized transmuted-G family of distributions. *Communications in Statistics-Theory and Methods*, **46**: 4119-4136.
- Ofori, J.B., Otchere, F., and Hesse. C.A. (2016). *Intermediate Statistical Methods*, Excellent Publication and Printing, Accra.
- O'Hagan, A., and Leonard, T. (1976). Bayes estimation subject to uncertainty about parameters constraints. *Biometrika*, **63**(1):201-203.
- Oguntunde, P.E., Adejumo, A.O. Okagbue, H.I. and Rastogi, M.K. (2016). Statistical properties and application of a new Lindley exponential distribution. *Gazi University journal of Sciences*, **29**(4):831-838.
- Oguntunde, P. E., Khaleel, M. A., Ahmed, M. T., Adejumo, A. O., and Odetunmbi, O. A. (2017). A new generalization of the Lomax distribution with increasing, decreasing, and constant failure rate. *Modelling and Simulation in Engineering*,



- Paula, G. A., Leiva, V., Barros, M., and Liu, S. (2012). Robust statistical modeling using the Birnbaum-Saunders-t distribution applied to insurance. *Applied Stochastic Models in Business and Industry*, **28**(1), 16-34.
- Pearson, K. (1895). Contributions to the mathematical theory of evolution, II: Skew variation in homogeneous material. *Philosophical Transactions of the Royal Society of London Series A*, **186**:343-414.
- Pearson, K. (1901). Mathematical contributions to the theory of evolution X: supplement to a memoir on skew of variation. *Philosophical Transactions of the Royal Society of London Series A*, **197**:343-414.
- Pearson, K. (1916). Mathematical contributions to the theory of evolution, XIX: second supplement to a memoir on skew of variation. *Philosophical Transactions of the Royal Society of London Series A*, **216**:429-457.
- Pinhoa, L. G. B., Cordeiroa, G. M., and Nobreb, J. S. (2012). The Harris Extended Exponential Distribution.
- Qin, X., Zhang, J. S., and Yan, X. D. (2012). Two improved mixture Weibull models for the analysis of wind speed data. *Journal of Applied Meteorology and Climatology*, **51**(7):1321-1332.
- Rahman, M. M., Al-Zahrani, B., and Shahbaz, M. Q. (2018). A general transmuted family of distributions. *Pakistan Journal of Statistics and Operation Research*, 451-469.



Rajab, M., Aleem, M., Nawaz, T., and Daniyal, M. (2013). On five parameter beta Lomax distribution. *Journal of Statistics*, **20**(1).

Ramos, M.W.A., Marinho, P.R.D., da Silva R.V. and Cordeiro, G.M.(2013) The exponentiated Lomax distribution.

Riffi, M.I., Ansari, S.I., and Hamdan, M.S (2019). A generalized transmuted Fréchet distribution. *Journal of Statistics Applications & Probability* **8**(2): 1-10

Rezaei, S., Marvasty, A.K, Nadarajah, S. and Alizadeh, (2017). A new exponentiated class of distributions: Properties and applications. *Communications in Statistics-Theory and Methods*. **46**(12):6054-6073

Ristić , M.M. and Balakrishna, N. (2012). The gamma-exponentiated exponential distribution. *Journal of Statistical Computation and Simulation* **82**:1191-1206

Salinas, H.S., Arellano-Valle, R.B., and Gomez, H.W. (2007). The extended skew-exponential power distribution and its derivation. *Communications in statistics-Theory and methods*, **30**(9):1673-1689.

Selim, M. A., and Badr, A. M. (2016). The Kumaraswamy generalized power Weibull distribution. *Math. Theo. Model*, **6**:110-124.

Shaked, M. and Shanthikumar, J.G. (1994). *Stochastic orders and their applications*. Academic press, New York.

Shanno, D. F. (1970). Conditioning of quasi-Newton methods for function minimization. *Mathematics of computation*, **24**(111), 647-656.



Shaw, W. and Buckley, I.(2007). The alchemy of probability distributions: beyond Gram-Charlier expansions and a skew-kurtotic-normal distribution from a rank transmutation map, *Research Report*

Smith, R. L., and Naylor, J. C. (1987). A comparison of maximum likelihood and Bayesian estimators for the three-parameter Weibull distribution. *Appl. Statist.* **36**:358–369.

Smirnov,N.V. (1939). On the estimation of the discrepancy between empirical curves of distributions for two independent samples. *Bulletin mathematique de l'Univerite de Moscou*, **2** :2.

Sugiura, G. (1978). Further analysis of data by Akaike's information criterion and theFinite corrections. *Communications in Statistics-Theory and Methods*, **7**(1):13-26.

Swartz, G. (1978). Estimating the dimension of a model. *The Annals of Statistics*, **6**(2):461-464.

Tablada, C. J. and Gauss M. Cordeiro,G.M.(2016). The modified Fréchet distribution and its properties, *Communication in Statistics- Theory and Methods*, Taylor and Francis Group,.

Tahir,M.H., Gauss, M.C., Cordeiro, G.,Mansoor M., Zubair, M. and MORAD Alizadeh, M (2014). The Weibull-Dagum Distribution: Properties and Applications. *Communication in Statistics- Theory and Methods* ·



- Tahir, M. H., Cordeiro, G. M., Mansoor, M., and Zubair, M. (2015). The Weibull-Lomax distribution: properties and applications. *Hacettepe Journal of Mathematics and Statistics*, **44**(2), 455-474.
- Thoman, D. R., Bain, L. J., and Antic, C. E. (1969). Inferences on the parameters of the Weibull distribution. *Technometrics*, **11**: 445-460.
- Tahir, A., Akhter, A. S., and Haq, M. A. (2018). Transmuted new Weibull-Pareto distribution and its applications. *Applications and Applied Mathematics-An International Journal*, **13**(1), 30-46.
- Tukey, J. W. (1960). The practical relationship between the common transformations of percentages of counts and amounts. Technical Report 36, Statistical Techniques Research Group, Princeton University, Princeton, N.J.
- Usman, A. U., and Yakubu, A. (2018). Generalized Transmuted-Generalized Rayleigh distribution: Its properties and application. *Journal of Experimental Research*, **6**(4).
- ul Haq, M. A., Yousof, H. M., and Hashmi, S. (2017). A new five-parameter Fréchet model for extreme values. *Pakistan Journal of Statistics and Operation Research*, 617-632.
- Ul-Haq, A. M., and Elgarhy, M. (2018). The odd Fréchet-G family of probability distributions. *Journal of Statistics Applications & Probability*, **7**(1), 185-201.



- Vallera, A. I., Bostrom, G.B., Hurd, D., and Ramsay, N.K.C. (1987). Comparison of autologous and allogeneic bone marrow transplantation for treatment of high-risk refractory acute lymphoblastic leukemia, *New England Journal of Medicine*, **317**:461–467.
- Weibull, W.A. (1951). A statistical distribution function of wide applicability. *J.Appl. Mech*, **18**(3):293-297.
- Willmot, G. E., and Lin, X. S. (2011). Risk modelling with the mixed Erlang distribution. *Applied Stochastic Models in Business and Industry*, **27**(1), 2-16.
- Youof, H.M., Afify, A.Z., Alizadeh, M., Butt, N.S., Hamedani, G.G., Ali, M.M. (2015). The transmuted exponential generalised-G family of distributions. *Pakistan Journal of Statistics and Operation Research*, **11**:441-464.
- Zhu H.P., Xia, X., and Chuan, H.Y (2011). Application of Weibull model for survival of patients with gastric cancer. *BMC, PubMed*
- Zografos, K. and Balakrishnan, N. (2009). On families of beta- and generalised gamma-generated distributions and associated inferences. *Statistical Methodology*. **6**:344-362



APPENDICES

Appendix A1: The tax revenue data and the application of the T-TIGER model

The Appendix A1 represents the first dataset known as the Tax Revenue data that was used to demonstrate the application of the T-TIGER distribution of the proposed generator.

Appendix A1: Tax Revenue Data

5.9	20.4	14.9	16.2	17.2	7.8	6.1	9.2
13.3	8.5	21.6	18.5	5.1	6.7	17.0	8.60
35.7	15.7	9.7	10.0	4.1	36	8.5	8.0
21.9	16.7	21.3	35.4	14.3	8.5	10.6	19.1
7.7	18.1	16.5	11.9	7.0	8.6	12.5	10.3
8.4	11	11.6	11.9	5.2	6.8	8.9	7.1
10.2	9.70	9.2	20.5	11.2	10.8	9.6	39.2
26.2	7.1	6.1					

Sources: (Nassar and Nada 2011; Klakattawi, 2019).



Appendix A2: The Kiamo dataset and the application of the T-TIGER model

This represents the second dataset known as the Kiamo Blowhole data that was used to demonstrate the application of the T-TIGER distribution of the proposed generator.

Appendix A2: Kiamo Blowhole data

83	51	87	60	28	95	8	27
15	10	18	16	29	54	91	8
17	55	10	35	47	77	36	17
21	36	18	40	10	7	34	27
28	56	8	25	68	146	89	18
73	69	9	37	10	82	29	8
60	61	61	18	169	25	8	26
11	83	11	42	17	14	9	12

Source: Pinho et al. (2012)



Appendix A3: The dataset and the application of the T-TIGER distribution

This represents the third dataset known as the Applied Life Analysis data that was used to demonstrate the application of the T-TIGER distribution of the proposed generator.

Appendix A3: Applied Life Analysis Data

0.96	4.15	0.19	0.78	8.01	31.75	7.35
32.52	3.16	4.85	2.78	4.67	1.31	12.06
6.50	36.71	8.27	72.89	33.91		

Sources: (Abbas and Tang, 2015; Nelson, 1982).



Appendix B: The Aircraft windshield failure rate dataset and the application of the T-TIGEW

This represents the fourth dataset known as the Aircraft windshield failure rate data that was used to demonstrate the application of the T-TIGEW model of the proposed generator.

Appendix B: Aircraft windshield failure rate data

0.040	1.866	2.385	3.443	0.301	1.876	2.481	3.467	0.309	1.899
0.557	1.911	2.625	3.578	0.943	1.912	2.632	3.595	1.070	1.914
1.124	1.981	2.661	3.779	1.248	2.010	2.688	3.924	1.281	2.038
4.035	1.281	2.085	2.890	4.121	1.303	2.089	2.902	4.167	1.432
4.240	1.480	2.135	2.962	4.255	1.505	2.154	2.964	4.278	1.506
4.305	1.568	2.194	3.103	4.376	1.615	2.223	3.114	4.449	1.619
4.485	1.652	2.229	3.166	4.570	1.652	2.300	3.344	4.602	1.757
4.663	2.610	3.478	2.646	3.699	2.820	3.000	2.097	2.934	2.190
3.000	2.224	3.117	2.324	3.376					

Sources:(Nasir et al.2019; Tahir et al.2015; Ramos et al. 2013; Murthy et al. 2004)



Appendix C1: The rainfall dataset and the application of the T-TIGEFr distribution

This represents the fifth dataset known as the rainfall dataset. This dataset was used to demonstrate the application of the T-TIGEFr distribution of the proposed generator.

Appendix C1: Rainfall Dataset

24.8	140.9	54.1	153.5	47.9	165.5	68.5	153.1
87.6	150.6	147.9	354.7	128.5	150.4	119.2	69.7
121.7	99.3	126.9	150.1	149.1	143	125.2	97.2
101	89.8	54.6	283.9	94.3	165.4	48.3	69.2
159.4	114.9	58.5	76.6	20.7	107.1	244.5	126
153.2	145.3	101.9	135.3	103.1	74.7	174	126
96.2	149.3	122.3	164.8	188.6	273.2	273.2	61.2
96.2	155.8	194.6	92	131	137	106.8	131.6
147.8	294.6	101.6	103.1	247.5	140.2	153.3	91.8
168.6	127.7	332.8	261.6	122.9	273.4	178	177
241	76	127.5	190	259.5	301.5	268.2	124.5
254.7	175.3	185.1	153.4	179.3	125.8	147.1	114.2
122.2	219.9	144.9	226.3	84.3	130.5	79.4	149.2
108.5	115	241	76	127.5	190	259.5	301.5

Source: Mansoor et al (2016).



Appendix C2: The breaking strength dataset and the application of the T-TIGEFr model

This represents the sixth dataset known as the breaking strength dataset. This dataset was used to demonstrate the application of the T-TIGEFr distribution of the proposed generator.

Appendix C2: Breaking Stress dataset

0.92	0.928	0.997	0.9971	1.061	1.117	1.162	1.183	1.187	1.192
1.196	1.213	1.215	1.2199	1.22,	1.224	1.225,	1.228	1.237	1.24
1.244	1.259	1.261	1.263	1.276	1.31	1.321	1.329	1.331	1.337
1.351	1.359	1.388	1.408	1.449	1.4497	1.45	1.459	1.471	1.475
1.477	1.48	1.489	1.501	1.507	1.515	1.53	1.5304	1.533	1.544
1.5443	1.552	1.556	1.562	1.566	1.585	1.586	1.599	1.602	1.614
1.616	1.617	1.628	1.684	1.711	1.718	1.733	1.738	1.743	1.759
1.777	1.794	1.799	1.806	1.814	1.816	1.828	1.83	1.884	1.892
1.944	1.972	1.984	1.987	2.02	2.0304	2.029	2.035	2.037	2.043
2.046	2.059	2.111	2.165	2.686	2.778	2.972	3.504	3.863	5.306

Sources: Mahmoud and Mandouh (2013)



Appendix D: The fibre strength dataset and application of the T-TIGEEE distribution

This represents the sixth dataset known as the breaking strength dataset. This dataset was used to demonstrate the application of the T-TIGEEE model of the proposed generator.

Appendix D: Fibre Strength Data

1.901	2.132	2.203	2.228	2.257	2.350	2.361	2.396
2.454	2.474	2.518	2.522	2.525	2.532	2.575	2.614
2.624	2.659	2.675	2.738	2.740	2.856	2.917	2.928
2.977	2.996	3.030	3.125	3.139	3.145	3.220	3.223
3.264	3.272	3.294	3.332	3.346	3.377	3.408	3.435
3.537	3.554	3.562	3.628	3.852	3.871	3.886	3.971
4.225	4.395	5.020	2.397	2.445	2.616	2.618	2.937
2.937	3.235	3.243	3.493	3.501	4.024	4.027	

Source: (Selim and Badr ,2016; Badar and Priest, 1982)

